Journal of Computational and Applied Mathematics 343 (2018) 662–707

Contents lists available at ScienceDirect

Journal of Computational and Applied Mathematics

journal homepage: www.elsevier.com/locate/cam

# $C^1$ sign, monotonicity and convexity preserving Hermite polynomial splines of variable degree

Nikolaos C. Gabrielides [a,*], Nickolas S. Sapidis [b]

[a] DNV GL — Digital Solutions, Veritasveien 1, 1363, Høvik, Norway
[b] Department of Mechanical Engineering, University of Western Macedonia, Bakola & Sialvera Str., GR-50132, Kozani, Greece

ARTICLE INFO

*Article history:*
Received 3 July 2017
Received in revised form 5 January 2018

*Keywords:*
1D shape-preserving interpolation
Sign, monotonicity, convexity criteria
Composite Bezier curves
Nodal derivative estimation method

ABSTRACT

This paper proposes an algorithm for constructing interpolatory Hermite polynomial splines of variable degree, which preserve the sign, the monotonicity and the convexity of the data. The polynomial segments are represented as Bézier curves. The degree of each segment plays the role of the tension parameter of the spline. We discuss extensively the monotonicity and convexity criteria, detailing a strict and a weak form of monotonicity preservation, as well as their implications on the Hermite interpolation. We also propose a global method for estimating the nodal derivatives of the spline. We evaluate the results of this method in an extensive set of examples, comparing them with a number of local derivative estimation methods from the pertinent literature. The algorithm is numerically stable, simple to implement, and it is of linear complexity, since the related mathematical conditions can be expressed as linear inequalities with respect to the control points of the spline.



## 1. Introduction

Scientific as well as engineering applications demand approximation methods representing physical reality as accurately as possible. For an accurate interpolation, we must carefully retain crucial properties implied by the data, thus reflecting the shape inferred by them. In 1D interpolation, shape preservation requirements make shape-preserving interpolation a constraint interpolation problem, subjected to sign, monotonicity and convexity constraints.

The motivation for this research was the reconstruction of the so-called "$p$–$y$" (soil resistance, $p$ as a function of the lateral deflection $y$ of the pile) and "$t$–$z$" (axial response $z$ of a pile subjected to vertical load $t$) curves. These curves are used in the design/evaluation of pile foundations; see [1] and [2]. They model the pile–soil interaction for a constant depth of the pile. Each one is known by a list of data points, which are to be interpolated by a smooth curve. The accuracy of the whole procedure depends on the shape characteristics of these curves, thus sign, monotonicity and convexity preservation turn out to be critical.

In Approximation Theory, the quality of an interpolation method is characterized primarily by the order of continuity of the interpolant and by the order of convergence as mesh spacing becomes arbitrarily small. However, none of these properties guarantees a geometrically/visually acceptable interpolant (see [3]). Moreover, frequently in practice, if we balance all requirements of an application (simplicity, controllability, efficiency regarding computing-time and storage, etc.) relatively low orders of continuity or rates of convergence can be proved to be sufficient, provided that the interpolant fully complies with the shape characteristics implied by the data (see, e.g., the planar three degree-of-freedom motion of a vehicle,

* Corresponding author.
*E-mail addresses:* nikolaos.gavriilidis@dnvgl.com (N.C. Gabrielides), nsapidis@uowm.gr (N.S. Sapidis).

https://doi.org/10.1016/j.cam.2018.03.020
0377-0427/

namely, the path planning problem and the guidance problem in [4], or the segmentation of tumor in images from CT scan or from ultrasonography (USG) in [5]).

In this work we deal with interpolation of an ordered set of points,

$$(x_i, f_i),\ i = 0, 1, \ldots, N \text{ with } a = x_0 < x_1 < \cdots < x_N = b \text{ and } f_i \in \mathbb{R} \tag{1}$$

from an unknown real function $f(x)$ of a real variable $x \in [a, b]$, seeking for a function, $c(x)$, such that:

$$c(x_i) = f_i,\ i = 0, \ldots, N \tag{2}$$

which preserves the sign, the monotonicity and the convexity of the data.

In the pertinent literature we can find numerous articles dealing with this problem (see [6–8] and the references therein). The flexibility of the Hermite interpolation scheme has let to its adoption by the majority of the shape-preservation methods. The data set of the standard $C^1$ Hermite interpolation consists of the ordered points (1) and the derivative values at them:

$$v_i \in \mathbb{R},\ i = 0, 1, \ldots, N \tag{3}$$

Methods for solving this interpolation problem with Hermite splines, usually, estimate derivative values at intermediate data points and assume the boundary ones, $v_0$ and $v_N$, as given.

The concept of shape-preserving interpolation in one dimension was introduced in classic works, on exponential splines in tension, by Schweikert [9] and Späth [10] in the sixties. Two decades later, a number of algorithms capable of practical use appeared (see, e.g., [3,11–13] and [14]) which are based on the Hermite interpolation scheme and construct polynomial segments. Such algorithms could have been adopted by software packages, due to their simplicity and stability, however, the use of non-standard basis functions, proved to be a major drawback for practical use (an interesting exception found in the NAG-library [15], which implements the method of [16]). Taking into account that along with the polynomial methods, shape preserving interpolation has been studied and solved also with the aid of rational polynomial splines (e.g. [17]) lets us characterize the problem as well studied, without any doubt. On the other hand, one may encounter another disadvantage of the methods in the existing literature, the monotonicity preservation criteria (see [7]) lead to over-constrained curves. Recently, a considerable number of articles, on polynomial splines (see [18–21]) on rational polynomial splines (see [22–31]) on exponential splines in tension (see [32,33]) on trigonometric splines (see [34]) on subdivision schemes (see [35–39]) and on fractal interpolation (see [40,41]) with tension properties, demonstrates that the interest in this subject is still high. However, one notes that most of these methods create non-polynomial splines, rendering them inappropriate for a commercial software package. The present research indeed focuses on polynomial splines, based on the convexity preserving splines of variable degree, introduced in [42]. This method lets the degrees of the spline segments vary using them as tension parameters, while restrictions are imposed on the structure of the control polygon of the curve. (In this respect, similar trends can also be found in [43] and [18]). The degrees increase in a semi-local manner and, after a finite number of iterations, the resulting spline is convexity preserving. Variable degree splines solve also the shape preservation problem in $\mathbb{R}^2$ [44] and in $\mathbb{R}^3$ [45], reaching even continuity order up to fourth order [46]. However, in order to use the method [42] for practical purposes, one may encounter that:

- It fails to construct monotonicity preserving curves (see Examples 1 and 2). (Studying deeply the method [42] we may deduce its ability to do so, though this has not been published yet).
- It implements a collinearity criterion which leads to extremely high degrees (see Example 4). A different way to be more consistent with the CAD practice needs to be implemented.
- The algorithms [44,45] and [46] curry a fundamental drawback of [42]: the difficulty in handling the degree increase and the unpredictable number of iterations, which leads to algorithms of complexity of $O((K-2)N)$, where $K$ is the maximum segment degree and $N$ is the given number of points.

Recently, the third disadvantage was overcome in [47] by relaxing the continuity order of the curves, from $C^2$ to $C^1$, and solving the Hermite interpolation problem. This method is of linear complexity $O(N)$ and has been implemented in the CAD/CAE system Genie [48].

In this paper, we develop an algorithm to calculate the $C^1$ Hermite piecewise polynomial shape-preserving curves of variable degree in one dimension. We construct a simple, robust algorithm of linear complexity with respect to the given number of points. Regarding the contents of the paper, we first set up the sign, monotonicity and convexity preservation criteria (Criteria 1–3) in the next section. In Section 3 we discuss in detail the shape preservation criteria and their implications in selecting the nodal derivatives (3). The discussion leads us to formulate an alternative monotonicity criterion (Criterion 4) which is more flexible than Criterion 2. The section ends with the formulation of the shape preserving interpolation problem. The next section deals with the representation of the interpolation curves. Moreover, it contains a geometric interpretation of the shape parameters and their influence on the interpolant. In Sections 5–8 we prove the ability of the variable degree Hermite polynomial spline to preserve Criteria 1–4, showing that the shape preserving interpolation problem in one dimension requires only the solution of a set of linear inequalities, leading to a linear complexity algorithm. In Section 9 we present (a) a number of local methods from the pertinent literature and (b) a new globally optimal method, which tends to reduce the polynomial degrees of the spline, for selecting the nodal derivatives. Based on the results of Sections 5–9, Section 10 presents analytically the steps of the algorithm. Section 11 addresses the convergence of the spline. Finally, in Section 12 we present the numerical experimentation of our method, giving comparisons with the algorithm [42], applied to examples from the CAD/CAE practice as well as examples of academic interest.

## 2. Sign, monotonicity and convexity criteria

Retaining sign (also found as 'positivity' in the literature) is important in many practical situations, when the data represent strictly positive (or negative) measurements (density, pressure etc.) as pointed out in [49]. When implementing a criterion expressing the positivity of a function, then for numerical stability reasons, we need to fix a small positive constant, $\epsilon_f$, in order to define a narrow band around zero, before we test the sign of the given values $f_i$ and $f_{i+1}$. In view of this remark, the *sign criterion* can be stated as:

**Criterion 1** (*Sign Criterion*). *The curve $c(x)$ which satisfies the interpolation conditions (2) preserves the sign of the data in $[x_i, x_{i+1}]$, iff:*

*If $|f_i|, |f_{i+1}| > \epsilon_f$ and $f_i f_{i+1} > 0$, then $c(x)f_I > 0,\ x \in [x_i, x_{i+1}]$, for $I = i, i+1$.*

The monotonicity of the polygonal arc $\mathcal{P}$ can be expressed in the interval $[x_i, x_{i+1}]$ by the divided difference:

$$s_i = \frac{f_{i+1} - f_i}{h_i}, \quad h_i = x_{i+1} - x_i, \quad i = 0, \ldots, N-1 \tag{4}$$

The slope $s_i$ is called *monotonicity indicator* of $\mathcal{P}$ in the interval $[x_i, x_{i+1}]$. The divided difference $s_i$ is equal to the tangent of the angle $\theta$ of the vector $\begin{pmatrix} x_{i+1} - x_i \\ f_{i+1} - f_i \end{pmatrix}$ with the $x$-axis. Now, setting a fixed small positive constant $\epsilon_\theta$ to be the tolerance of the zero angle $\theta$, the *monotonicity preservation criterion* can be stated as follows:

**Criterion 2** (*Monotonicity Criterion*). *The curve $c(x)$ which satisfies the interpolation conditions (2) preserves the monotonicity of the data in $[x_i, x_{i+1}]$ iff:*

A. *If $|s_i| < \epsilon_\theta$ then $c(x) = f_i \frac{x_{i+1} - x}{x_{i+1} - x_i} + f_{i+1} \frac{x - x_i}{x_{i+1} - x_i},\ x \in [x_i, x_{i+1}]$ (constant value).*

B. *If $|s_i| > \epsilon_\theta$ then $c'(x)s_i \geq 0,\ x \in [x_i, x_{i+1}]$.*

A more careful observation of the monotonicity criterion, can easily make us realize that it actually overlaps with the sign criterion, in the following sense:

**Lemma 1.** *If the curve $c(x)$ is monotonicity preserving, satisfying Criterion 2, then it also retains the sign of the data, in the sense of Criterion 1.*

**Proof.** If the curve $c(x)$ satisfies Criterion 2 in $[x_i, x_{i+1}]$, one of the following cases holds:

Case A. $|s_i| < \epsilon_\theta$: the monotonicity criterion implies $c(x) = f_i(1-t) + f_{i+1}t$, for $t = \frac{x - x_i}{x_{i+1} - x_i},\ x \in [x_i, x_{i+1}]$. Now, if $|f_i|, |f_{i+1}| > \epsilon_f$ and $f_i f_{i+1} > 0$, then, $c(x)f_I = f_i f_I (1-t) + f_{i+1} f_I t$, for $I = i, i+1$, which is always positive, since $f_i f_{i+1} > 0$, i.e. the sign criterion holds.

Case B. $|s_i| > \epsilon_\theta$: the monotonicity criterion implies $c'(x)s_i \geq 0,\ x \in [x_i, x_{i+1}]$, i.e., the function $c(x)$ has either positive (if $f_i < f_{i+1}$) or negative (if $f_i > f_{i+1}$) derivative in $[x_i, x_{i+1}]$. Then, taking into account the prerequisites of the sign criterion, i.e. $|f_i|, |f_{i+1}| > \epsilon_f$ and $f_i f_{i+1} > 0$, the function $c(x)$ shares the same sign with $f_i$ and $f_{i+1}$ necessarily. □

In the next section we shall give a less restrictive version of the monotonicity criterion. Then, if the weak version of the criterion is employed, the positivity criterion begins to play an important role of its own.

The convexity of $\mathcal{P}$ at the point $(x_i, f_i)$ can be expressed by the difference of slopes of the adjacent segments, i.e.:

$$\delta_i = s_i - s_{i-1}, \quad i = 1, \ldots, N-1 \tag{5}$$

The quantity $\delta_i$ is the so-called *convexity indicator* of the polygon $\mathcal{P}$ at the point $(x_i, f_i)$ (see [42]). It is quite convenient to define also the convexity indicators at the end points, where the slopes $s_0$ and $s_{N-1}$ are given, as:

$$\delta_0 = s_0 - v_0 \qquad \text{and} \qquad \delta_N = v_N - s_{N-1} \tag{6}$$

The (almost) zero $\delta_i$ indicates that the three consecutive points, with indices $i-1$, $i$ and $i+1$, can be regarded as *collinear*. We define a small positive constant $\epsilon_\delta$ and we extend the convexity preservation notion from the point $(x_i, f_i)$ over the whole interval $[x_i, x_{i+1}]$, by adopting the following:

**Criterion 3** (*Convexity Criterion*). *A curve $c(x)$ which satisfies the interpolation conditions (2) preserves the convexity of the data in $[x_i, x_{i+1}]$ iff:*

A. *If $\delta_i < \epsilon_\delta$ or $\delta_{i+1} < \epsilon_\delta$, then $c(x) = f_i \frac{x_{i+1} - x}{x_{i+1} - x_i} + f_{i+1} \frac{x - x_i}{x_{i+1} - x_i},\ x \in [x_i, x_{i+1}]$ (collinearity).*

B. *Else If $\delta_i \delta_{i+1} > 0$ then $c''(x)\delta_I \geq 0,\ x \in [x_i, x_{i+1}]$ for $I = i, i+1$.*

C. *Else If $\delta_i \delta_{i+1} < 0$ then $c''(x)$ changes sign only once in $[x_i, x_{i+1}]$.*

Since the constant value Criterion 2.A and the collinearity Criterion 3.A, lead to uniquely defined linear segments, we would give the following corollaries, which have trivial proofs:

**Corollary 1.** *Given a sequence of points (1) if the convexity indicators $\delta_{i-1}$ and $\delta_{i+1}$ are (almost) zero while $\delta_i$ is not, i.e. $|\delta_{i+1}| < \epsilon_\delta$ and $|\delta_{i-1}| < \epsilon_\delta$ and $|\delta_i| > \epsilon_\delta$ then any function $c(x)$ interpolating the data, which satisfies Criterion 2.A, is necessarily $C^0$ continuous at $(x_i, f_i)$.*

**Corollary 2.** *Given a sequence of points (1) if the monotonicity indicator $s_i$ and the convexity indicator $\delta_{i-1}$ (or $\delta_{i+2}$) are (almost) zero, i.e. $|s_i| < \epsilon_\theta$ and $|\delta_{i-1}| < \epsilon_\delta$ (or $|\delta_{i+2}| < \epsilon_\delta$) then any function $c(x)$ interpolating the data, which satisfies Criterion 2.A and Criterion 3.A is necessarily $C^0$ continuous at $(x_i, f_i)$.*

The fact that the above corollaries contradict our intention to create $C^1$ continuous curves over the whole interval $[a, b]$, could characterize the validity of the criteria questionable. Nevertheless, one could hardly argue against the fact that the polygonal arc of the data points, $\mathcal{P}$, indicates discontinuity of the derivative of the interpolating curve in such cases. In our opinion, such a behavior of any interpolation method is acceptable in the shape-preservation context (see also [47]).

## 3. Monotonicity and convexity preservation in Hermite interpolation

Since we have adopted Criteria 2 and 3, for monotonicity/convexity preservation,the nodal derivatives $v_i$, should be estimated in accordance to (they should not violate) these two criteria. Since $v_i$ denotes the first derivative at $(x_i, f_i)$, then the convexity indicator at that point can equivalently be defined by:

$$\delta_i^- = v_i - s_{i-1} \quad \text{and} \quad \delta_i^+ = s_i - v_i \tag{7}$$

The restriction on $v_i$, imposed by the convexity criterion, is that the convexity indicators $\delta_i^-$ and $\delta_i^+$ should have the same sign with $\delta_i$, i.e., $\exists \beta_i, \gamma_i > 0$ such that: $\delta_i^- = \beta_i \delta_i$ and $\delta_i^+ = \gamma_i \delta_i$. These two equalities, along with (7), yield:

$$v_i = s_{i-1}(1-\beta_i) + s_i \beta_i \quad \text{and} \quad v_i = s_{i-1}\gamma_i + s_i(1-\gamma_i)$$

Equalizing the right-hand side of the above equations, we obtain $\beta_i + \gamma_i = 1$, which necessarily leads to (cf. [47] -rel. (13)):

$$v_i = (1-\alpha_i)s_{i-1} + \alpha_i s_i, \text{ or } v_i = s_{i-1} + \alpha_i \delta_i \text{ with } 0 \le \alpha_i \le 1 \tag{8}$$

Apart from the convexity criterion, the implication of the monotonicity criterion has to be taken into account as well. In this respect, we consider, first, the estimation of $v_i$ with respect to $[x_{i-1}, x_i]$. If $s_i \neq 0$, then Criterion 2.B requires at $x = x_i$:

$$s_{i-1} v_i \ge 0 \Longleftrightarrow (1-\alpha_i)s_{i-1}^2 + \alpha_i s_{i-1} s_i \ge 0 \tag{9}$$

Analogously, in $x \in [x_i, x_{i+1}]$ Criterion 2.B dictates at $x = x_i$:

$$s_i v_i \ge 0 \Longleftrightarrow (1-\alpha_i)s_{i-1} s_i + \alpha_i s_i^2 \ge 0 \tag{10}$$

If $s_{i-1}$ and $s_i$ have the same sign, then the inequalities (9) and (10) hold, since $0 \le \alpha_i \le 1$. However, in case when $s_{i-1}s_i < 0$, multiplying the latter by the positive quantity $\frac{-s_i s_{i-1}}{s_i^2}$ yields:

$$-(1-\alpha_i)s_{i-1}^2 - \alpha_i s_{i-1} s_i \ge 0 \tag{11}$$

The only way to satisfy both (9) and (11) is to set:

$$(1-\alpha_i)s_{i-1}^2 + \alpha_i s_{i-1} s_i = 0 \Longrightarrow s_{i-1} v_i = 0 \Longrightarrow v_i = 0.$$

The constraints in the selection of the derivatives, $v_i$, due to Criteria 2 and 3 are summarized in the following:

**Lemma 2.** *The standard Hermite spline, which interpolates the set of points (1) and the tangent vectors (3) is able to preserve the convexity of the data in the sense of Criterion 3 iff the nodal derivatives are represented as in (8). Moreover, it is able to preserve the monotonicity of the data in the sense of Criterion 2 iff the derivative $v_i$ is set explicitly equal to zero, when $|s_{i-1}|, |s_i| > \epsilon_\theta$ and $s_{i-1}s_i < 0$.*

Fig. 1 shows all possible distinct cases that the polygon $\mathcal{P}$, between the points with indices $(i-1)$ and $(i+2)$, may fall into (the figure does not contain configurations of (almost) zero monotonicity indicators). Lemma 2 says that if monotonicity preservation is enforced by Criterion 2, then one obtains curves with vanishing derivative at the following cases/points: Case II/point $i$, Case III/point $(i+1)$ and Case IV/points $i$ and $(i+1)$. Only the nodal derivatives of Case I are not affected by this restriction. This leads necessarily to local minimum or maximum at those points. In this sense, the monotonicity Criterion 2 can be characterized as *strict* (see also [21]). The idea here is to relax Criterion 2, so as the minimum/maximum do not appear exactly at the nodes of interpolation but in a wider range around them. In other words, we may shorten the interval in which

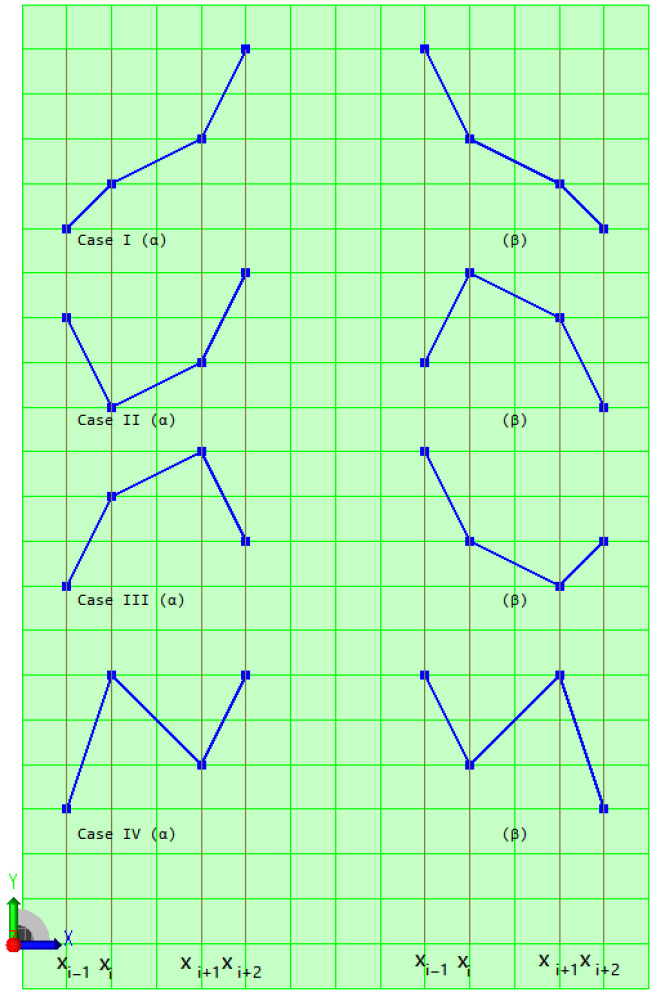


**Fig. 1.** **Case I** ($s_{i-1}s_i > 0$ and $s_is_{i+1} > 0$). Possible configurations: ($\alpha$) $s_{i-1}, s_i, s_{i+1} > 0$ and ($\beta$) $s_{i-1}, s_i, s_{i+1} < 0$. **Case II** ($s_{i-1}s_i < 0$ and $s_is_{i+1} > 0$). Possible configurations: ($\alpha$) $s_{i-1} < 0$ and $s_i, s_{i+1} > 0$ ($\beta$) $s_{i-1} > 0$ and $s_i, s_{i+1} < 0$. **Case III** ($s_{i-1}s_i > 0$ and $s_is_{i+1} < 0$). Possible configurations: ($\alpha$) $s_{i-1}, s_i < 0$ and $s_{i+1} > 0$ ($\beta$) $s_{i-1}, s_i > 0$ and $s_{i+1} < 0$. **Case IV** ($s_{i-1}s_i < 0$ and $s_is_{i+1} < 0$). Possible configurations: ($\alpha$) $s_{i-1}, s_{i+1} > 0$ and $s_i < 0$ ($\beta$) $s_{i-1}, s_{i+1} < 0$ and $s_i > 0$.

$c'(x)s_i \geq 0$, thus forming a weak version of the monotonicity criterion. Such a relaxation may be desirable when a particular application allows it. Since the vectors $v_i$ are given, the weak form of the monotonicity criterion should preferably accept $s_iv_i < 0$, in the Case II and IV (analogously $s_iv_{i+1} < 0$, in the Case III and IV). In this sense, the interval $[x_i, x_{i+1}]$, where the inequality $c'(x)s_i > 0$ holds, might be shortened by a length percentage $0 < \lambda < \frac{1}{2}$ near $x_i$ (and/or near $x_{i+1}$ respectively). Thus, the weak formulation of the monotonicity criterion can be stated as follows:

**Criterion 4** (*Weak Monotonicity Criterion*)**.** *A curve $c(x)$ which satisfies the interpolation conditions (2) preserves the monotonicity of the data in $[x_i, x_{i+1}]$:*

A. *If $|s_i| < \epsilon_\theta$ then $c(x) = f_i\frac{x_{i+1}-x}{x_{i+1}-x_i} + f_{i+1}\frac{x-x_i}{x_{i+1}-x_i}$, $x \in [x_i, x_{i+1}]$ (constant value).*
B. *If $|s_i| > \epsilon_\theta$, then:*

I. *If $v_is_i > 0$ and $s_iv_{i+1} > 0$, then $c'(x)s_i \geq 0$ in $[x_i, x_{i+1}]$.*
II. *If $v_is_i < 0$ and $s_iv_{i+1} > 0$, then $c'(x)s_i \geq 0$ in $[x_i + \lambda h_i, x_{i+1}]$.*
III. *If $v_is_i > 0$ and $s_iv_{i+1} < 0$, then $c'(x)s_i \geq 0$ in $[x_i, x_{i+1} - \lambda h_i]$.*
IV. *If $v_is_i < 0$ and $s_iv_{i+1} < 0$, then $c'(x)s_i \geq 0$ in $[x_i + \lambda h_i, x_{i+1} - \lambda h_i]$.*

If the weak monotonicity criterion is employed, then in the cases II–IV, Lemma 1 does not hold, so the curve does not retain the sign of the data necessarily and the sign criterion 1 plays an important role of its own, nearby the ends of the interval $[x_i, x_{i+1}]$, since it restrains the resulting curve from changing its sign. In the case I, the sign criterion constraint

is automatically satisfied by the constraints of the monotonicity criterion above. Based on the discussion in the last two sections, the paper proposes a method to solve the following problem:

**Problem 1.** Given the sequence of points (1) construct a curve, $c(x)$, which satisfies (2) and preserves, in every interval, positivity in the sense of Criterion 1, monotonicity in the sense of Criterion 2 or 4 and convexity in the sense of Criterion 3.

## 4. $C^1$ Hermite splines of variable degree

The shape preservation properties of the curves in the family $\Gamma$ introduced in [42] propel us to attempt solving Problem 1 with $C^1$ Hermite splines of variable degree, using the polynomial degree as the local tension parameter of the curve. If we represent the $C^1$ Hermite spline of variable degree as a composite Bézier curve, then each segment is given by:

$$c_i(t) = \sum_{j=0}^{k_i} b_{ij} B_j^{k_i}(t),\ t = \frac{x - x_i}{x_{i+1} - x_i},\ x \in [x_i, x_{i+1}],\ i = 0, 1, \ldots, N-1 \tag{12}$$

where the Bernstein basis functions are given by $B_j^{k_i}(t) = \frac{k_i!}{j!(k_i-j)!}(1-t)^{k_i-j}t^j$, with $k_i \geq 3$ denoting the polynomial degree of the segment $c_i$. If, apart from the end point values, $f_i$ and $f_{i+1}$, the first derivatives, $v_i$ and $v_{i+1}$, at the end points of the $i$th segment are given, then the following Bézier control points can be determined:

$$b_{i,0} = f_i, \quad b_{i,1} = f_i + v_i \frac{h_i}{k_i}, \quad b_{i,k_i-1} = f_{i+1} - v_{i+1}\frac{h_i}{k_i}, \quad b_{i,k_i} = f_{i+1} \tag{13}$$

Then, the rest of them is given by (see [50]):

$$b_{i,j} = b_{i,1}\left(1 - \frac{j-1}{k_i - 2}\right) + b_{i,k_i-1}\frac{j-1}{k_i-2}, \quad j = 2, \ldots, k_i - 2 \tag{14}$$

The derivative of $c_i(t)$ with respect to $x$ can be written as:

$$c_i'(t) = \frac{k_i}{h_i}\sum_{j=0}^{k_i-1} \Delta b_{ij} B_j^{k_i-1}(t) \tag{15}$$

where the control point-differences are:

$$\begin{aligned}
\Delta b_{i,0} &= b_{i,1} - b_{i,0} = v_i \frac{h_i}{k_i} \\
\Delta b_{i,j} &= b_{i,j+1} - b_{i,j} = b_{i,1}(1 - s_{j+1}) + b_{i,k_i-1}s_{j+1} - b_{i,1}(1-s_j) - b_{i,k_i-1}s_j \\
&= \left(b_{i,k_i-1} - b_{i,1}\right)(s_{j+1} - s_j) = \frac{b_{i,k_i-1} - b_{i,1}}{k_i - 2} \\
&= \frac{(f_{i+1} - f_i) - (v_i + v_{i+1})\frac{h_i}{k_i}}{k_i - 2} \\
&= \frac{h_i}{k_i}\left(\frac{k_i s_i - (v_i + v_{i+1})}{k_i - 2}\right), \quad j = 1, \ldots, k_i - 2 \\
\Delta b_{i,k_i-1} &= b_{i,k_i} - b_{i,k_i-1} = v_{i+1}\frac{h_i}{k_i}
\end{aligned} \tag{16}$$

Based on the above, the derivative can alternatively be written as:

$$c_i'(t) = v_i(1-t)^{k_i-1} + v_{i+1}t^{k_i-1} + \left(\frac{s_i k_i - (v_i + v_{i+1})}{k_i - 2}\right)\sum_{j=1}^{k_i-2} B_j^{k_i-1}(t) \tag{17}$$

The second order derivative of the curve (12) is given by:

$$c_i''(t) = \frac{k_i(k_i-1)}{h_i^2}\sum_{j=0}^{k_i-2} \Delta^2 b_{ij} B_j^{k_i-2}(t) \tag{18}$$

where

$$\begin{aligned}\Delta^2 b_{i,0} &= \Delta b_{i,1} - \Delta b_{i,0} = \frac{h_i}{k_i}\left[\frac{k_i}{k_i-2}s_i - \frac{v_i+v_{i+1}}{k_i-2} - v_i\right] \\ &= \frac{h_i}{k_i}\left[\frac{k_i(s_i-v_i)-(v_{i+1}-v_i)}{k_i-2}\right] \\ \Delta^2 b_{i,j} &= 0, \quad j = 1,\ldots,k_i-3 \\ \Delta^2 b_{i,k_i-2} &= \Delta b_{i,k_i-1} - \Delta b_{i,k_i-2} = \frac{h_i}{k_i}\left[v_{i+1} - \frac{k_i}{k_i-2}s_i + \frac{v_i+v_{i+1}}{k_i-2}\right] \\ &= \frac{h_i}{k_i}\left[\frac{k_i(v_{i+1}-s_i)-(v_{i+1}-v_i)}{k_i-2}\right]\end{aligned} \tag{19}$$

Thus, (18) becomes:

$$c_i''(t) = \frac{k_i-1}{h_i}\left[\frac{k_i(s_i-v_i)-(v_{i+1}-v_i)}{k_i-2}(1-t)^{k_i-2} + \frac{k_i(v_{i+1}-s_i)-(v_{i+1}-v_i)}{k_i-2}t^{k_i-2}\right] \tag{20}$$

### 4.1. The behavior of the curve for large segment degrees

Investigating the behavior of the spline when the tension parameter increases leads to some interesting results, which predispose us to use these basis functions, as an adequate choice for shape preserving interpolation. To investigate how the tension parameter changes the shape of the interpolating function, let us introduce the operator:

$$D\left(c_i^{(m)}(x), L_i^{(m)}(x)\right) := \max_{x\in[x_i,x_{i+1}]}\left|c_i^{(m)}(x) - L_i^{(m)}(x)\right|$$

where $L_i(x)$ represents the line segment connecting $(x_i, f_i)$ and $(x_{i+1}, f_{i+1})$ :

$$L_i(x) = f_i + (x-x_i)s_i, \quad x \in [x_i, x_{i+1}]$$

If we elevate the degree of $L_i(x)$ to $k_i$, then $D^{(m)}\left(c_i^{(m)}(x), L_i^{(m)}(x)\right)$ is bounded above by the maximum of the absolute values of the corresponding control points:

$$D\left(c_i^{(m)}(x), L_i^{(m)}(x)\right) = \max_{x\in[x_i,x_{i+1}]}\left|\sum_{j=0}^{k_i-m}(\Delta^m b_{ij} - \Delta^m L_{ij})B_j^{k_i-m}(t)\right| \tag{21}$$

$$\leq \max_{x\in[x_i,x_{i+1}]}\sum_{j=0}^{k_i}\left|\Delta^m b_{ij} - \Delta^m L_{ij}\right| B_j^{k_i-m}(t) \tag{22}$$

$$\leq \max_{j=0,\ldots,k_i-m}\{\left|\Delta^m b_{ij} - \Delta^m L_{ij}\right|\} \tag{23}$$

where $L_{ij} = L_i(x_i + jh_i/k_i)$. We are interested in calculating the above distances for $m = 0, 1, 2$. Beginning with $m = 0$, and noting that the shape of the curve segment (12) is fully determined by the four control points given in (13), the above distances are bounded above by:

$$\left|b_{i,1} - L_i\left(x_i + \frac{h_i}{k_i}\right)\right| = \frac{h_i}{k_i}|v_i - s_i|$$

and/or

$$\left|b_{i,k_i-1} - L_i\left(x_{i+1} - \frac{h_i}{k_i}\right)\right| = \frac{h_i}{k_i}|s_i - v_{i+1}|$$

i.e.

$$D(c_i(x), L_i(x)) \leq \frac{h_i}{k_i}\max\{|v_i - s_i|, |s_i - v_{i+1}|\} = O(k_i^{-1})$$

which implies that the distance from the curve to the line segment $L_i(x)$ is proportional to the inverse of the degree of the polynomial segment. Obviously, for any $\epsilon > 0$ there exists a degree $k_i$ such that the above distance is less than $\epsilon$. Thus, using Landau notation, we may write $D(c_i(x), L_i(x)) = O(k_i^{-1})$, to imply that the Hermite spline segment $c_i(x)$ tends to the linear interpolant of the data points, as the degree $k_i$ increases. However, in order to comprehend the way that this convergence takes place (if it is oscillatory or not) we need to further investigate the behavior of the derivatives of $c_i(x)$ for large segment degrees.

Starting from the expression (17) of the derivative of $c_i(x)$, and exploiting the partition of unity of the Bernstein basis functions, we may substitute $\sum_{j=1}^{k_i-2} B_j^{k_i-1}(t)$ with $1-(1-t)^{k_i-1}-t^{k_i-1}$ and readily obtain:

$$\begin{aligned} c_i'(t) &= v_i(1-t)^{k_i-1} + v_{i+1}t^{k_i-1} + \left(\frac{s_i k_i - (v_i+v_{i+1})}{k_i-2}\right)\left(1-(1-t)^{k_i-1}-t^{k_i-1}\right) \\ &= (v_i - W)(1-t)^{k_i-1} + (v_{i+1}-W)t^{k_i-1} + W \end{aligned}$$

where

$$W = \left(\frac{s_i k_i - (v_i+v_{i+1})}{k_i-2}\right)$$

from which we easily deduce $W \longrightarrow s_i$ as $k_i \longrightarrow \infty$ and moreover that $W - s_i = O(K_i^{-1})$. Now, since $v_i(1-t)^{k_i-1}$ and $v_{i+1}t^{k_i-1}$ tend exponentially to 0, in any closed subinterval of $[0,1]$, while they are equal to $v_i$ for $t=0$ and to $v_{i+1}$ for $t=1$, we may state that: $c_i'(t) \longrightarrow s_i$ as $k_i \longrightarrow \infty$, in any closed subinterval of $[0,1]$, and moreover: $c_i(t) - s_i = O(k_i^{-1})$ or in the notation introduced above:

$$D(c_i'(x), L_i'(x)) = O(k_i^{-1})$$

As for the second order derivative of $c_i(x)$ from (18) we see that inside any closed subinterval of $[x_i, x_{i+1}]$ tends exponentially to zero, while at the ends with the aid of (19) we see that $\Delta b_{i,0} = O(k_i^{-1})$ and $\Delta b_{i,k_i-2} = O(k_i^{-1})$, so we may state $c_i''(t) \longrightarrow 0$ as $k_i \longrightarrow \infty$, in any closed subinterval of $[0,1]$, i.e. $c_i''(t) = O(k_i^{-1})$ or in the notation we use here:

$$D(c_i''(x), L_i''(x)) = O(k_i^{-1})$$

## 5. Satisfaction of the sign Criterion 1

A sufficient condition can be obtained directly from the convex hull property of the curve $c_i(x)$:

$$f_I b_{i,1} > 0 \quad \text{and} \quad f_I b_{i,k_i-1} > 0, \quad \text{where } I = i, i+1.$$

From the expressions in (13) we obtain the following two inequalities:

$$k_i = \max\left\{3, -\frac{v_i h_i}{f_i}, \frac{v_{i+1}h_i}{f_{i+1}}\right\} \tag{24}$$

(Note that by definition of the criterion, $f_i, f_{i+1} \neq 0$). Now we can state the following:

**Theorem 1.** *The $C^1$ Hermite spline defined by (12)–(14), which interpolates the ordered set of points (1) and the nodal derivative values, satisfies the sign criterion in any interval $[x_i, x_{i+1}]$ as long as the degrees $k_i$ satisfy (24).*

Note that the degree which satisfies the above inequality is always bounded above by $\max\left\{3, \frac{|v_i|h_i}{\epsilon_f}, \frac{|v_{i+1}|h_i}{\epsilon_f}\right\}$.

## 6. Satisfaction of the strict monotonicity Criterion 2

If $|s_i| < \epsilon_\theta$ then selecting $k_i = 3$ and $v_i = v_{i+1} = 0$, the relations (13) and (14) show that all the Bézier points lie on the same line, i.e. by construction the curve defined by (12)–(14) satisfies the Part A of the criterion.

If $|s_i| > \epsilon_\theta$, then the relation (15) multiplied by $s_i$ gives:

$$s_i c_i'(t) = s_i \frac{k_i}{h_i} \sum_{j=0}^{k_i-1} \Delta b_{ij} B_j^{k_i-1}(t)$$

Obviously, if all products $s_i \Delta b_{ij},\ j = 0, \ldots, k_i - 1$, are nonnegative, then the function (12) is monotone. At both ends we have:

$$s_i \Delta b_{i0} = \frac{h_i}{k_i} s_i v_i \geq 0 \text{ and } s_i \Delta b_{i,k_i-1} = \frac{k_i}{h_i} s_i v_{i+1} \geq 0$$

Since the products $s_i \Delta b_{ij},\ j = 1, \ldots, k_i - 2$ are independent of $j$ (see rel. (14)) they are positive if:

$$s_i \Delta b_{ij} = s_i \frac{k_i s_i - (v_i + v_{i+1})}{k_i - 2} = \frac{1}{k_i - 2}\left(k_i s_i^2 - s_i(v_i + v_{i+1})\right) \geq 0$$

from which, taking into account that $k_i \geq 3$, we arrive at the following sufficient condition:

$$k_i \geq \max\left\{3, \frac{v_i + v_{i+1}}{s_i}\right\} \tag{25}$$

which ensures monotonicity of the curve in $[x_i, x_{i+1}]$. This completes the proof of the following:

**Theorem 2.** *The $C^1$ Hermite spline defined by (12)–(14), which interpolates the ordered set of points (1) and the nodal derivative values which conform with Lemma 2, satisfies the strict monotonicity Criterion 2 in any interval $[x_i, x_{i+1}]$ as long as the degrees $k_i$ satisfy (25).*

Note that the degree which satisfies the above inequality is always bounded above by $\max\left\{3, \frac{|v_i+v_{i+1}|}{\epsilon_\theta}\right\}$.

## 7. Satisfaction of the weak monotonicity Criterion 4

Criterion 4.A is identical with Criterion 2.A, thus we proceed on with the cases B.I–B.IV.

**Case B.I:** The criterion is the same with the strict version of it, which was proved to be fulfilled if the sufficient condition given by the inequality (25) is satisfied.

**Case B.II:** Since $s_i v_i < 0$ and $s_i v_{i+1} > 0$, if we assume that $k_i$ satisfies (25) then the control polygon of $s_i c_i'(t)$ will have only one intersection with the $x$-axis, which implies that $s_i c_i'(t)$ has one root in $[x_i, x_{i+1}]$. In view of this remark, a sufficient condition for Criterion 4 to be satisfied is the following:

$$s_i c_i'(\lambda) \geq 0 \tag{26}$$

It remains to establish that (26) will eventually be satisfied for a sufficiently large $k_i$. Substituting (17) into (26) for $t = \lambda$ we obtain:

$$s_i c_i'(\lambda) = s_i v_i (1-\lambda)^{k_i-1} + s_i v_{i+1} \lambda^{k_i-1} + \sigma(k_i) r(\lambda) \tag{27}$$

where

$$\sigma(k_i) = \frac{k_i}{k_i - 2}\left(s_i^2 - s_i \frac{v_i + v_{i+1}}{k_i}\right) \geq 0 \tag{28}$$

and

$$r(\lambda) = \sum_{j=1}^{k_i-2} B_j^{k_i-1}(\lambda) = 1 - (1-\lambda)^{k_i-1} - \lambda^{k_i-1} \tag{29}$$

Then, using (27), (26) is written as follows:

$$s_i c_i'(\lambda) = (s_i v_i - \sigma(k_i))(1-\lambda)^{k_i-1} + (s_i v_{i+1} - \sigma(k_i))\lambda^{k_i-1} + \sigma(k_i) \geq 0 \tag{30}$$

Now, since in Case B.II, $(s_i v_i - \sigma(k_i)) < (s_i v_{i+1} - \sigma(k_i))$, if the inequality:

$$(s_i v_i - \sigma(k_i))\left((1-\lambda)^{k_i-1} + \lambda^{k_i-1}\right) + \sigma(k_i) > 0 \tag{31}$$

is satisfied, then (30) and thus (26) hold true. Moreover, since $(s_i v_i - \sigma(k_i)) < 0$ if we divide the above inequality by this quantity, then we strengthen (26) even more:

$$(1-\lambda)^{k_i-1} + \lambda^{k_i-1} < \frac{\sigma(k_i)}{(\sigma(k_i) - s_i v_i)} \tag{32}$$

Finally, since $0 < \lambda < \frac{1}{4}$, $1 - \lambda > \lambda$, the next inequality is an even stronger version of the previous ones:

$$(1-\lambda)^{k_i-1} < \frac{\sigma(k_i)}{2(\sigma(k_i) - s_i v_i)} \tag{33}$$

Since, $\sigma(k_i)$ tends to $s_i^2$ and $2(1-\lambda)^{k_i-1}$ tends to zero as $k_i$ increases, the above inequality proves that the condition (26) will eventually be satisfied. Now, the question is if we can deduce an explicit solution for the above inequality. We will prove the following:

$$s_i c_i'(\lambda) > 0, \quad \text{for} \quad \lambda = \frac{1}{k_i} \tag{34}$$

by proving the validity of (33) for $\lambda = k_i^{-1}$, i.e.

$$(1 - k_i^{-1})^{k_i-1} < \frac{\sigma(k_i)}{2(\sigma(k_i) - s_i v_i)} \tag{35}$$

The right hand side is bounded above $\frac{1}{2}$, provided that (25) holds. Then, it is straightforward to confirm that the above inequality holds for $k_i = 3$. For $k_i > 3$, we need to elaborate a little more on (35), which can equivalently be written as:

$$(k_i - 1)\ln(1 - k_i^{-1}) < \ln\left(\frac{\sigma(k_i)}{2(\sigma(k_i) - s_i v_i)}\right) \tag{36}$$

Then, applying the basic inequality of the logarithmic function, $\ln(1+x) \leq x,\ x > -1$, to the right hand side of (36) we further strengthen it to:

$$-\frac{k_i-1}{k_i} = -1+\frac{1}{k_i} < \ln\left(\frac{\sigma(k_i)}{2(\sigma(k_i)-s_i v_i)}\right) \tag{37}$$

This can equivalently be written as:

$$e^{-1+\frac{1}{k_i}} < \frac{\sigma(k_i)}{2(\sigma(k_i)-s_i v_i)} \tag{38}$$

Then, since the right hand side of (38) is bounded above by $\frac{1}{2}$, provided that (25) holds, we may write:

$$\frac{\sqrt[k_i]{e}}{e} < \frac{1}{2} \tag{39}$$

which holds for $k_i > 3$, thus proving the validity of (33). Taking into account that the inequality (33) holds for $k_i = 3$, it holds for $k_i \geq 3$. Now we can state that, given any $0 < \lambda < \frac{1}{2}$, if the degree $k_i$ is greater or equal to $\lambda^{-1}$, the condition (26) of the Criterion 4 Case B.II holds, i.e.

$$k_i \geq \max\left\{3, \frac{v_i+v_{i+1}}{s_i}, \lambda^{-1}\right\} \tag{40}$$

**Case B.III and Case B.IV:** These cases are treated exactly the same way as the Case B.II. Thus, we can state the following:

**Theorem 3.** *The $C^1$ Hermite spline defined by (12)–(14), which interpolates the ordered set of points (1) and the associated nodal derivatives, which conform with (8), satisfies the weak monotonicity criterion if the degrees satisfy (40).*

Note that the degree which satisfies the above inequality is always bounded above by $\max\left\{3, \frac{|v_i+v_{i+1}|}{\epsilon_\theta}, \lambda^{-1}\right\}$.

## 8. Satisfaction of the convexity Criterion 3

Part A of Criterion 3 creates the linear segment connecting $(x_i, f_i)$ and $(x_{i+1}, f_{i+1})$, thus (12) is able to represent it by setting $k_i = 3$ and $v_i = v_{i+1} = s_i$.

Regarding Parts B and C of the criterion, we notice at once in (20) that the function has constant sign in $[0, 1]$ if and only if the coefficients of $t^{k_i-2}$ and $(1-t)^{k_i-2}$ have the same sign, otherwise the sign changes only once in $[0, 1]$ (due to the structure of the Bézier control polygon and the variation diminishing property). Clearly, if $\delta_i\delta_{i+1} > 0$, then $\delta_I c_i''(t)$ has constant sign for $t \in [0, 1]$ if and only if:

$$[k_i(s_i - v_i) - (v_{i+1} - v_i)]\,\delta_I \geq 0, \text{ for } I = i, i+1$$

and

$$[k_i(v_{i+1} - s_i) - (v_{i+1} - v_i)]\,\delta_I \geq 0, \text{ for } I = i, i+1$$

which, along with $k_i \geq 3$, yield the following condition:

$$k_i \geq \max\left\{\left|\frac{v_{i+1}-v_i}{s_i-v_i}\right|, \left|\frac{v_{i+1}-v_i}{v_{i+1}-s_i}\right|, 3\right\} \tag{41}$$

If $\delta_i\delta_{i+1} < 0$, then $\delta_I c_i''(t)$ changes sign only once, thus we can state the following:

**Theorem 4.** *The $C^1$ Hermite spline defined by (12)–(14), which interpolates the ordered set of points (1), and the nodal derivatives at them conform with (8), satisfies the convexity criterion in any interval $[x_i, x_{i+1}]$ as long as the degrees $k_i$ satisfy (41).*

The application of expression (41) raises a numerical issue when either $s_i - v_i$ or $v_{i+1} - s_i$ are almost zero. Let us analyze how we can avoid the possibility of falling into a division by zero case. The expression (41) can equivalently be written as:

$$k_i \geq \max\left\{\left|1+\frac{v_{i+1}-s_i}{s_i-v_i}\right|, \left|1+\frac{s_i-v_i}{v_{i+1}-s_i}\right|, 3\right\} \tag{42}$$

From (8) we may substitute

$$v_{i+1} - s_i = \alpha_{i+1}\delta_{i+1} \qquad \text{and} \qquad s_i - v_i = (1-\alpha_i)\delta_i$$

thus getting:

$$k_i \geq \max\left\{\left|1 + \frac{\alpha_{i+1}\delta_{i+1}}{(1-\alpha_i)\delta_i}\right|, \left|1 + \frac{(1-\alpha_i)\delta_i}{\alpha_{i+1}\delta_{i+1}}\right|, 3\right\}$$

Now, if $\alpha_i = 1$ the denominator of the first fraction in the above relation makes $k_i$ tend to infinity. The same happens with the second fraction if $\alpha_{i+1} = 0$. It is evident that we need to further restrict all $\alpha_i$'s in a way that the maximum degree $k_{max} = \max_i k_i$, needed in order to satisfy the convexity criterion, is bounded above by a fixed number. In other words, if we assume a fixed – relatively high – integer $K$, then:

$$\frac{\alpha_{i+1}\delta_{i+1}}{(1-\alpha_i)\delta_i} < K \qquad \text{and} \qquad \frac{(1-\alpha_i)\delta_i}{\alpha_{i+1}\delta_{i+1}} < K$$

or

$$\frac{\alpha_{i+1}\delta_{i+1}}{K\delta_i} < (1-\alpha_i) \qquad \text{and} \qquad \frac{(1-\alpha_i)\delta_i}{K\delta_{i+1}} < \alpha_{i+1}$$

Since $\alpha_{i+1} < 1$, and $(1-\alpha_i) < 1$, we strengthen the above inequalities by setting:

$$\frac{\delta_{i+1}}{K\delta_i} \leq \frac{\alpha_{i+1}\delta_{i+1}}{K\delta_i} < (1-\alpha_i) \qquad \text{and} \qquad \frac{\delta_i}{K\delta_{i+1}} \leq \frac{(1-\alpha_i)\delta_i}{K\delta_{i+1}} < \alpha_{i+1}$$

from which we obtain the following:

$$\alpha_i \leq 1 - \frac{\delta_{i+1}}{K\delta_i} \qquad \text{and} \qquad \frac{\delta_i}{K\delta_{i+1}} \leq \alpha_{i+1}$$

If we change the index $i$ in the second inequality to $i-1$ we finally arrive at the following restriction for $\alpha_i$:

$$\frac{\delta_{i-1}}{K\delta_i} \leq \alpha_i \leq 1 - \frac{\delta_{i+1}}{K\delta_i}$$

The above can always be satisfied, i.e. we can always find a large but bounded integer $K$, by fixing a small positive number $\zeta$, such that:

$$\alpha_i \in [\zeta, 1-\zeta], \qquad 0 < \zeta < \frac{1}{2} \tag{43}$$

Then,

$$K = \frac{1}{\zeta}\max_i\left\{\max\left[\frac{\delta_{i-1}}{\delta_i}, \frac{\delta_{i+1}}{\delta_i}\right]\right\} \quad \text{provided that :} \quad \delta_i\delta_{i+1} > 0 \text{ and } \delta_i\delta_{i-1} > 0$$

The constant $\zeta$ will be particularly useful if the method for estimating the derivatives $v_i$ (and consequently the constants $\alpha_i$) returns $\alpha_i \leq \zeta$ or $\alpha_i \geq 1-\zeta$. Then, the value of $\alpha_i$ should be corrected accordingly, by setting it explicitly equal to $\zeta$ or $1-\zeta$, respectively. For each particular example, the value of $\zeta$ gives the possible highest degree $K$, which may be needed in order to satisfy the convexity criterion and which is always finite.

## 9. Estimation of the nodal derivatives

As we have already seen, the constant value Criterion 2.A (or 4.A) along with the collinearity Criterion 3.A, impose derivative values at the following points:

- If $|s_i| < \epsilon_\theta$ holds in $[x_i, x_{i+1}]$ then $v_i = 0$ and $v_{i+1} = 0$.
- If $|\delta_i| < \epsilon_\delta$ holds at $x_i$, then $v_{i-1} = v_i = v_{i+1} = \frac{f_{i+1}-f_{i-1}}{x_{i+1}-x_{i-1}}$.

Now, let us assume that the derivatives $v_m$ and $v_{m+\ell}$ have already been calculated as above or they are given, while the estimation of the derivatives at the points with indices $i = m+1, \ldots, m+\ell-1$ remains to be done. At these points, the derivative can be estimated by adopting any rule, which satisfies (8). In the works of Hyman [3] and Aràndiga [51] one can fine very thorough analyses of such estimations. We may distinguish the methods into two main categories; the local and the global. In this work we have tested the following local methods, and we developed a new global method, with which we deal in the following sub-sections.

### 9.1. Local methods for derivative estimation

We have taken from the literature a number of local methods, which are the following:

- *The parabolic estimation*, according to which the derivative at $x_i$ is equal to the derivative of the parabola interpolating three points at $x_{i-1}, x_i, x_{i+1}$:
$$v_i = \frac{h_i}{h_{i-1}+h_i}s_{i-1} + \frac{h_{i-1}}{h_{i-1}+h_i}s_i, \quad i = m+1, \ldots, m+\ell-1 \tag{44}$$
- *The finite difference estimation*, according to which the derivative at $x_i$ is equal to the slope of the two points adjacent to $(x_i, f_i)$, i.e.:
$$\begin{aligned} v_i &= \frac{f_{i+1}-f_{i-1}}{h_{i-1}+h_i} = \frac{(f_{i+1}-f_i)+(f_i-f_{i-1})}{h_{i-1}+h_i} \\ &= \frac{h_i}{h_{i-1}+h_i}s_i + \frac{h_{i-1}}{h_{i-1}+h_i}s_{i-1}, \quad i = m+1, \ldots, m+\ell-1 \end{aligned} \tag{45}$$
- *Fritsch–Butland [16] method*, according to which, when $s_{i-1}s_i > 0$, the derivative at $x_i$ is given by:
$$v_i = \begin{cases} \dfrac{3s_{i-1}s_i}{s_{i-1+2}s_i} & \text{if} \quad |s_i| \le |s_{i-1}| \\ \dfrac{3s_{i-1}s_i}{2s_{i-1}+s_i} & \text{if} \quad |s_i| > |s_{i-1}| \end{cases}, \quad i = m+1, \ldots, m+\ell-1 \tag{46}$$
otherwise $v_i = 0$.
- *Brodlie [52] method*, according to which, when $s_{i-1}s_i > 0$, the derivative at $x_i$ is given by:
$$v_i = \frac{3(h_{i-1}+h_i)s_{i-1}s_i}{(h_{i-1}+2h_i)s_i + (2h_{i-1}+h_i)s_{i-1}}, \quad i = m+1, \ldots, m+\ell-1 \tag{47}$$
otherwise $v_i = 0$.
- *Aràndiga weighted harmonic [51] method*, according to which, when $s_{i-1}s_i > 0$, the derivative at $x_i$ is given by:
$$v_i = \frac{(h_{i-1}+h_i)s_{i-1}s_i}{h_i s_i + h_{i-1}s_{i-1}}, \quad i = m+1, \ldots, m+\ell-1 \tag{48}$$
otherwise $v_i = 0$.
- *Aràndiga alternative [51] method*, according to which, when $s_{i-1}s_i > 0$, the derivative at $x_i$ is given by:
$$v_i = \frac{h_i s_{i-1} + h_{i-1}s_i}{h_{i-1}+h_i}\frac{4s_{i-1}s_i}{(s_i+s_{i-1})^2}, \quad i = m+1, \ldots, m+\ell-1 \tag{49}$$
otherwise $v_i = 0$.

For the first two methods it is evident that (8) always holds. For the next three methods, it is not hard to prove that (8) is always fulfilled. For the last method one needs to further restrict the result in a way that $\alpha_i = (v_i - s_{i-1})/\delta_i$ is actually in $[0, 1]$.

### 9.2. Derivatives estimation for minimum degree distribution

The question that arises at this point is if we can estimate the derivatives at $i = m+1, \ldots, m+\ell-1$ in a way to reduce the degrees of the corresponding intervals. This sub-section focuses on this problem and we give an optimal solution to it. As we saw, the convexity criterion condition (41), which can easily be written as in (42). The latter can also be written in the form:
$$k_i \ge \max\left\{3, |\xi_i+1|, \left|\frac{1}{\xi_i}+1\right|\right\}, \quad \text{where} \quad \xi_i = \frac{v_{i+1}-s_i}{s_i-v_i}, \ i = 0, \ldots, N-1 \tag{50}$$
We aim to minimize the sum of the squares of the factors $|\xi_i+1|$ and $\left|\frac{1}{\xi_i}+1\right|$, i.e.:
$$\min_{\xi_i} \sum_{i=1}^{N-1} \left( |\xi_i+1|^2 + \left|\frac{1}{\xi_i}+1\right|^2 \right)$$
Elementary analysis shows that for each $i$, the above function has local minimum at $\xi_i = \pm 1$. For $\xi_i = -1$, the definition of $\xi_i$ gives $v_i = v_{i+1}$, which is meaningless for our analysis. On the contrary, for $\xi_i = 1$, by the definition of $\xi_i$ we obtain:
$$v_{i+1} - s_i = s_i - v_i \Longrightarrow v_i + v_{i+1} = 2s_i, \quad i = 0, \ldots, N-1 \tag{51}$$

which minimizes also the monotonicity criterion constraint (25), since $\frac{v_i+v_{i+1}}{s_i}$ becomes equal to 2. Since $v_0$ and $v_N$ are given, we may write Equations (51) in matrix form as:

$$\mathbb{A}V = b, \text{ with } \mathbb{A} = \begin{bmatrix} 1 & 0 & \dots & 0 \\ 1 & 1 & \dots & 0 \\ 0 & 1 & \dots & 0 \\ \vdots & \vdots & \ddots & \vdots \\ 0 & 0 & \dots & 1 \end{bmatrix}, \; V = \begin{bmatrix} v_1 \\ v_2 \\ v_3 \\ \vdots \\ v_{N-1} \end{bmatrix}, b = \begin{bmatrix} 2s_0 - v_0 \\ 2s_1 \\ 2s_2 \\ \vdots \\ 2s_{N-1} - v_N \end{bmatrix}$$

The number of equations is $N$ while the number of unknowns is $N-1$. The system may approximately be solved by minimizing the error $\|\mathbb{A}V - b\|$, i.e. solving the minimization problem:

$$\min \|\mathbb{A}V - b\|^2, \; v_i(\alpha_i) \in R^{N-1}, \text{ subject to } 0 \le \alpha_i \le 1, \; i = 1, \dots, N-1 \tag{52}$$

The partial derivatives of the objective function, $\|\mathbb{A}V - b\|^2$, are zero when:

$$\mathbb{A}^T\mathbb{A}V = \mathbb{A}^T b \tag{53}$$

The matrix $\mathbb{A}^T\mathbb{A}$ is $(N-1)\times(N-1)$ tridiagonal, symmetric and positive definite and the system:

$$\begin{bmatrix} 2 & 1 & 0 & \dots & 0 \\ 1 & 2 & 1 & \dots & 0 \\ 0 & 1 & 2 & \dots & 0 \\ \vdots & \vdots & \vdots & \ddots & \vdots \\ 0 & 0 & 0 & \dots & 2 \end{bmatrix} \begin{bmatrix} v_1 \\ v_2 \\ v_3 \\ \vdots \\ v_{N-1} \end{bmatrix} = \begin{bmatrix} 2s_0 + 2s_1 - v_0 \\ 2s_1 + 2s_2 \\ 2s_2 + 2s_3 \\ \vdots \\ 2s_{N-2} + 2s_{N-1} - v_N \end{bmatrix} \tag{54}$$

has a unique solution. The objective function (52) is quadratic, thus convex. On the other hand, the solution for each $v_i$ is acceptable as long as it can be written in the form (8) i.e. the corresponding $\alpha_i$'s are inside [0, 1]. This implies that the feasible space is a hypercube in $R^{N-1}$, thus also convex, so the constraint minimization problem (52) has a unique solution. The solution can be obtained by, first, solving (53) then calculating $\alpha_i$, for $i = 1, \dots, N-1$, in accordance with (8). If any $\alpha_i$ is outside $[\zeta, 1-\zeta]$, we set it explicitly equal to the closest end, so as to fulfill the constraints in (52) and we re-calculate $v_i$ from (8). The above linear system can be solved by a Cholesky factorization of $\mathbb{A}^T\mathbb{A}$, which is of linear complexity with respect to $N$, for a tridiagonal matrix.

*9.2.1. Rates of convergence*

We assume uniform distribution of the interpolation nodes on $x$-axis, i.e., $h_i = h = (x_N - x_0)/N, \; i = 0, \dots, N-1$, and we consider the error bounds of the methods presented in the previous sub-sections. The local (linear and non-linear) derivative estimations have rates of convergence given by the following proposition (see [51]):

**Proposition 1.** *The following asymptotic estimates hold:*

- *Parabolic estimation:*

$$v_i - f_i' = O(h^2) \quad \text{and} \quad v_{i+1} - f_{i+1}' = O(h^2) \tag{55}$$

- *Finite difference estimation:*

$$v_i - f_i' = O(h^2) \quad \text{and} \quad v_{i+1} - f_{i+1}' = O(h^2) \tag{56}$$

- *Fritsch–Butland method:*

$$v_i - f_i' = O(h) \quad \text{and} \quad v_{i+1} - f_{i+1}' = O(h) \tag{57}$$

- *Brodlie's method:*

$$v_i - f_i' = O(h^2) \quad \text{and} \quad v_{i+1} - f_{i+1}' = O(h^2) \tag{58}$$

- *Aràndiga's weighted harmonic method:*

$$v_i - f_i' = O(h^2) \quad \text{and} \quad v_{i+1} - f_{i+1}' = O(h^2) \tag{59}$$

- *Aràndiga's alternative method:*

$$v_i - f_i' = O(h^2) \quad \text{and} \quad v_{i+1} - f_{i+1}' = O(h^2) \tag{60}$$

As for the optimal method for minimum degree distribution, we may assert the following:

**Lemma 3.** *If we estimate the derivatives by solving (53), then we obtain the following asymptotic estimates:*

$$v_i - f_i' = O(h) \qquad \text{and} \qquad v_{i+1} - f_{i+1}' = O(h) \tag{61}$$

*Proof.* We start from (53) and we re-write the $i$th equation of it:

$$v_{i-1} + 2v_i + v_{i+1} = 2(s_i + s_{i+1}) = 4\psi_i, \quad \text{where } \psi_i = \frac{f_{i+1} - f_{i-1}}{2h} \tag{62}$$

The above equation can be written, now, as:

$$(v_{i-1} - \psi_i) + 2(v_i - \psi_i) + (v_{i+1} - \psi_i) = 0 \tag{63}$$

In order to investigate the behavior of the factors of the above equation, we begin with the Taylor expansion of $f$ around $x_i$:

$$f(x) = f_i + (x - x_i)f_i' + (x - x_i)^2\frac{f_i''}{2!} + (x - x_i)^3\frac{f_i'''}{3!} + (x - x_i)^4\frac{f_i^{(4)}}{4!} + O((x - x_i)^5) \tag{64}$$

Setting $x = x_{i-1}$ and $x = x_{i+1}$ we get:

$$f_{i-1} = f_i - hf_i' + h^2\frac{f_i''}{2!} - h^3\frac{f_i'''}{3!} + h^4\frac{f_i^{(4)}}{4!} + O(h^5) \tag{65}$$

$$f_{i+1} = f_i + hf_i' + h^2\frac{f_i''}{2!} + h^3\frac{f_i'''}{3!} + h^4\frac{f_i^{(4)}}{4!} + O(h^5) \tag{66}$$

From (66) we readily obtain the following asymptotic estimate:

$$s_i - f_i' = O(h) \tag{67}$$

and if we subtract (66) from (65) we get:

$$f_i' - \psi_i = O(h^2)$$

Now, based on the definition of $\psi_i$ we may calculate:

$$(f_{i+1}' - \psi_i) + (f_{i-1}' - \psi_i) = (f_{i+1}' - s_{i+1}) + (f_{i-1}' - s_{i-1}) \tag{68}$$

which in view of (67) gives the following result:

$$(f_{i+1}' - \psi_i) + (f_{i-1}' - \psi_i) = O(h) \tag{69}$$

Clearly the addition of the left hand sides of (68) and (69) gives:

$$(f_{i+1}' - \psi_i) + 2(f_i' - \psi_i) + (f_{i-1}' - \psi_i) = O(h) \tag{70}$$

or

$$(f_{i+1}' - v_{i+1} + v_{i+1} - \psi_i) + 2(f_i' - v_i + v_i - \psi_i) + (f_{i-1}' - v_{i-1} + v_{i-1} - \psi_i) = O(h) \tag{71}$$

which in view of (63) can equivalently be written as:

$$(f_{i+1}' - v_{i+1}) + 2(f_i' - v_i) + (f_{i-1}' - v_{i-1}) = O(h) \tag{72}$$

which proves the validity of (61). □

## 10. The algorithm

Based on Lemma 2 and Theorems 1–4, we can present here an algorithm solving Problem 1, i.e., computing the degree distribution for a $C^1$ Hermite spline, $c(x)$, which satisfies Sign Criterion 1, Strict Monotonicity Criterion 2 or Weak Monotonicity Criterion 4 and Convexity Criterion 3. The algorithm is of linear complexity with respect to the number of points to be interpolated. We have grouped the steps of the algorithm and we present each one of them analytically in the following sub-sections.

### 10.1. Preparatory steps

Step 0. Read the list of data points $\mathcal{P} = \{(x_i, f_i),\ i = 0, \ldots, N\}$ and the first order derivatives at the end points $v_0$, $v_N$.
Step 1. Fix the tolerances $\epsilon_f, \epsilon_\theta, \epsilon_\delta, \zeta \ll 1$ and the constant $0 < \lambda < 0.5$.
Step 2. Define the list of $(N+1)$ real numbers $\mathcal{V}$, which contains the derivatives at the given points and initialize the elements of it as:

$$\mathcal{V} = \{v_0, v_1 = v_2 = \cdots v_{N-1} = 0.0, v_N\}$$

Step 3. Calculate:

- the monotonicity indicators, $s_i,\ i = 0, \ldots, N-1$, using (4), and
- the convexity indicators, $\delta_i,\ i = 0, \ldots, N$, using (5) and (6)

### 10.2. Distinction between linear and curved segments

Define a list of $N$ integers, $\mathcal{L}$, with elements $\mathcal{L}_i = \begin{cases} -1, & \text{if } s_i < -\epsilon_\theta \\ 0, & \text{if the segment is linear} \\ 1, & \text{if } s_i > \epsilon_\theta \end{cases}$

The elements of $\mathcal{L}$ distinguish the segments to linear, curved downward and curved upward. Evaluate the elements of $\mathcal{L}$ in the following steps:

Step 4. Apply the constant value Criterion 2.A or 4.A:
For $i = 0, \ldots, N-1$
If $(|s_i| < \epsilon_\theta)$
$\mathcal{L}_i = 0$
Step 5. Employ Collinearity Criterion 3.A:
For $i = 1, \ldots, N-1$
If $(|d_i| < \epsilon_\delta)$
$v_{i-1} = s_i$
$\mathcal{L}_{i-1} = 0$
$v_i = s_i$
$\mathcal{L}_i = 0$
$v_{i+1} = s_i$
Step 6. Distinguish the upward and downward curved segments:
For $i = 0, \ldots, N-1$
If $(|s_i| > \epsilon_\theta)$
$\mathcal{L}_i = sign(s_i)$

### 10.3. Calculation of the nodal derivatives

In Section 9 we saw two local methods and one global method for obtaining an estimation of the nodal derivatives: (a) the use of any local rule which satisfies (8) such as (44) or (45) and (b) the optimal estimation presented in sub-section 9.2.
If the user has chosen (a), then the following step gives the remaining derivative estimations:

Step 8a. If Strict Monotonicity Criterion 2 has been employed, then:
For $i = 0, \ldots, N-1$
If $(\mathcal{L}_{i-1}\mathcal{L}_i = 1)$
Calculate $v_i$ by using one of (44)–(49)
Step 8b. If Weak Monotonicity Criterion 4 has been employed, then:
For $i = 0, \ldots, N-1$
If $(\mathcal{L}_{i-1}\mathcal{L}_i \neq 0)$
Calculate $v_i$ by using one of (44)–(49)

If the user has chosen (b), then the calculation of the nodal derivatives is done by grouping the segments, according to their $\mathcal{L}_i$ value and the type of the chosen monotonicity criterion:

Step 8c. If Strict Monotonicity Criterion 2 has been employed, then:
For $i = 1, \ldots, N-1$ Define a set of indices $\mathcal{I}$.
While $(\mathcal{L}_{i-1}\mathcal{L}_i = 1)$
Insert index $i$ into $\mathcal{I}$.
Calculate the derivative estimations at the points
with indices in $\mathcal{I}$ by solving (53).

Step 8d. If Weak Monotonicity Criterion 4 has been employed, then:
For $i = 1, \ldots, N-1$ Define a set of indices $\mathcal{I}$.
While $(\mathcal{L}_{i-1}\mathcal{L}_i \neq 0)$
Insert index $i$ into $\mathcal{I}$.
Calculate the derivative estimations at the points
with indices in $\mathcal{I}$ by solving (53).

*10.4. Degree distribution of the curved segments*

Step 9. Define the list of $N$ integers $\mathcal{K}$, which contains the polynomial degrees of the segments. We initialize it by setting $\mathcal{K}_i = 3$, for $i = 0, \ldots, N-1$.

Step 10. Compute the degree distribution, so as to fulfill the criteria:
For $i = 0, \ldots, N-1$
If $\mathcal{L}_i = \pm 1$
Set $k_{positive} = 3$, $k_{monotone} = 3$ and $k_{convex} = 3$.
If Strict Monotonicity Criterion 2 is employed: $k_{monotone}$ is the minimum value satisfying (25).
Else If Weak Monotonicity Criterion 4 is employed: $k_{monotone}$ is the minimum value satisfying (40).
If Sign Criterion 1 is employed: $k_{positive}$ is the minimum value satisfying (24).
If Convexity Criterion 3 is employed: $k_{convex}$ is the minimum value satisfying (41).
Set $\mathcal{K}_i = \max\{k_{monotone}, k_{convex}, k_{positive}\}$

*10.5. Bézier Segments Definition*

Step 11. Compute the control points of the composite Bézier curve (12) using (13) and (14).

## 11. Convergence of the spline

The objective of this section is to investigate the error bounds of the interpolating spline $c_i(x; k_i)$, and the order of approximation of it to any function of sufficiently high continuity order, $f(x)$, as the length of intervals $h_i$ tend to zero. For the sake of simplicity, we are considering the uniform distribution of the interpolation nodes on $x$-axis, i.e. $h_i = x_{i+1} - x_i = h = (x_N - x_0)/N$ for each $i = 0, \ldots, N-1$. In order to take into account that the degree(s) of the spline may vary as $h$ tends to zero, while the order of continuity remains the same and equal to 1, it is convenient to split the remainder into two differences, i.e.:

$$f(x) - c_i(x; k_i) = [f(x) - c_i(x; 3)] + [c_i(x; 3) - c_i(x; k_i)] \tag{73}$$

where $c_i(x; k_i)$ represents the variable degree spline segment, with $k_i \geq 3$, and $c_i(x; 3)$ denotes the cubic Hermite spline segment, both interpolating the values $f(x_i) = f_i$ and $f(x_{i+1}) = f_{i+1}$ and the derivative estimations $v_i$, and $v_{i+1}$ at these points. We are going to deal separately with the two terms of (73). This split can be characterized as 'natural', since the first difference expresses the Hermite spline interpolation error, and the second expresses the difference due to degree increase (equality holds for $k_i = 3$).

The error bounds for the first difference are given by the following generic result for Hermite interpolation (see [51]):

**Proposition 2.** *Let us assume $f \in C^1_{[x_0, x_N]}$ be given. If $(v_i - f_i') = O(h^{m_i})$ and $(v_{i+1} - f_{i+1}') = O(h^{m_{i+1}})$, then the cubic Hermite interpolant, $c_i(x; 3)$ satisfies*

$$c_i(x; 3) - f(x) = O(h^m), \qquad \text{where} \quad m = \min(4, m_i + 1, m_{i+1} + 1) \tag{74}$$

Based on Proposition 1 we may, now, assert the following:

**Corollary 3.** *Let $f(x)$ be a $C^1$ continuous function on $[a, b]$ and $a = x_0 < x_1 < \cdots < x_N = b$ a uniform discretization of $[a, b]$ with length $h$. Let also $c_i(x; 3)$ denote the cubic Hermite spline, which interpolates $f(x)$ at the nodes $x_i$ with derivative estimates, $v_i$. Then, the difference $[f(x) - c_i(x; 3)]$ tends to zero, as $h$ tends to zero, with the following asymptotic estimates:*

- *If the derivative estimations are given by (44), (45), (47), (48) or (49), then*

$$f(x) - c_i(x; 3) = O(h^3)$$

- *If the derivative estimations are given by (46) or by solving (53), then*

$$f(x) - c_i(x; 3) = O(h^2)$$

Next, we consider the second difference, $[c_i(x;3) - c_i(x;k_i)]$. Instead of using the Bézier representation, we employ the representation of the family $\Gamma$, found in [42], i.e.:

$$c_i(x;k_i) = f_i(1-t) + f_{i+1}t + h^2 q_i F(1-t;k_i) + h^2 q_{i+1} F(t;k_i), \qquad t = \frac{x-x_i}{h}$$

where $q_i$ is the second order derivative of the spline at $x_i$, and $F(1-t;k_i) = \frac{t^{k_i}-t}{k_i(k_i-1)}$. Setting $k_i = 3$ we have the representation of:

$$c_i(x;3) = f_i(1-t) + f_{i+1}t + h^2 q_i^c F(1-t;3) + h^2 q_{i+1}^c F(t;3), \qquad t = \frac{x-x_i}{h}$$

where $q_i^c$ is the second order derivative of the cubic Hermite spline at $x_i$. From (19) we have:

$$\begin{aligned} h^2 q_i &= \frac{k_i-1}{k_i-2} h\left(k_i(s_i - v_i) - (v_{i+1} - v_i)\right) = \frac{k_i-1}{k_i-2} h\left((k_i-1)(s_i - v_i) - (v_{i+1} - s_i)\right) \\ h^2 q_{i+1} &= \frac{k_i-1}{k_i-2} h\left(k_i(v_{i+1} - s_i) - (v_{i+1} - v_i)\right) = \frac{k_i-1}{k_i-2} h\left((k_i-1)(v_{i+1} - s_i) - (s_i - v_i)\right) \end{aligned}$$

and setting $k_i = 3$ in the above expressions, we also obtain:

$$\begin{aligned} h^2 q_i^c &= 2h\left(2(s_i - v_i) - (v_{i+1} - v_i)\right) \\ h^2 q_{i+1}^c &= 2h\left(2(v_{i+1} - s_i) - (v_{i+1} - v_i)\right) \end{aligned}$$

Straightforwardly, since $F(t;k_i)$ for $k_i \geq 3$ is bounded above by $|F\left(\sqrt[k_i-1]{1/k_i};k_i\right)|$, and the degree $k_i$, which satisfies the sign, monotonicity and convexity criteria is always finite, i.e. $O(k_i) = O(1)$, as $h$ tends to zero, the rate of convergence of $c_i(x;3) - c_i(x;k_i)$ is given by:

$$O\left(c_i(x;3) - c_i(x;k_i)\right) = \max\{h(s_i - v_i), h(v_{i+1} - s_i)\} \tag{75}$$

Based on the above expression, we state and prove the following:

**Lemma 4.** *Let $a = x_0 < x_1 < \cdots < x_N = b$ be a uniform discretization of $[a,b]$, with length $h$. Let also $c_i(x;3)$ and $c_i(x;k_i)$ represent the cubic and the $k_i$-degree Hermite polynomial spline, which interpolate a $C^1$ continuous function $f(x)$, $x \in [a,b]$, at the nodes $x_i$ and the estimations of the derivative of $f$, $v_i$ and $v_{i+1}$. Then, the following asymptotic estimate holds, as $h$ tends to zero:*

$$O\left(c_i(x;3) - c_i(x;k_i)\right) = O(h^2) \tag{76}$$

*Proof.* We consider separately each of the factors of (75). Since the restriction (8) holds,

$$v_i = s_{i-1} + \alpha_i\delta_i \Longrightarrow s_i - v_i = (1-\alpha_i)\delta_i \Longrightarrow h(s_i - v_i) = \frac{\alpha_i\delta_i}{h}h^2$$

Now, If we add (66) and (65) we readily get:

$$\frac{\delta_i}{h} - f_i'' = O(h^2) \tag{77}$$

and consequently:

$$h(v_i - s_{i-1}) = h^2 f_i'' + O(h^4) \quad \text{or} \quad h(v_i - s_{i-1}) = O(h^2) \tag{78}$$

The next estimate can be proved in the same manner:

$$h(v_{i+1} - s_i) = O(h^2) \tag{79}$$

Now, substituting (78) and (79) into (75) the estimate (76) follows readily. □

Finally, summarizing the results of Corollary 3, and Lemma 4 we arrive at the following result:

**Theorem 5.** *Let $f(x)$ be a $C^1$ continuous function on $[a,b]$ and $a = x_0 < x_1 < \cdots < x_N = b$ a uniform discretization of $[a,b]$ with length $h$. Let also $c_i(x;k_i)$ be the $k_i$-degree Hermite polynomial spline, which interpolates $f(x)$ and the derivative estimates, $v_i$, at the nodes $x_i$. Then, the difference $[f(x) - c_i(x;k_i)]$ tends to zero, as $h$ tends to zero, with the asymptotic estimate:*

$$f(x) - c_i(x;k_i) = O(h^2) \tag{80}$$

*either when the derivative estimations are given by the local estimation methods, (44)–(49) or when the derivative estimations are given by the optimal estimation method.*

## 12. Numerical results and discussion

In this section we present the results of the algorithm on an extensive set of examples and we evaluate the fairness of the resulting curves for all derivative estimation methods, presented in Section 9. Each example is followed by three tables:

- In the first table we give the data as well as the degree distributions for the algorithm [42], namely $\mathcal{K}_{[42]}$, and the present algorithm, with the derivatives provided by the parabolic estimation, $\mathcal{K}_{par}$, by the finite difference estimation, $\mathcal{K}_{fd}$, by Fritsch–Butland estimation, $\mathcal{K}_{FB}$, by Brodlie's method, $\mathcal{K}_{Br}$, by Aràndiga's weighted harmonic method, $\mathcal{K}_{Aw}$, by Aràndiga's alternative method, $\mathcal{K}_{Aa}$, and our optimal method $\mathcal{K}_{Opt}$ (see Section 9.2). The last two rows of the table contain the maximum segment degree and the sum of the segment degrees for each method.
- In the second table we give the results of three fairness measures, related to the second derivative of the interpolating curves, for each derivative estimation method. They measure how far each interpolant is from being $C^2$ continuous. They are:
  - The maximum absolute difference of the second order derivative values at the internal nodes of interpolation: $\max_{1\le i\le N-1}|c''_{i-1}(x_i) - c''_i(x_i)|$.
  - The sum of the absolute differences of the second order derivative values at the internal nodes of interpolation: $\sum_{i=1}^{N-1}|c''_{i-1}(x_i) - c''_i(x_i)|$.
  - The integral of the square of the second order derivative of the interpolant over the whole domain: $\sum_{i=0}^{N-1}\int(c''_i(x))^2dx$.
- In the third table we give the results of four fairness measures, related to the curvature of the interpolating curves, for each derivative estimation method. They measure how far each interpolant is from being $G^2$ continuous. They are:
  - The maximum absolute difference of the curvature values at the internal nodes of interpolation: $\max_{1\le i\le N-1}|\kappa_{i-1}(x_i) - \kappa_i(x_i)|$.
  - The sum of the absolute differences of the curvature values at the internal nodes of interpolation: $\sum_{i=1}^{N-1}|\kappa_{i-1}(x_i) - \kappa_i(x_i)|$.
  - The integral of the square of the curvature of the interpolants over the whole domain: $\sum_{i=0}^{N-1}\int(\kappa_i(x))^2dx$.

In the last column of each table we give the method(s) which give(s) the best results, i.e. the minimum values. Each example is followed by the graphical representation of the resulting curve with derivative estimates based on the method *Opt*, compared with one or more curves of one of the other derivative estimation methods, which in most of the cases appear to have the lowest degree distribution.

In the end of this section we have gathered the results from all the examples in Tables 1–3, thus proposing a way to evaluate "statistically" the results of all methods. Our interpretation is given in the conclusions of the paper.

The first group of examples, consists of two typical data-sets, which model pile–soil interaction; one "$p$–$y$" curve (soil resistance, $p$ as a function of the lateral deflection $y$ of the pile) and one "$t$–$z$" curve (axial response $z$ of a pile subjected to vertical load $t$). We have employed the strict monotonicity criterion, which ensures that the curve will lie in between its minimum and maximum values (see Lemma 1). The derivative at the first end has been estimated by the derivative of the parabola interpolating the first three points. The derivative at the other end is equal to zero due to the shape of these curves. The degree increase has been activated in all cases. In the figures shown in the sequel we have compared the resulting curve with the $C^2$ parametric non-uniform degree spline of [42]. Note that since all these curves become constant for $x \ge$ some specific abscissa and since the spline of [42] interprets co-linearity in a different way, we have calculated that curve up to the point where it meets the linear segment at the end. The figures clearly show that convexity preservation is not sufficient for an acceptable result.

**Example 1.** A "$p$–$y$" curve: data, degree distributions and fairness measures for various derivative estimation methods. The results are shown in Fig. 2.

| Points $(x_i, f_i)$ | $\mathcal{K}_{Opt}$ | $\mathcal{K}_{par}$ | $\mathcal{K}_{fd}$ | $\mathcal{K}_{FB}$ | $\mathcal{K}_{Br}$ | $\mathcal{K}_{Aw}$ | $\mathcal{K}_{Aa}$ | $\mathcal{K}$ [42] | |
|---|---|---|---|---|---|---|---|---|---|
| (0,0) | 3 | 3 | 4 | 4 | 4 | 4 | 4 | 3 | |
| (0.23,4.07459) | 5 | 23 | 5 | 6 | 3 | 7 | 3 | 5 | |
| (0.69,5.8459) | 3 | 7 | 3 | 3 | 3 | 4 | 7 | 5 | |
| (2.29,8.8582) | 3 | 3 | 5 | 3 | 5 | 3 | 9 | 3 | |
| (6.86,12.7566) | 3 | 3 | 3 | 3 | 3 | 3 | 3 | 3 | |
| (34.31,3.25984) | 1 | 1 | 1 | 1 | 1 | 1 | 1 | 1 | |
| (68.63,3.25984) | | | | | | | | | |
| End point derivatives: $v_0 = 22.3373$ and $v_6 = 0$. | | | | | | | | | |
| | | | | | | | | | Min |
| Max degree | 5 | 23 | 5 | 6 | 5 | 7 | 9 | | Opt,fd,Br |
| Sum of degrees | 18 | 40 | 21 | 20 | 19 | 22 | 27 | | Opt |

| 2nd Derivative | $\mathcal{K}_{Opt}$ | $\mathcal{K}_{par}$ | $\mathcal{K}_{fd}$ | $\mathcal{K}_{FB}$ | $\mathcal{K}_{Br}$ | $\mathcal{K}_{Aw}$ | $\mathcal{K}_{Aa}$ | Min |
|---|---|---|---|---|---|---|---|---|
| $\max_i \lvert c''_{i-1}(x_i) - c''_i(x_i)\rvert$ | 7.28 | 73.63 | 101.55 | 104.56 | 189.49 | 95.08 | 217.32 | Opt |
| $\sum_i \lvert c''_{i-1}(x_i) - c''_i(x_i)\rvert$ | 9.53 | 106.53 | 107.94 | 105.52 | 195.28 | 98.22 | 233.76 | Opt |
| $\sum_i \int (c''_i(x))^2 dx$ | 15.96 | 14.68 | 67.11 | 74.46 | 119.13 | 74.43 | 142.74 | par |
| Curvature | $\mathcal{K}_{Opt}$ | $\mathcal{K}_{par}$ | $\mathcal{K}_{fd}$ | $\mathcal{K}_{FB}$ | $\mathcal{K}_{Br}$ | $\mathcal{K}_{Aw}$ | $\mathcal{K}_{Aa}$ | Min |
| $\max_i \lvert \kappa_{i-1}(x_i) - \kappa_i(x_i)\rvert$ | 0.22 | 2.97 | 0.84 | 0.46 | 0.88 | 0.42 | 1.67 | Opt |
| $\sum_i \lvert \kappa_{i-1}(x_i) - \kappa_i(x_i)\rvert$ | 0.50 | 3.58 | 1.72 | 0.76 | 2.40 | 0.75 | 5.76 | Opt |
| $\sum_i \int (\kappa_i(x))^2 dx$ | 2.0e−03 | 0.03 | 1.8e−03 | 1.9e−03 | 1.8e−03 | 2.1e−03 | 1.7e−03 | Aa |

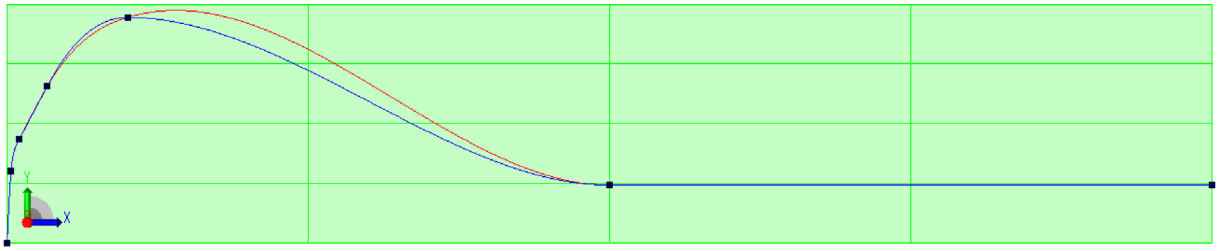


**Fig. 2.** Example 1: The $C^1$ shape preserving curve with its nodal derivatives estimated using the *Opt* method (blue) and the $C^2$ convexity preserving curve of [42] (red). (For interpretation of the references to color in this figure legend, the reader is referred to the web version of this article.)

In particular for Example 1, we give analytically the results of the algorithm, for the optimal degree distribution. We have employed the strict monotonicity criterion, thus the tolerance $\epsilon_f$ and the constant $\lambda$ play no role in this example. Apart from them, we have fixed the tolerances $\epsilon_\theta = 10^{-3}$, $\epsilon_\delta = 10^{-3}$ and the parameter $\zeta = 0$. We compute the monotonicity indicators, $s_i,\ i = 0, \ldots, 5$, using (4), and the convexity indicators, $\delta_i,\ i = 0, \ldots, 6$, using (5) and (6). Based on $s_i$'s and $d_i$'s, we computed the elements of the list $\mathcal{L} = \{1, 1, 1, 1, -1, 0\}$, corresponding to the intervals of the spline, which in turn determine the derivatives at the points with indices 4 and 5. Both are equal to zero, since the last segment is parallel to the $x$-axis and the point $(x_4, y_4)$ is a local maximum. The list $\mathcal{L}$ splits the spline into three parts; the first one between the points with indices 0 and 4, the second a single curved segment connecting the points with indices 4 and 5 and the third one a linear segment between the points 5 and 6.

The optimal degree distribution can be applied only to the first part of the curve, i.e. between the points 0 and 4, since the other parts consist of one segment with known derivatives at the end points. Following the analysis of Section 9.2, the derivative estimations were obtained by solving a $3 \times 3$ linear system of the form:

$$\begin{bmatrix} 2 & 1 & 0 \\ 1 & 2 & 1 \\ 0 & 1 & 2 \end{bmatrix} \cdot \begin{bmatrix} v_1 \\ v_2 \\ v_3 \end{bmatrix} = \begin{bmatrix} 2s_0 + 2s_1 - v_0 \\ 2s_1 + 2s_2 \\ 2s_2 + 2s_3 - v_4 \end{bmatrix} \Longrightarrow \begin{bmatrix} v_1 \\ v_2 \\ v_3 \end{bmatrix} = \begin{bmatrix} 11.231 \\ -1.666 \\ 3.569 \end{bmatrix}$$

The solution of the system is further restricted, since for each $v_i$, $i = 1, 2, 3$, the corresponding $\alpha_i = \frac{v_i - s_{i-1}}{s_i - s_{i-1}}$ must be in $[\zeta, 1 - \zeta]$ (equal to $[0, 1]$ since we have chosen $\zeta = 0$). The formula gives:

$$\begin{bmatrix} \alpha_1 \\ \alpha_2 \\ \alpha_3 \end{bmatrix} = \begin{bmatrix} 0.468 \\ 2.804 \\ -1.638 \end{bmatrix} \quad \text{which become} \quad \begin{bmatrix} \alpha_1 \\ \alpha_2 \\ \alpha_3 \end{bmatrix} = \begin{bmatrix} 0.468 \\ 1.000 \\ 0.000 \end{bmatrix}$$

Then, the nodal derivatives take their final values:

$$\begin{bmatrix} v_1 \\ v_2 \\ v_3 \end{bmatrix} = \begin{bmatrix} 11.231 \\ 1.883 \\ 1.883 \end{bmatrix}$$

The interested reader may observe that the above combination of $\alpha_2$ and $\alpha_3$ linearizes the segment, since $v_2 = v_3 = s_2$.

Next, we consider the strict monotonicity and the convexity criteria, for each curved segment separately. The second segment of the curve, i.e. that between the points with indices 1 and 2 is most interesting, since both criteria are violated; the strict monotonicity criterion returns minimum degree equal to 4, while the convexity criterion returns minimum degree equal to 5, which is the minimum acceptable degree for that segment. For all the other curved segments no degree increase is required.

Based on the degree distribution of the previous step, the Bézier control points of (12) can be calculated using (13) and (14).

**Example 2.** A "$t$–$z$" curve: data, degree distributions and fairness measures for various derivative estimation methods. The results are shown in Fig. 3.

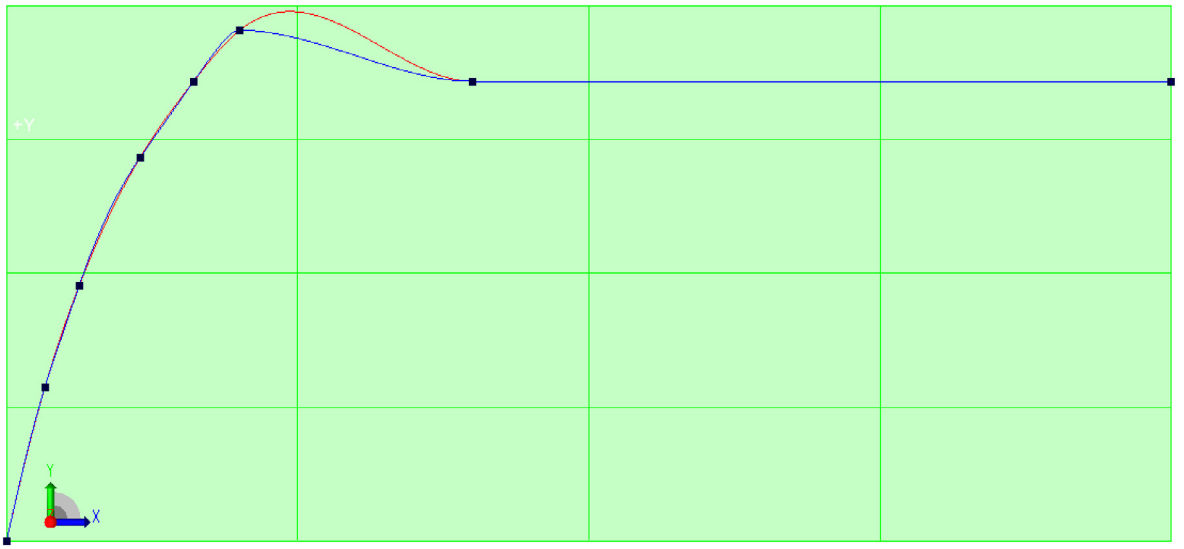


**Fig. 3.** Example 2: The $C^1$ shape preserving curve with its nodal derivatives estimated using the *Opt* method (blue) and the $C^2$ convexity preserving curve of [42] (red). (For interpretation of the references to color in this figure legend, the reader is referred to the web version of this article.)

| Points $(x_i, f_i)$ | $\mathcal{K}_{Opt}$ | $\mathcal{K}_{par}$ | $\mathcal{K}_{fd}$ | $\mathcal{K}_{FB}$ | $\mathcal{K}_{Br}$ | $\mathcal{K}_{Aw}$ | $\mathcal{K}_{Aa}$ | $\mathcal{K}$ [42] | |
|---|---|---|---|---|---|---|---|---|---|
| (0,0) | 3 | 3 | 3 | 3 | 3 | 3 | 3 | 3 | |
| (1,4.0153) | 7 | 3 | 3 | 3 | 3 | 3 | 3 | 3 | |
| (1.9,6.6804) | 3 | 3 | 3 | 3 | 3 | 3 | 3 | 3 | |
| (3.5,10.038) | 3 | 3 | 4 | 5 | 3 | 3 | 3 | 3 | |
| (4.9,12.0283) | 5 | 9 | 8 | 7 | 9 | 10 | 9 | 3 | |
| (6.1,13.3608) | 3 | 3 | 3 | 3 | 3 | 3 | 3 | 3 | |
| (12.2,12.0283) | 1 | 1 | 1 | 1 | 1 | 1 | 1 | 1 | |
| (30.5,12.0283) | | | | | | | | | |
| End point derivatives: $v_0 = 4.57008$ and $v_7 = 0$. | | | | | | | | | |
| | | | | | | | | | Min |
| Max degree | 7 | 9 | 8 | 7 | 9 | 10 | 9 | | Opt,FB |
| Sum of degrees | 25 | 25 | 25 | 25 | 25 | 26 | 25 | | Opt,par,fd,FB,Br,Aa |

| 2nd Derivative | $\mathcal{K}_{Opt}$ | $\mathcal{K}_{par}$ | $\mathcal{K}_{fd}$ | $\mathcal{K}_{FB}$ | $\mathcal{K}_{Br}$ | $\mathcal{K}_{Aw}$ | $\mathcal{K}_{Aa}$ | Min |
|---|---|---|---|---|---|---|---|---|
| $\max_i \lvert c''_{i-1}(x_i) - c''_i(x_i)\rvert$ | 4.37 | 8.11 | 7.18 | 6.26 | 8.11 | 9.04 | 8.10 | Opt |
| $\sum_i \lvert c''_{i-1}(x_i) - c''_i(x_i)\rvert$ | 6.67 | 9.86 | 9.20 | 9.94 | 9.99 | 9.92 | 10.46 | Opt |
| $\sum_i \int (c''_i(x))^2 dx$ | 0.38 | 0.99 | 0.81 | 0.62 | 1.02 | 1.21 | 1.03 | Opt |
| Curvature | $\mathcal{K}_{Opt}$ | $\mathcal{K}_{par}$ | $\mathcal{K}_{fd}$ | $\mathcal{K}_{FB}$ | $\mathcal{K}_{Br}$ | $\mathcal{K}_{Aw}$ | $\mathcal{K}_{Aa}$ | Min |
| $\max_i \lvert \kappa_{i-1}(x_i) - \kappa_i(x_i)\rvert$ | 4.37 | 8.11 | 7.18 | 6.26 | 8.11 | 9.04 | 8.10 | Opt |
| $\sum_i \lvert \kappa_{i-1}(x_i) - \kappa_i(x_i)\rvert$ | 4.79 | 8.42 | 7.52 | 6.69 | 8.42 | 9.31 | 8.44 | Opt |
| $\sum_i \int (\kappa_i(x))^2 dx$ | 3.1e−03 | 3.2e−03 | 3.3e−03 | 3.5e−03 | 3.1e−03 | 3.1e−03 | 3.1e−03 | Opt,Br,Aw |

The algorithm presented in Section 10 has been also applied to a number of academic examples. Starting with the Examples 3–9, we compare the results of our algorithm with the results presented in [42]. The reason for this comparison stems from the fact that the underlying Bézier structure of the polynomial segments used in both algorithms is the same, and the tension parameter, which is the polynomial degree, is the same in both of them. At this point, let us remark, again, that the method in [42] preserves only the convexity and the collinearity of the data. The convexity criterion is the same as the one employed here, however, the collinearity criterion differs from ours, giving extremely high degrees for [42] (see e.g. Example 4). The algorithm in [42] is iterative and global and converges to a $C^2$ convexity preserving interpolant. In each iteration a linear system needs to be solved. The algorithm presented here solves the interpolation problem satisfying also the monotonicity criteria, is of linear complexity and simpler for implementation, however, the resulting curve is only $C^1$ continuous.

Regarding this group of examples, our main remarks are the following:

- In Examples 3–5 we observe that all the degree distributions are of the same order of magnitude with those of $\mathcal{K}_{[42]}$, while the degree distributions $\mathcal{K}_{Opt}$ are lower in all cases.
- The Examples 6–9, where the algorithm has been applied to sharply bent data sets, reveal the necessity of the number $\zeta$ to be set for numerical stability reasons. The polynomial degrees in some of the polynomial segments are still very high for the optimal method.

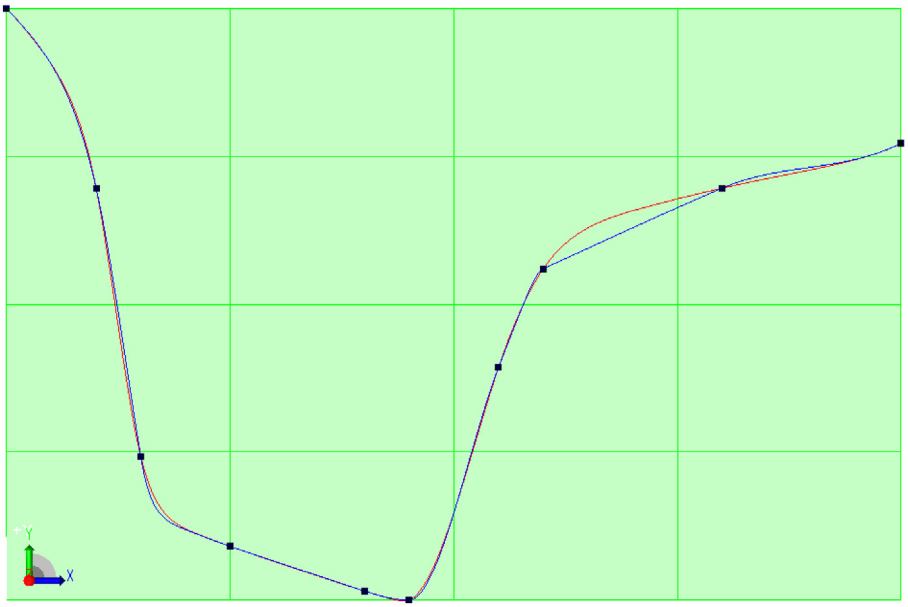

**Fig. 4.** Example 3: The $C^1$ shape preserving curve with its nodal derivatives estimated using the *Opt* method (blue) and the $C^2$ convexity preserving curve of [42] (red). (For interpretation of the references to color in this figure legend, the reader is referred to the web version of this article.)

Finally, the third group of examples, 10–30, contains benchmark data sets from the pertinent literature, showing the differences between the methods for derivative estimation, we gave in Section 9. The tables accompanying each example have the same structure as the one we described in the beginning of the section. In all cases the strict monotonicity criterion has been employed, which mostly complies with all these methods.

**Example 3.** Data from Späth [10]: data, degree distributions and fairness measures for various derivative estimation methods. The results are shown in Fig. 4.

| Points $(x_i, f_i)$ | $\mathcal{K}_{Opt}$ | $\mathcal{K}_{par}$ | $\mathcal{K}_{fd}$ | $\mathcal{K}_{FB}$ | $\mathcal{K}_{Br}$ | $\mathcal{K}_{Aw}$ | $\mathcal{K}_{Aa}$ | $\mathcal{K}$ [42] | |
|---|---|---|---|---|---|---|---|---|---|
| (0,10) | 4 | 4 | 3 | 3 | 3 | 3 | 3 | 5 | |
| (1,8) | 3 | 3 | 3 | 3 | 3 | 3 | 3 | 3 | |
| (1.5,5) | 9 | 14 | 6 | 5 | 3 | 4 | 3 | 6 | |
| (2.5,4) | 3 | 6 | 10 | 6 | 4 | 4 | 4 | 8 | |
| (4,3.5) | 3 | 8 | 4 | 4 | 5 | 11 | 4 | 7 | |
| (4.5,3.4) | 3 | 3 | 3 | 3 | 3 | 3 | 3 | 3 | |
| (5.5,6) | 6 | 4 | 7 | 6 | 9 | 10 | 9 | 3 | |
| (6,7.1) | 3 | 15 | 5 | 7 | 3 | 8 | 116 | 6 | |
| (8,8) | 4 | 4 | 4 | 4 | 4 | 4 | 4 | 6 | |
| (10,8.5) | | | | | | | | | |
| End point derivatives: $v_0 = -1$ and $v_9 = 0.5$. | | | | | | | | | |
| | | | | | | | | | Min |
| Max degree | 9 | 15 | 10 | 7 | 9 | 11 | 116 | | FB |
| Sum of degrees | 38 | 61 | 45 | 41 | 37 | 50 | 149 | | Br |

| 2nd Derivative | $\mathcal{K}_{Opt}$ | $\mathcal{K}_{par}$ | $\mathcal{K}_{fd}$ | $\mathcal{K}_{FB}$ | $\mathcal{K}_{Br}$ | $\mathcal{K}_{Aw}$ | $\mathcal{K}_{Aa}$ | Min |
|---|---|---|---|---|---|---|---|---|
| $\max_i \lvert c''_{i-1}(x_i) - c''_i(x_i)\rvert$ | 38.77 | 27.99 | 31.33 | 33.47 | 46.61 | 34.64 | 51.43 | par |
| $\sum_i \lvert c''_{i-1}(x_i) - c''_i(x_i)\rvert$ | 77.59 | 58.29 | 93.84 | 92.27 | 130.96 | 93.95 | 147.67 | par |
| $\sum_i \int (c''_i(x))^2 dx$ | 4.45 | 4.26 | 11.82 | 12.14 | 19.70 | 13.04 | 23.51 | par |
| Curvature | $\mathcal{K}_{Opt}$ | $\mathcal{K}_{par}$ | $\mathcal{K}_{fd}$ | $\mathcal{K}_{FB}$ | $\mathcal{K}_{Br}$ | $\mathcal{K}_{Aw}$ | $\mathcal{K}_{Aa}$ | Min |
| $\max_i \lvert \kappa_{i-1}(x_i) - \kappa_i(x_i)\rvert$ | 15.85 | 7.74 | 9.17 | 9.12 | 15.93 | 6.57 | 492.98 | Aw |
| $\sum_i \lvert \kappa_{i-1}(x_i) - \kappa_i(x_i)\rvert$ | 26.56 | 10.44 | 21.67 | 17.90 | 34.31 | 14.42 | 541.20 | par |
| $\sum_i \int (\kappa_i(x))^2 dx$ | 0.64 | 0.75 | 0.68 | 0.67 | 0.67 | 0.68 | 0.68 | Opt |

**Example 4.** Data from Rentrop [53]: data, degree distributions and fairness measures for various derivative estimation methods. The results are shown in Fig. 5.

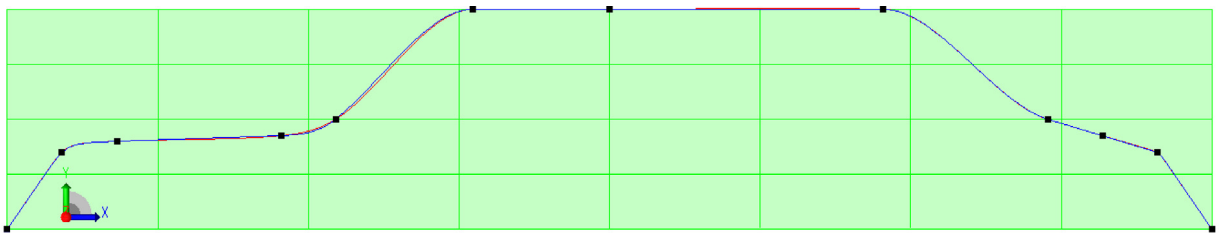

**Fig. 5.** Example 4: The $C^1$ shape preserving curve with its nodal derivatives estimated using the *Opt* method (blue) and the $C^2$ convexity preserving curve of [42] (red). (For interpretation of the references to color in this figure legend, the reader is referred to the web version of this article.)

| Points $(x_i, f_i)$ | $\mathcal{K}_{Opt}$ | $\mathcal{K}_{par}$ | $\mathcal{K}_{fd}$ | $\mathcal{K}_{FB}$ | $\mathcal{K}_{Br}$ | $\mathcal{K}_{Aw}$ | $\mathcal{K}_{Aa}$ | $\mathcal{K}$ [42] | |
|---|---|---|---|---|---|---|---|---|---|
| (−11,0) | 11 | 13 | 13 | 20 | 22 | 22 | 22 | 10 | |
| (−10,1.4) | 6 | 16 | 6 | 4 | 3 | 3 | 3 | 6 | |
| (−9,1.6) | 3 | 12 | 6 | 5 | 4 | 6 | 3 | 6 | |
| (−6,1.7) | 3 | 4 | 3 | 3 | 3 | 5 | 3 | 3 | |
| (−5,2) | 3 | 3 | 3 | 3 | 3 | 3 | 3 | 3 | |
| (−2.5,4) | 1 | 1 | 1 | 1 | 1 | 1 | 1 | 355 | |
| (0,4) | 1 | 1 | 1 | 1 | 1 | 1 | 1 | 398 | |
| (5,4) | 3 | 3 | 3 | 3 | 3 | 3 | 3 | 3 | |
| (8,2) | 1 | 1 | 1 | 1 | 1 | 1 | 1 | 71 | |
| (9,1.7) | 1 | 1 | 1 | 1 | 1 | 1 | 1 | 398 | |
| (10,1.4) | 23 | 23 | 23 | 23 | 23 | 23 | 23 | 23 | |
| (11,0) | | | | | | | | | |
| End point derivatives: $v_0 = 1.45$ and $v_{11} = -1.45$. | | | | | | | | | |
| | | | | | | | | | Min |
| Max degree | 23 | 23 | 23 | 23 | 23 | 23 | 23 | | Opt,par,fd,FB,Br,Aw,Aa |
| Sum of degrees | 56 | 78 | 61 | 65 | 65 | 69 | 64 | | Opt |

| 2nd Derivative | $\mathcal{K}_{Opt}$ | $\mathcal{K}_{par}$ | $\mathcal{K}_{fd}$ | $\mathcal{K}_{FB}$ | $\mathcal{K}_{Br}$ | $\mathcal{K}_{Aw}$ | $\mathcal{K}_{Aa}$ | Min |
|---|---|---|---|---|---|---|---|---|
| $\max_i \lvert c''_{i-1}(x_i) - c''_i(x_i)\rvert$ | 7.87 | 8.34 | 7.87 | 7.87 | 7.87 | 7.87 | 7.87 | Opt,fd,FB,Br,Aw,Aa |
| $\sum_i \lvert c''_{i-1}(x_i) - c''_i(x_i)\rvert$ | 12.74 | 21.48 | 15.85 | 19.20 | 20.87 | 21.07 | 20.66 | Opt |
| $\sum_i \int (c''_i(x))^2 dx$ | 1.47 | 2.18 | 1.84 | 2.28 | 2.32 | 2.33 | 2.32 | Opt |
| Curvature | $\mathcal{K}_{Opt}$ | $\mathcal{K}_{par}$ | $\mathcal{K}_{fd}$ | $\mathcal{K}_{FB}$ | $\mathcal{K}_{Br}$ | $\mathcal{K}_{Aw}$ | $\mathcal{K}_{Aa}$ | Min |
| $\max_i \lvert \kappa_{i-1}(x_i) - \kappa_i(x_i)\rvert$ | 325.40 | 325.40 | 325.40 | 325.40 | 325.40 | 325.40 | 325.40 | Opt,par,fd,FB,Br,Aw,Aa |
| $\sum_i \lvert \kappa_{i-1}(x_i) - \kappa_i(x_i)\rvert$ | 329.40 | 372.22 | 330.99 | 504.43 | 601.58 | 601.82 | 601.40 | Opt,fd |
| $\sum_i \int (\kappa_i(x))^2 dx$ | 0.08 | 10.11 | 0.09 | 0.06 | 0.06 | 0.08 | 0.06 | Aa |

**Example 5.** Data from McAllister et al. [6]: data, degree distributions and fairness measures for various derivative estimation methods. The results are shown in Fig. 6.

| Points $(x_i, f_i)$ | $\mathcal{K}_{Opt}$ | $\mathcal{K}_{par}$ | $\mathcal{K}_{fd}$ | $\mathcal{K}_{FB}$ | $\mathcal{K}_{Br}$ | $\mathcal{K}_{Aw}$ | $\mathcal{K}_{Aa}$ | $\mathcal{K}$ [42] | |
|---|---|---|---|---|---|---|---|---|---|
| (−2,0.25) | 3 | 18 | 13 | 4 | 3 | 3 | 3 | 6 | |
| (−1,1) | 3 | 21 | 3 | 3 | 3 | 6 | 3 | 6 | |
| (−0.3,11.1) | 3 | 9 | 3 | 3 | 3 | 3 | 3 | 3 | |
| (−0.2,25) | | | | | | | | | |
| End point derivatives: $v_0 = 0.25$ and $v_3 = 250$. | | | | | | | | | |
| | | | | | | | | | Min |
| Max degree | 3 | 21 | 13 | 4 | 3 | 6 | 3 | | Opt,Br,Aa |
| Sum of degrees | 9 | 48 | 19 | 10 | 9 | 12 | 9 | | Opt,Br,Aa |

| 2nd Derivative | $\mathcal{K}_{Opt}$ | $\mathcal{K}_{par}$ | $\mathcal{K}_{fd}$ | $\mathcal{K}_{FB}$ | $\mathcal{K}_{Br}$ | $\mathcal{K}_{Aw}$ | $\mathcal{K}_{Aa}$ | Min |
|---|---|---|---|---|---|---|---|---|
| $\max_i \lvert c''_{i-1}(x_i) - c''_i(x_i)\rvert$ | 2186.5 | 174.43 | 2074.0 | 1819.3 | 2466.3 | 220.57 | 2992.9 | par |
| $\sum_i \lvert c''_{i-1}(x_i) - c''_i(x_i)\rvert$ | 2223.6 | 239.09 | 2145.7 | 1823.8 | 2518.8 | 237.86 | 3079.7 | par,Aw |
| $\sum_i \int (c''_i(x))^2 dx$ | 6570.2 | 115157.0 | 6900.0 | 7572.7 | 5871.3 | 13498.9 | 4722.2 | Aa |
| Curvature | $\mathcal{K}_{Opt}$ | $\mathcal{K}_{par}$ | $\mathcal{K}_{fd}$ | $\mathcal{K}_{FB}$ | $\mathcal{K}_{Br}$ | $\mathcal{K}_{Aw}$ | $\mathcal{K}_{Aa}$ | Min |
| $\max_i \lvert \kappa_{i-1}(x_i) - \kappa_i(x_i)\rvert$ | 11.00 | 2.25 | 0.27 | 0.39 | 10.99 | 2.27 | 22.81 | fd |
| $\sum_i \lvert \kappa_{i-1}(x_i) - \kappa_i(x_i)\rvert$ | 11.10 | 2.28 | 0.34 | 0.43 | 11.23 | 2.27 | 25.57 | fd |
| $\sum_i \int (\kappa_i(x))^2 dx$ | 0.55 | 0.33 | 1.8e−03 | 7.4e−03 | 0.43 | 0.04 | 0.91 | fd |

**Example 6.** Data from Fritsch and Carlson [12]: data, degree distributions and fairness measures for various derivative estimation methods. The results are shown in Fig. 7.

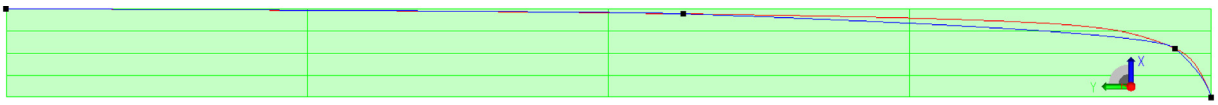

**Fig. 6.** Example 5: The $C^1$ shape preserving curve with its nodal derivatives estimated using the *Opt* method (blue) and the $C^2$ convexity preserving curve of [42] (red). (For interpretation of the references to color in this figure legend, the reader is referred to the web version of this article.)

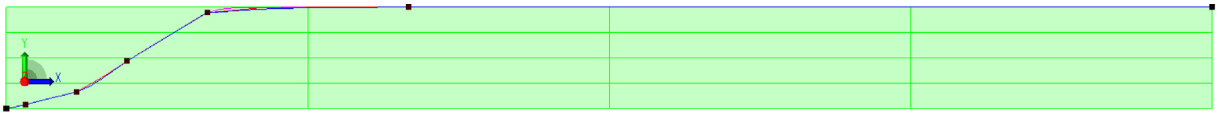

**Fig. 7.** Example 6: The $C^1$ shape preserving curve with its nodal derivatives estimated using the *Opt* method (blue) and the $C^2$ convexity preserving curve of [42] (red). (For interpretation of the references to color in this figure legend, the reader is referred to the web version of this article.)

| Points $(x_i, f_i)$ | $\mathcal{K}_{Opt}$ | $\mathcal{K}_{par}$ | $\mathcal{K}_{fd}$ | $\mathcal{K}_{FB}$ | $\mathcal{K}_{Br}$ | $\mathcal{K}_{Aw}$ | $\mathcal{K}_{Aa}$ | $\mathcal{K}$ [42] | |
|---|---|---|---|---|---|---|---|---|---|
| (8,0) | 1 | 1 | 1 | 1 | 1 | 1 | 1 | 14 | |
| (8.19,0.0437) | 3 | 13 | 13 | 12 | 8 | 8 | 8 | 11 | |
| (8.7,0.169) | 3 | 3 | 3 | 3 | 3 | 3 | 3 | 7 | |
| (9.2,0.469) | 80 | 44 | 170 | 126 | 192 | 134 | 237 | 7 | |
| (10,0.944) | 4 | 16 | 7 | 3 | 3 | 4 | 8 | 13 | |
| (12,1) | 1 | 1 | 1 | 1 | 1 | 1 | 1 | 107 | |
| (20,1) | | | | | | | | | |
| End point derivatives: $v_0 = 0.23$ and $v_6 = 0$. | | | | | | | | | |
| | | | | | | | | | Min |
| Max degree | 80 | 44 | 170 | 126 | 192 | 134 | 237 | | par |
| Sum of degrees | 92 | 78 | 195 | 146 | 208 | 151 | 258 | | par |

| 2nd Derivative | $\mathcal{K}_{Opt}$ | $\mathcal{K}_{par}$ | $\mathcal{K}_{fd}$ | $\mathcal{K}_{FB}$ | $\mathcal{K}_{Br}$ | $\mathcal{K}_{Aw}$ | $\mathcal{K}_{Aa}$ | Min |
|---|---|---|---|---|---|---|---|---|
| $\max_i \lvert c''_{i-1}(x_i) - c''_i(x_i)\rvert$ | 5.75 | 4.90 | 5.14 | 5.17 | 5.44 | 5.40 | 5.46 | par |
| $\sum_i \lvert c''_{i-1}(x_i) - c''_i(x_i)\rvert$ | 13.00 | 12.19 | 12.04 | 11.73 | 10.33 | 10.10 | 10.47 | Aw |
| $\sum_i \int (c''_i(x))^2 dx$ | 0.74 | 0.95 | 0.87 | 0.83 | 0.78 | 0.77 | 0.79 | Opt |
| Curvature | $\mathcal{K}_{Opt}$ | $\mathcal{K}_{par}$ | $\mathcal{K}_{fd}$ | $\mathcal{K}_{FB}$ | $\mathcal{K}_{Br}$ | $\mathcal{K}_{Aw}$ | $\mathcal{K}_{Aa}$ | Min |
| $\max_i \lvert \kappa_{i-1}(x_i) - \kappa_i(x_i)\rvert$ | 2536.2 | 172.14 | 9174.7 | 6725.5 | 16642.3 | 7429.9 | 26111.9 | par |
| $\sum_i \lvert \kappa_{i-1}(x_i) - \kappa_i(x_i)\rvert$ | 2539.7 | 175.07 | 9177.4 | 6727.6 | 16643.2 | 7430.6 | 26112.8 | par |
| $\sum_i \int (\kappa_i(x))^2 dx$ | 0.04 | 0.34 | 0.01 | 9.6e−03 | 0.02 | 0.02 | 0.02 | FB |

**Example 7.** Data from McAllister & Roulier [54]: data and degree distributions for various derivative estimation methods.

| Points $(x_i, f_i)$ | $\mathcal{K}_{Opt}$ | $\mathcal{K}_{par}$ | $\mathcal{K}_{fd}$ | $\mathcal{K}_{FB}$ | $\mathcal{K}_{Br}$ | $\mathcal{K}_{Aw}$ | $\mathcal{K}_{Aa}$ | $\mathcal{K}$ [42] | |
|---|---|---|---|---|---|---|---|---|---|
| (0,0) | 35 | 52 | 52 | 10 | 6 | 6 | 6 | 16 | |
| (2,2) | 15 | 21 | 21 | 29 | 41 | 41 | 41 | 3 | |
| (4,44) | 3 | 3 | 3 | 3 | 3 | 3 | 3 | 3 | |
| (6,88) | | | | | | | | | |
| End point derivatives: $v_0 = 0.8$ and $v_3 = 22.5$. | | | | | | | | | |
| | | | | | | | | | Min |
| Max degree | 35 | 52 | 52 | 29 | 41 | 41 | 41 | | FB |
| Sum of degrees | 53 | 76 | 76 | 42 | 50 | 50 | 50 | | FB |

**Example 8.** Data from McAllister & Roulier [54]: data and degree distributions for various derivative estimation methods.

| Points $(x_i, f_i)$ | $\mathcal{K}_{Opt}$ | $\mathcal{K}_{par}$ | $\mathcal{K}_{fd}$ | $\mathcal{K}_{FB}$ | $\mathcal{K}_{Br}$ | $\mathcal{K}_{Aw}$ | $\mathcal{K}_{Aa}$ | $\mathcal{K}$ [42] | |
|---|---|---|---|---|---|---|---|---|---|
| (0,0) | 3 | 52 | 52 | 10 | 6 | 6 | 6 | 33 | |
| (2,2) | 21 | 21 | 21 | 29 | 41 | 41 | 41 | 15 | |
| (4,44) | 3 | 22 | 22 | 12 | 22 | 22 | 22 | 4782 | |
| (6,88) | 6500 | 9561 | 9561 | 2322 | 808 | 808 | 808 | 4782 | |
| (8,132.1) | 3062 | 9560 | 9560 | 13178 | 18313 | 18313 | 18313 | 4783 | |
| (10,1132.1) | 3 | 3 | 3 | 3 | 3 | 3 | 3 | 4783 | |
| (12,2132.2) | | | | | | | | | |
| End point derivatives: $v_0 = 0.8$ and $v_6 = 500.075$. | | | | | | | | | |
| | | | | | | | | | Min |
| Max degree | 6500 | 9561 | 9561 | 13178 | 18313 | 18313 | 18313 | | Opt |
| Sum of degrees | 9592 | 19219 | 19219 | 15554 | 19193 | 19193 | 19193 | | Opt |

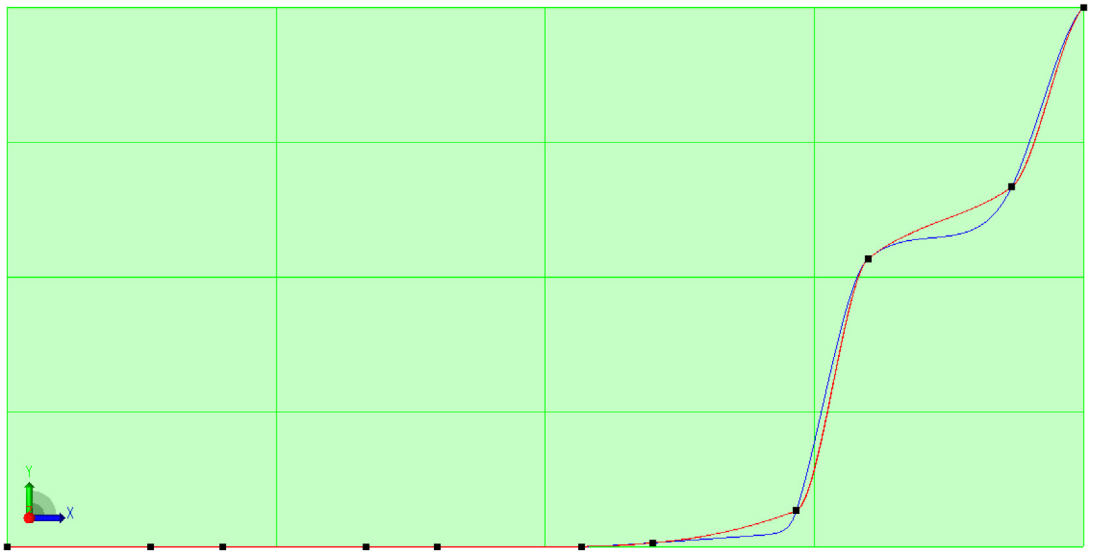

**Fig. 8.** Example 10: The $C^1$ shape preserving curve with its nodal derivatives estimated using the *Opt* method (blue) and the *Aa*, *Br* methods (red). (For interpretation of the references to color in this figure legend, the reader is referred to the web version of this article.)

**Example 9.** Data from McAllister & Roulier [54]: data and degree distributions for various derivative estimation methods.

| Points $(x_i, f_i)$ | $\mathcal{K}_{Opt}$ | $\mathcal{K}_{par}$ | $\mathcal{K}_{fd}$ | $\mathcal{K}_{FB}$ | $\mathcal{K}_{Br}$ | $\mathcal{K}_{Aw}$ | $\mathcal{K}_{Aa}$ | $\mathcal{K}$ [42] | |
|---|---|---|---|---|---|---|---|---|---|
| (0,0) | 3 | 3 | 3 | 3 | 3 | 3 | 3 | 596 | |
| (1,0.001) | 3 | 1000 | 1000 | 1498 | 1999 | 1999 | 1999 | 877 | |
| (2,1.001) | 17001 | 17002 | 17002 | 5102 | 1792 | 1792 | 1792 | 877 | |
| (3,2.002) | 3 | 10 | 10 | 13 | 18 | 18 | 18 | 25 | |
| (4,20.003) | 40 | 40 | 40 | 32 | 14 | 14 | 14 | 25 | |
| (5,40.1) | 3 | 3 | 3 | 4 | 5 | 5 | 5 | 18 | |
| (6,140.1) | 25 | 25 | 25 | 13 | 6 | 6 | 6 | 18 | |
| (7,282) | 3 | 5 | 5 | 6 | 8 | 8 | 8 | 36 | |
| (8,1400) | 86 | 86 | 86 | 23 | 9 | 9 | 9 | 36 | |
| (9,2800) | 3 | 31 | 31 | 42 | 59 | 59 | 59 | 23 | |
| (10,28000) | 26 | 26 | 26 | 40 | 19 | 19 | 19 | 23 | |
| (11,54000) | 3 | 3 | 3 | 3 | 3 | 3 | 3 | 3 | |
| (12,100000) | | | | | | | | | |
| End point derivatives: $v_0 = 0$ and $v_{12} = 5768$. | | | | | | | | | |
| | | | | | | | | | Min |
| Max degree | 17001 | 17002 | 17002 | 5102 | 1999 | 1999 | 1999 | | Br,Aw,Aa |
| Sum of degrees | 17199 | 18234 | 18234 | 6779 | 3935 | 3935 | 3935 | | Br,Aw,Aa |

**Example 10.** Data from Akima [55]: data, degree distributions and fairness measures for various derivative estimation methods. The results are shown in Fig. 8.

| Points $(x_i, f_i)$ | $\mathcal{K}_{Opt}$ | $\mathcal{K}_{par}$ | $\mathcal{K}_{fd}$ | $\mathcal{K}_{FB}$ | $\mathcal{K}_{Br}$ | $\mathcal{K}_{Aw}$ | $\mathcal{K}_{Aa}$ | |
|---|---|---|---|---|---|---|---|---|
| (0,1) | 1 | 1 | 1 | 1 | 1 | 1 | 1 | |
| (2,1) | 1 | 1 | 1 | 1 | 1 | 1 | 1 | |
| (3,1) | 1 | 1 | 1 | 1 | 1 | 1 | 1 | |
| (5,1) | 1 | 1 | 1 | 1 | 1 | 1 | 1 | |
| (6,1) | 1 | 1 | 1 | 1 | 1 | 1 | 1 | |
| (8,1) | 3 | 3 | 4 | 3 | 3 | 4 | 3 | |
| (9,1.05) | 20 | 20 | 20 | 5 | 3 | 4 | 3 | |
| (11,1.5) | 3 | 3 | 3 | 3 | 3 | 3 | 3 | |
| (12,5) | 6 | 9 | 6 | 5 | 4 | 5 | 3 | |
| (14,6) | 3 | 3 | 3 | 3 | 3 | 3 | 3 | |
| (15,8.5) | | | | | | | | |
| End point derivatives: $v_0 = 0$ and $v_{10} = 1$. | | | | | | | | |
| | | | | | | | | Min |
| Max degree | 20 | 20 | 20 | 5 | 4 | 5 | 3 | Aa |
| Sum of degrees | 40 | 43 | 41 | 24 | 21 | 24 | 20 | Aa |

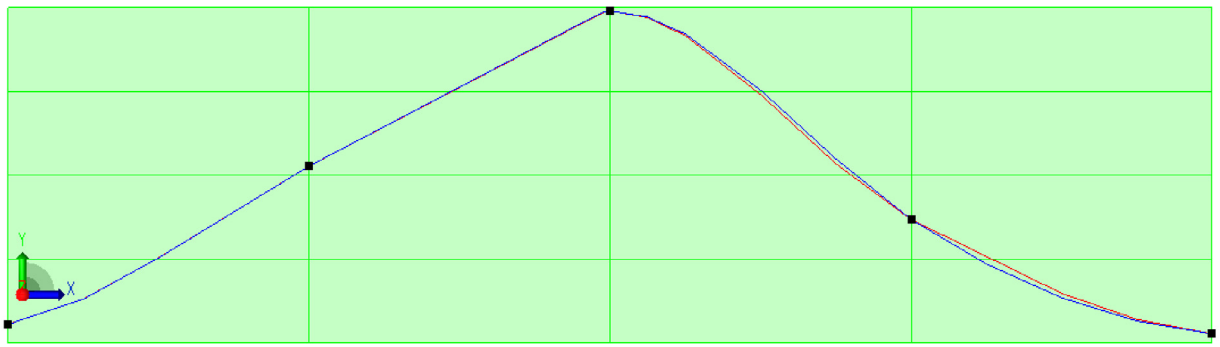


**Fig. 9.** Example 11: The $C^1$ shape preserving curve with its nodal derivatives estimated using the *Opt* method (blue) and the *FB* method (red). (For interpretation of the references to color in this figure legend, the reader is referred to the web version of this article.)

| 2nd Derivative | $\mathcal{K}_{Opt}$ | $\mathcal{K}_{par}$ | $\mathcal{K}_{fd}$ | $\mathcal{K}_{FB}$ | $\mathcal{K}_{Br}$ | $\mathcal{K}_{Aw}$ | $\mathcal{K}_{Aa}$ | Min |
|---|---|---|---|---|---|---|---|---|
| $\max_i \lvert c''_{i-1}(x_i) - c''_i(x_i)\rvert$ | 8.45 | 6.30 | 12.99 | 15.36 | 17.66 | 15.55 | 18.47 | par |
| $\sum_i \lvert c''_{i-1}(x_i) - c''_i(x_i)\rvert$ | 14.20 | 11.83 | 27.51 | 35.22 | 42.99 | 35.55 | 45.92 | par |
| $\sum_i \int (c''_i(x))^2 dx$ | 2.87 | 2.56 | 3.27 | 4.05 | 4.86 | 4.05 | 5.25 | par |
| Curvature | $\mathcal{K}_{Opt}$ | $\mathcal{K}_{par}$ | $\mathcal{K}_{fd}$ | $\mathcal{K}_{FB}$ | $\mathcal{K}_{Br}$ | $\mathcal{K}_{Aw}$ | $\mathcal{K}_{Aa}$ | Min |
| $\max_i \lvert \kappa_{i-1}(x_i) - \kappa_i(x_i)\rvert$ | 8.47 | 15.19 | 27.69 | 9.71 | 14.35 | 9.83 | 16.24 | Opt |
| $\sum_i \lvert \kappa_{i-1}(x_i) - \kappa_i(x_i)\rvert$ | 12.82 | 15.73 | 31.12 | 15.56 | 26.58 | 15.82 | 32.43 | Opt |
| $\sum_i \int (\kappa_i(x))^2 dx$ | 0.03 | 0.04 | 0.04 | 0.07 | 0.11 | 0.07 | 0.13 | Opt |

**Example 11.** Five points from the function $e^{x^2}, x \in [-1.7, 1.9]$, from Hyman [3]: data, degree distributions and fairness measures for various derivative estimation methods. The results are shown in Fig. 9.

| Points $(x_i, f_i)$ | $\mathcal{K}_{Opt}$ | $\mathcal{K}_{par}$ | $\mathcal{K}_{fd}$ | $\mathcal{K}_{FB}$ | $\mathcal{K}_{Br}$ | $\mathcal{K}_{Aw}$ | $\mathcal{K}_{Aa}$ | |
|---|---|---|---|---|---|---|---|---|
| (−1.7,0.0555762) | 3 | 3 | 3 | 3 | 3 | 3 | 3 | |
| (−0.8,0.527292) | 53 | 105 | 105 | 79 | 106 | 106 | 106 | |
| (0.1,0.99005) | 3 | 3 | 3 | 3 | 3 | 3 | 3 | |
| (1,0.367879) | 3 | 3 | 3 | 3 | 4 | 4 | 4 | |
| (1.9,0.0270518) | | | | | | | | |
| End point derivatives: $v_0 = 0.188959$ and $v_4 = -0.102797$. | | | | | | | | |
| | | | | | | | | Min |
| Max degree | 53 | 105 | 105 | 79 | 106 | 106 | 106 | Opt |
| Sum of degrees | 62 | 114 | 114 | 88 | 116 | 116 | 116 | Opt |

| 2nd Derivative | $\mathcal{K}_{Opt}$ | $\mathcal{K}_{par}$ | $\mathcal{K}_{fd}$ | $\mathcal{K}_{FB}$ | $\mathcal{K}_{Br}$ | $\mathcal{K}_{Aw}$ | $\mathcal{K}_{Aa}$ | Min |
|---|---|---|---|---|---|---|---|---|
| $\max_i \lvert c''_{i-1}(x_i) - c''_i(x_i)\rvert$ | 4.04 | 4.13 | 4.13 | 4.10 | 4.13 | 4.13 | 4.13 | Opt |
| $\sum_i \lvert c''_{i-1}(x_i) - c''_i(x_i)\rvert$ | 5.09 | 6.30 | 6.30 | 6.21 | 6.60 | 6.60 | 6.60 | Opt |
| $\sum_i \int (c''_i(x))^2 dx$ | 0.62 | 0.69 | 0.69 | 0.68 | 0.71 | 0.71 | 0.71 | Opt |
| Curvature | $\mathcal{K}_{Opt}$ | $\mathcal{K}_{par}$ | $\mathcal{K}_{fd}$ | $\mathcal{K}_{FB}$ | $\mathcal{K}_{Br}$ | $\mathcal{K}_{Aw}$ | $\mathcal{K}_{Aa}$ | Min |
| $\max_i \lvert \kappa_{i-1}(x_i) - \kappa_i(x_i)\rvert$ | 1046.2 | 4155.3 | 4155.3 | 2343.1 | 4235.2 | 4235.2 | 4235.2 | Opt |
| $\sum_i \lvert \kappa_{i-1}(x_i) - \kappa_i(x_i)\rvert$ | 1047.1 | 4157.1 | 4157.1 | 2345.1 | 4237.2 | 4237.2 | 4237.2 | Opt |
| $\sum_i \int (\kappa_i(x))^2 dx$ | 0.13 | 0.15 | 0.15 | 0.15 | 0.16 | 0.16 | 0.16 | Opt |

**Example 12.** Data from Pruess [7]: data, degree distributions and fairness measures for various derivative estimation methods. The results are shown in Fig. 10.

| Points $(x_i, f_i)$ | $\mathcal{K}_{Opt}$ | $\mathcal{K}_{par}$ | $\mathcal{K}_{fd}$ | $\mathcal{K}_{FB}$ | $\mathcal{K}_{Br}$ | $\mathcal{K}_{Aw}$ | $\mathcal{K}_{Aa}$ |
|---|---|---|---|---|---|---|---|
| (0,0) | 6 | 4 | 4 | 3 | 3 | 3 | 3 |
| (0.1,0.25) | 3 | 3 | 3 | 3 | 3 | 3 | 3 |
| (0.2,1.675) | 23 | 17 | 17 | 3 | 3 | 3 | 3 |
| (0.3,1.65) | 3 | 3 | 3 | 3 | 3 | 3 | 3 |
| (0.4,0.825) | 23 | 18 | 18 | 3 | 3 | 3 | 3 |
| (0.5,0.8) | 1 | 1 | 1 | 1 | 1 | 1 | 1 |
| (0.6,0.8) | 1 | 1 | 1 | 1 | 1 | 1 | 1 |
| (0.7,0.8) | 1 | 1 | 1 | 1 | 1 | 1 | 1 |

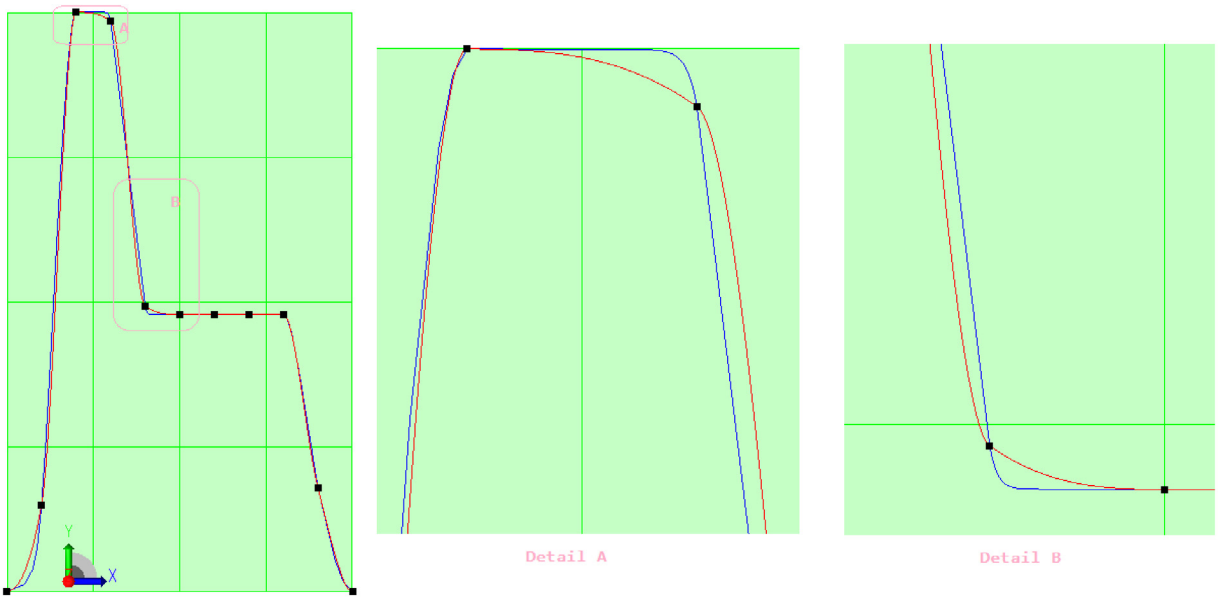


**Fig. 10.** Example 12: The $C^1$ shape preserving curve with its nodal derivatives estimated using the *Opt* method (blue) and the *FB* method (red). (For interpretation of the references to color in this figure legend, the reader is referred to the web version of this article.)

(*continued*)

| Points $(x_i, f_i)$ | $\mathcal{K}_{Opt}$ | $\mathcal{K}_{par}$ | $\mathcal{K}_{fd}$ | $\mathcal{K}_{FB}$ | $\mathcal{K}_{Br}$ | $\mathcal{K}_{Aw}$ | $\mathcal{K}_{Aa}$ | |
|---|---|---|---|---|---|---|---|---|
| (0.8,0.8) | 3 | 3 | 3 | 3 | 3 | 3 | 3 | |
| (0.9,0.3) | 3 | 4 | 4 | 4 | 5 | 6 | 6 | |
| (1,0) | | | | | | | | |
| End point derivatives : $v_0 = 0$ and $v_{10} = 0$. | | | | | | | | |
| | | | | | | | | Min |
| Max degree | 23 | 18 | 18 | 4 | 5 | 6 | 6 | FB |
| Sum of degrees | 67 | 55 | 55 | 25 | 26 | 27 | 27 | FB |

| 2nd Derivative | $\mathcal{K}_{Opt}$ | $\mathcal{K}_{par}$ | $\mathcal{K}_{fd}$ | $\mathcal{K}_{FB}$ | $\mathcal{K}_{Br}$ | $\mathcal{K}_{Aw}$ | $\mathcal{K}_{Aa}$ | Min |
|---|---|---|---|---|---|---|---|---|
| $\max_i \lvert c''_{i-1}(x_i) - c''_i(x_i)\rvert$ | 569.78 | 687.50 | 687.50 | 743.10 | 764.63 | 764.63 | 764.63 | Opt |
| $\sum_i \lvert c''_{i-1}(x_i) - c''_i(x_i)\rvert$ | 1549.0 | 1793.1 | 1793.1 | 2533.8 | 2732.6 | 2723.2 | 2723.2 | Opt |
| $\sum_i \int (c''_i(x))^2 dx$ | 1087.5 | 797.82 | 797.82 | 1021.8 | 1096.1 | 1106.9 | 1106.9 | par,fd |
| Curvature | $\mathcal{K}_{Opt}$ | $\mathcal{K}_{par}$ | $\mathcal{K}_{fd}$ | $\mathcal{K}_{FB}$ | $\mathcal{K}_{Br}$ | $\mathcal{K}_{Aw}$ | $\mathcal{K}_{Aa}$ | Min |
| $\max_i \lvert \kappa_{i-1}(x_i) - \kappa_i(x_i)\rvert$ | 557.22 | 687.50 | 687.50 | 743.10 | 764.63 | 764.63 | 764.63 | Opt |
| $\sum_i \lvert \kappa_{i-1}(x_i) - \kappa_i(x_i)\rvert$ | 960.52 | 1118.7 | 1118.7 | 1445.2 | 1677.5 | 1677.4 | 1677.4 | Opt |
| $\sum_i \int (\kappa_i(x))^2 dx$ | 11.18 | 11.00 | 11.00 | 4.91 | 9.64 | 9.64 | 9.64 | FB |

**Example 13.** Data from Butt & Brodlie [56]: data, degree distributions and fairness measures for various derivative estimation methods. The results are shown in Fig. 11.

| Points $(x_i, f_i)$ | $\mathcal{K}_{Opt}$ | $\mathcal{K}_{par}$ | $\mathcal{K}_{fd}$ | $\mathcal{K}_{FB}$ | $\mathcal{K}_{Br}$ | $\mathcal{K}_{Aw}$ | $\mathcal{K}_{Aa}$ | |
|---|---|---|---|---|---|---|---|---|
| (0,20.8) | 3 | 3 | 3 | 3 | 3 | 3 | 3 | |
| (2,8.8) | 3 | 6 | 3 | 3 | 3 | 3 | 3 | |
| (4,4.2) | 3 | 4 | 3 | 3 | 4 | 3 | 10 | |
| (10,0.5) | 3 | 6 | 3 | 3 | 4 | 5 | 3 | |
| (28,3.9) | 3 | 4 | 5 | 4 | 5 | 3 | 6 | |
| (30,6.2) | 4 | 3 | 3 | 3 | 3 | 3 | 3 | |
| (32,9.6) | | | | | | | | |
| End point derivatives: $v_0 = -7.85$ and $v_6 = 1.975$. | | | | | | | | |
| | | | | | | | | Min |
| Max degree | 4 | 6 | 5 | 4 | 5 | 5 | 10 | Opt,FB |
| Sum of degrees | 19 | 26 | 20 | 19 | 22 | 20 | 28 | Opt,FB |

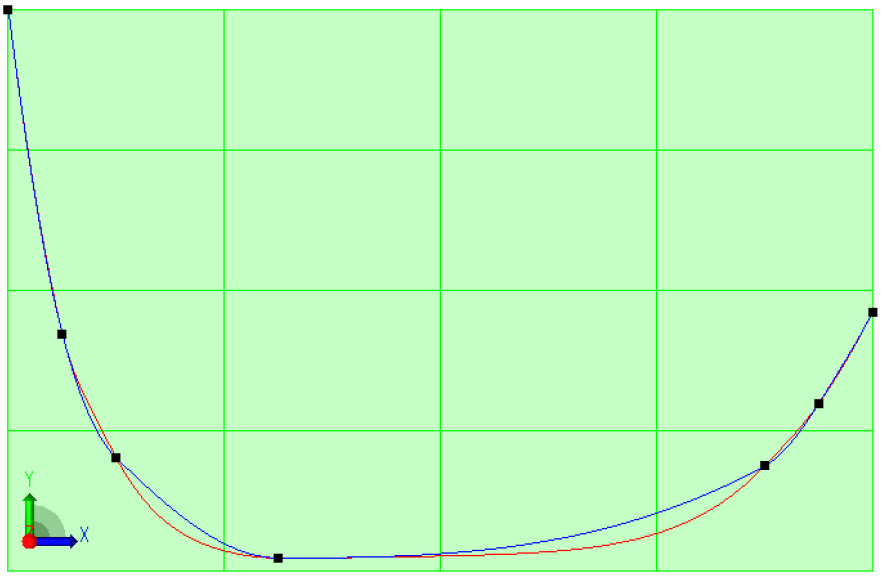


**Fig. 11.** Example 13: The $C^1$ shape preserving curve with its nodal derivatives estimated using the *Opt* method (blue) and the *par* method (red). (For interpretation of the references to color in this figure legend, the reader is referred to the web version of this article.)

| 2nd Derivative | $\mathcal{K}_{Opt}$ | $\mathcal{K}_{par}$ | $\mathcal{K}_{fd}$ | $\mathcal{K}_{FB}$ | $\mathcal{K}_{Br}$ | $\mathcal{K}_{Aw}$ | $\mathcal{K}_{Aa}$ | Min |
|---|---|---|---|---|---|---|---|---|
| $\max_i \lvert c''_{i-1}(x_i) - c''_i(x_i)\rvert$ | 1.04 | 3.67 | 2.12 | 1.36 | 2.86 | 2.38 | 3.06 | Opt |
| $\sum_i \lvert c''_{i-1}(x_i) - c''_i(x_i)\rvert$ | 2.80 | 4.99 | 3.67 | 2.20 | 7.53 | 3.80 | 9.59 | FB |
| $\sum_i \int (c''_i(x))^2 dx$ | 0.20 | 0.12 | 0.11 | 0.16 | 0.42 | 0.35 | 0.52 | fd |
| Curvature | $\mathcal{K}_{Opt}$ | $\mathcal{K}_{par}$ | $\mathcal{K}_{fd}$ | $\mathcal{K}_{FB}$ | $\mathcal{K}_{Br}$ | $\mathcal{K}_{Aw}$ | $\mathcal{K}_{Aa}$ | Min |
| $\max_i \lvert \kappa_{i-1}(x_i) - \kappa_i(x_i)\rvert$ | 0.48 | 0.14 | 1.89 | 1.06 | 1.96 | 0.20 | 2.97 | par |
| $\sum_i \lvert \kappa_{i-1}(x_i) - \kappa_i(x_i)\rvert$ | 1.20 | 0.40 | 2.36 | 1.37 | 3.20 | 0.58 | 5.30 | par |
| $\sum_i \int (\kappa_i(x))^2 dx$ | 6.0e−03 | 8.5e−04 | 0.06 | 0.02 | 0.06 | 2.2e−03 | 0.12 | par |

**Example 14.** Eleven points from the function $f(x) = 1 + \frac{2^{x+1}}{2^x - 1}$ from Conti & Morandi [57]: data, degree distributions and fairness measures for various derivative estimation methods. The results are shown in Fig. 12.

| Points $(x_i, f_i)$ | $\mathcal{K}_{Opt}$ | $\mathcal{K}_{par}$ | $\mathcal{K}_{fd}$ | $\mathcal{K}_{FB}$ | $\mathcal{K}_{Br}$ | $\mathcal{K}_{Aw}$ | $\mathcal{K}_{Aa}$ | |
|---|---|---|---|---|---|---|---|---|
| (0.1,30.8655) | 7 | 12 | 12 | 8 | 7 | 7 | 7 | |
| (0.59,6.95846) | 3 | 17 | 17 | 6 | 3 | 3 | 3 | |
| (1.08,4.79527) | 5 | 5 | 5 | 4 | 3 | 3 | 3 | |
| (1.57,4.01572) | 3 | 4 | 4 | 4 | 3 | 3 | 3 | |
| (2.06,3.63094) | 3 | 3 | 3 | 4 | 3 | 3 | 3 | |
| (2.55,3.41183) | 3 | 3 | 3 | 4 | 3 | 3 | 3 | |
| (3.04,3.27682) | 3 | 3 | 3 | 4 | 3 | 3 | 3 | |
| (3.53,3.18955) | 3 | 3 | 3 | 4 | 3 | 3 | 3 | |
| (4.02,3.13138) | 3 | 3 | 3 | 4 | 3 | 3 | 3 | |
| (4.51,3.09181) | 3 | 3 | 3 | 3 | 3 | 3 | 3 | |
| (5,3.06452) | | | | | | | | |
| End point derivatives: $v_0 = -288.101$ and $v_{10} = -0.0463289$. | | | | | | | | |
| | | | | | | | | Min |
| Max degree | 7 | 17 | 17 | 8 | 7 | 7 | 7 | Opt,Br,Aw,Aa |
| Sum of degrees | 36 | 56 | 56 | 45 | 34 | 34 | 34 | Br,Aw,Aa |

| 2nd Derivative | $\mathcal{K}_{Opt}$ | $\mathcal{K}_{par}$ | $\mathcal{K}_{fd}$ | $\mathcal{K}_{FB}$ | $\mathcal{K}_{Br}$ | $\mathcal{K}_{Aw}$ | $\mathcal{K}_{Aa}$ | Min |
|---|---|---|---|---|---|---|---|---|
| $\max_i \lvert c''_{i-1}(x_i) - c''_i(x_i)\rvert$ | 65.97 | 24.24 | 24.24 | 26.08 | 9.72 | 9.72 | 9.72 | Br,Aw,Aa |
| $\sum_i \lvert c''_{i-1}(x_i) - c''_i(x_i)\rvert$ | 98.62 | 44.84 | 44.84 | 37.68 | 12.06 | 12.06 | 12.06 | Br,Aw,Aa |
| $\sum_i \int (c''_i(x))^2 dx$ | 25.72 | 7.18 | 7.18 | 18.54 | 0.88 | 0.88 | 0.88 | Br,Aw,Aa |
| Curvature | $\mathcal{K}_{Opt}$ | $\mathcal{K}_{par}$ | $\mathcal{K}_{fd}$ | $\mathcal{K}_{FB}$ | $\mathcal{K}_{Br}$ | $\mathcal{K}_{Aw}$ | $\mathcal{K}_{Aa}$ | Min |
| $\max_i \lvert \kappa_{i-1}(x_i) - \kappa_i(x_i)\rvert$ | 1.00 | 0.70 | 0.70 | 0.83 | 0.12 | 0.12 | 0.12 | Br,Aw,Aa |
| $\sum_i \lvert \kappa_{i-1}(x_i) - \kappa_i(x_i)\rvert$ | 3.44 | 2.58 | 2.58 | 2.95 | 0.40 | 0.40 | 0.40 | Br,Aw,Aa |
| $\sum_i \int (\kappa_i(x))^2 dx$ | 9.3e−03 | 0.01 | 0.01 | 0.01 | 3.2e−03 | 3.2e−03 | 3.2e−03 | Br,Aw,Aa |

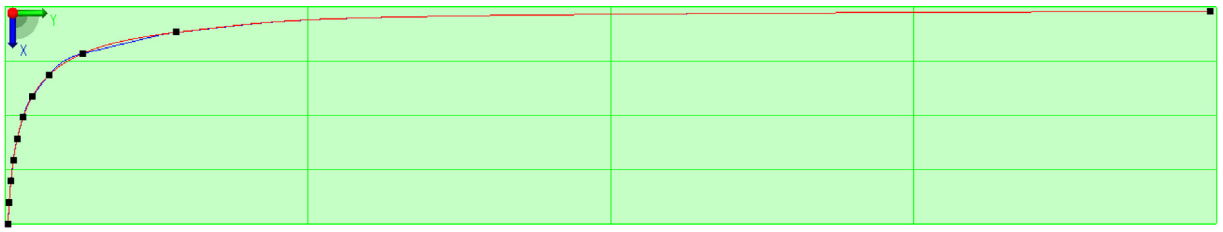

**Fig. 12.** Example 14: The $C^1$ shape preserving curve with its nodal derivatives estimated using the *Opt* method (blue) and the *Br* method (red). (For interpretation of the references to color in this figure legend, the reader is referred to the web version of this article.)

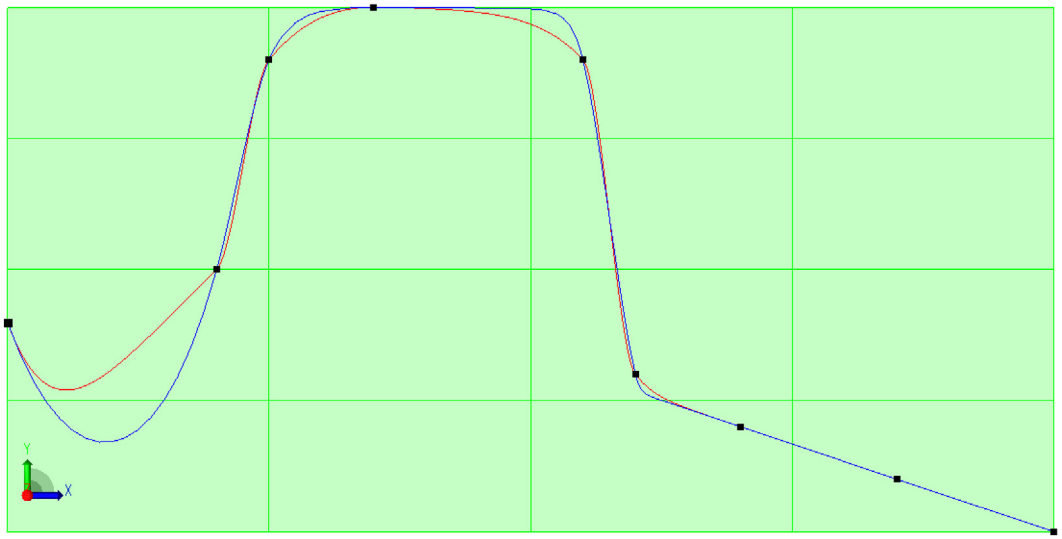

**Fig. 13.** Example 15: The $C^1$ shape preserving curve with its nodal derivatives estimated using the *Opt* method (blue) and the *Aw* method (red). (For interpretation of the references to color in this figure legend, the reader is referred to the web version of this article.)

**Example 15.** Data from Späth [58]: data, degree distributions and fairness measures for various derivative estimation methods. The results are shown in Fig. 13.

| Points $(x_i, f_i)$ | $\mathcal{K}_{Opt}$ | $\mathcal{K}_{par}$ | $\mathcal{K}_{fd}$ | $\mathcal{K}_{FB}$ | $\mathcal{K}_{Br}$ | $\mathcal{K}_{Aw}$ | $\mathcal{K}_{Aa}$ | |
|---|---|---|---|---|---|---|---|---|
| (0,2) | 5 | 3 | 5 | 9 | 21 | 5 | 105 | |
| (2,2.5) | 3 | 3 | 3 | 3 | 3 | 3 | 3 | |
| (2.5,4.5) | 5 | 6 | 4 | 3 | 3 | 3 | 5 | |
| (3.5,5) | 17 | 20 | 6 | 3 | 3 | 5 | 7 | |
| (5.5,4.5) | 3 | 3 | 3 | 3 | 3 | 3 | 3 | |
| (6,1.5) | 24 | 23 | 12 | 6 | 4 | 6 | 3 | |
| (7,1) | 1 | 1 | 1 | 1 | 1 | 1 | 1 | |
| (8.5,0.5) | 1 | 1 | 1 | 1 | 1 | 1 | 1 | |
| (10,0) | | | | | | | | |
| End point derivatives: $v_0 = -2.75$ and $v_8 = -0.333333$. | | | | | | | | |
| | | | | | | | | Min |
| Max degree | 24 | 23 | 12 | 9 | 21 | 6 | 105 | Aw |
| Sum of degrees | 59 | 60 | 35 | 29 | 39 | 27 | 128 | Aw |

| 2nd Derivative | $\mathcal{K}_{Opt}$ | $\mathcal{K}_{par}$ | $\mathcal{K}_{fd}$ | $\mathcal{K}_{FB}$ | $\mathcal{K}_{Br}$ | $\mathcal{K}_{Aw}$ | $\mathcal{K}_{Aa}$ | Min |
|---|---|---|---|---|---|---|---|---|
| $\max_i \lvert c''_{i-1}(x_i) - c''_i(x_i)\rvert$ | 22.11 | 20.01 | 48.03 | 60.68 | 65.32 | 56.26 | 67.90 | par |
| $\sum_i \lvert c''_{i-1}(x_i) - c''_i(x_i)\rvert$ | 51.82 | 47.05 | 133.70 | 187.14 | 211.04 | 177.33 | 221.38 | par |
| $\sum_i \int (c''_i(x))^2 dx$ | 6.35 | 4.17 | 20.87 | 30.41 | 36.29 | 28.79 | 39.25 | par |
| Curvature | $\mathcal{K}_{Opt}$ | $\mathcal{K}_{par}$ | $\mathcal{K}_{fd}$ | $\mathcal{K}_{FB}$ | $\mathcal{K}_{Br}$ | $\mathcal{K}_{Aw}$ | $\mathcal{K}_{Aa}$ | Min |
| $\max_i \lvert \kappa_{i-1}(x_i) - \kappa_i(x_i)\rvert$ | 16.11 | 15.44 | 11.79 | 33.73 | 51.99 | 17.87 | 235.01 | fd |
| $\sum_i \lvert \kappa_{i-1}(x_i) - \kappa_i(x_i)\rvert$ | 22.01 | 21.14 | 26.79 | 77.48 | 132.63 | 51.60 | 362.51 | par |
| $\sum_i \int (\kappa_i(x))^2 dx$ | 0.80 | 0.77 | 0.68 | 2.04 | 12.25 | 0.71 | 5074.3 | fd |

**Example 16.** Ten points from the function $f(x) = (1 + (x + a)^{1/3})/(2 - (x + a)^{1/3})$, $a = 10^{-}4$, from Manni [59]: data, degree distributions and fairness measures for various derivative estimation methods. The results are shown in Fig. 14.

| Points $(x_i, f_i)$ | $\mathcal{K}_{Opt}$ | $\mathcal{K}_{par}$ | $\mathcal{K}_{fd}$ | $\mathcal{K}_{FB}$ | $\mathcal{K}_{Br}$ | $\mathcal{K}_{Aw}$ | $\mathcal{K}_{Aa}$ | |
|---|---|---|---|---|---|---|---|---|
| (−0.8,0.0244925) | 3 | 3 | 3 | 3 | 3 | 3 | 3 | |
| (−0.6,0.0550802) | 4 | 4 | 4 | 5 | 3 | 3 | 3 | |
| (−0.4,0.0961928) | 3 | 6 | 5 | 5 | 3 | 4 | 3 | |
| (−0.2,0.160674) | 12 | 22 | 10 | 6 | 3 | 5 | 3 | |
| (−0.04,0.281115) | 3 | 3 | 3 | 3 | 3 | 3 | 3 | |
| (0.04,0.809714) | 9 | 12 | 6 | 8 | 4 | 6 | 3 | |
| (0.2,1.11999) | 3 | 6 | 5 | 7 | 4 | 5 | 4 | |
| (0.4,1.37505) | 4 | 4 | 4 | 6 | 4 | 4 | 4 | |
| (0.6,1.59399) | 3 | 3 | 3 | 3 | 3 | 3 | 3 | |
| (0.8,1.79944) | | | | | | | | |
| End point derivatives: $v_0 = 0.135337$ and $v_9 = 1.46544$. | | | | | | | | |
| | | | | | | | | Min |
| Max degree | 12 | 22 | 10 | 8 | 4 | 6 | 4 | Br,Aa |
| Sum of degrees | 44 | 63 | 43 | 46 | 30 | 36 | 29 | Aa |

| 2nd Derivative | $\mathcal{K}_{Opt}$ | $\mathcal{K}_{par}$ | $\mathcal{K}_{fd}$ | $\mathcal{K}_{FB}$ | $\mathcal{K}_{Br}$ | $\mathcal{K}_{Aw}$ | $\mathcal{K}_{Aa}$ | Min |
|---|---|---|---|---|---|---|---|---|
| $\max_i \lvert c''_{i-1}(x_i) - c''_i(x_i)\rvert$ | 260.94 | 147.88 | 195.28 | 271.33 | 354.42 | 278.07 | 382.60 | par |
| $\sum_i \lvert c''_{i-1}(x_i) - c''_i(x_i)\rvert$ | 504.54 | 283.15 | 362.09 | 477.51 | 665.03 | 495.06 | 733.37 | par |
| $\sum_i \int (c''_i(x))^2 dx$ | 194.00 | 19.15 | 92.80 | 75.93 | 107.12 | 74.93 | 124.15 | par |
| Curvature | $\mathcal{K}_{Opt}$ | $\mathcal{K}_{par}$ | $\mathcal{K}_{fd}$ | $\mathcal{K}_{FB}$ | $\mathcal{K}_{Br}$ | $\mathcal{K}_{Aw}$ | $\mathcal{K}_{Aa}$ | Min |
| $\max_i \lvert \kappa_{i-1}(x_i) - \kappa_i(x_i)\rvert$ | 1.93 | 68.15 | 6.31 | 29.57 | 87.45 | 30.31 | 136.66 | Opt |
| $\sum_i \lvert \kappa_{i-1}(x_i) - \kappa_i(x_i)\rvert$ | 10.07 | 75.37 | 16.38 | 41.69 | 101.46 | 38.97 | 160.02 | Opt |
| $\sum_i \int (\kappa_i(x))^2 dx$ | 0.01 | 0.04 | 0.04 | 0.15 | 0.44 | 0.14 | 0.75 | Opt |

**Example 17.** Data from Sarfraz et al. [23]: data, degree distributions and fairness measures for various derivative estimation methods. The results are shown in Fig. 15.

| Points $(x_i, f_i)$ | $\mathcal{K}_{Opt}$ | $\mathcal{K}_{par}$ | $\mathcal{K}_{fd}$ | $\mathcal{K}_{FB}$ | $\mathcal{K}_{Br}$ | $\mathcal{K}_{Aw}$ | $\mathcal{K}_{Aa}$ | |
|---|---|---|---|---|---|---|---|---|
| (0,0.5) | 7 | 8 | 5 | 3 | 3 | 3 | 5 | |
| (2,1.5) | 3 | 3 | 3 | 3 | 3 | 3 | 3 | |
| (3,7) | 12 | 11 | 5 | 5 | 3 | 5 | 3 | |
| (7,9) | 3 | 3 | 3 | 3 | 3 | 3 | 3 | |
| (11,13) | | | | | | | | |
| End point derivatives: $v_0 = 0$ and $v_4 = 1.25$. | | | | | | | | |
| | | | | | | | | Min |
| Max degree | 12 | 11 | 5 | 5 | 3 | 5 | 5 | Br |
| Sum of degrees | 25 | 25 | 16 | 14 | 12 | 14 | 14 | Br |

| 2nd Derivative | $\mathcal{K}_{Opt}$ | $\mathcal{K}_{par}$ | $\mathcal{K}_{fd}$ | $\mathcal{K}_{FB}$ | $\mathcal{K}_{Br}$ | $\mathcal{K}_{Aw}$ | $\mathcal{K}_{Aa}$ | Min |
|---|---|---|---|---|---|---|---|---|
| $\max_i \lvert c''_{i-1}(x_i) - c''_i(x_i)\rvert$ | 8.37 | 4.65 | 21.25 | 24.35 | 27.89 | 23.22 | 29.80 | par |
| $\sum_i \lvert c''_{i-1}(x_i) - c''_i(x_i)\rvert$ | 10.54 | 10.18 | 39.01 | 49.09 | 55.81 | 44.97 | 59.20 | par |
| $\sum_i \int (c''_i(x))^2 dx$ | 3.02 | 5.03 | 7.03 | 8.30 | 10.18 | 6.89 | 11.41 | Opt |
| Curvature | $\mathcal{K}_{Opt}$ | $\mathcal{K}_{par}$ | $\mathcal{K}_{fd}$ | $\mathcal{K}_{FB}$ | $\mathcal{K}_{Br}$ | $\mathcal{K}_{Aw}$ | $\mathcal{K}_{Aa}$ | Min |
| $\max_i \lvert \kappa_{i-1}(x_i) - \kappa_i(x_i)\rvert$ | 0.64 | 0.86 | 3.63 | 5.77 | 13.52 | 5.50 | 22.39 | Opt |
| $\sum_i \lvert \kappa_{i-1}(x_i) - \kappa_i(x_i)\rvert$ | 0.73 | 0.97 | 5.17 | 11.76 | 26.12 | 8.11 | 39.43 | Opt |
| $\sum_i \int (\kappa_i(x))^2 dx$ | 4.9e−03 | 2.2e−03 | 0.03 | 0.23 | 0.90 | 0.22 | 1.64 | par |

**Example 18.** Data from Gerald & Wheatley [60]: data, degree distributions and fairness measures for various derivative estimation methods. The results are shown in Fig. 16.

| Points $(x_i, f_i)$ | $\mathcal{K}_{Opt}$ | $\mathcal{K}_{par}$ | $\mathcal{K}_{fd}$ | $\mathcal{K}_{FB}$ | $\mathcal{K}_{Br}$ | $\mathcal{K}_{Aw}$ | $\mathcal{K}_{Aa}$ | |
|---|---|---|---|---|---|---|---|---|
| (0,0.302) | 6 | 3 | 3 | 4 | 6 | 6 | 6 | |
| (0.05,0.278) | 3 | 3 | 3 | 3 | 3 | 3 | 3 | |
| (0.1,0.1) | 6 | 9 | 9 | 3 | 3 | 3 | 3 | |
| (0.15,0.268) | 3 | 3 | 3 | 3 | 3 | 3 | 3 | |
| (0.2,3) | | | | | | | | |
| End point derivatives: $v_0 = 1.06$ and $v_4 = 80.28$. | | | | | | | | |
| | | | | | | | | Min |
| Max degree | 6 | 9 | 9 | 4 | 6 | 6 | 6 | FB |
| Sum of degrees | 18 | 18 | 18 | 13 | 15 | 15 | 15 | FB |

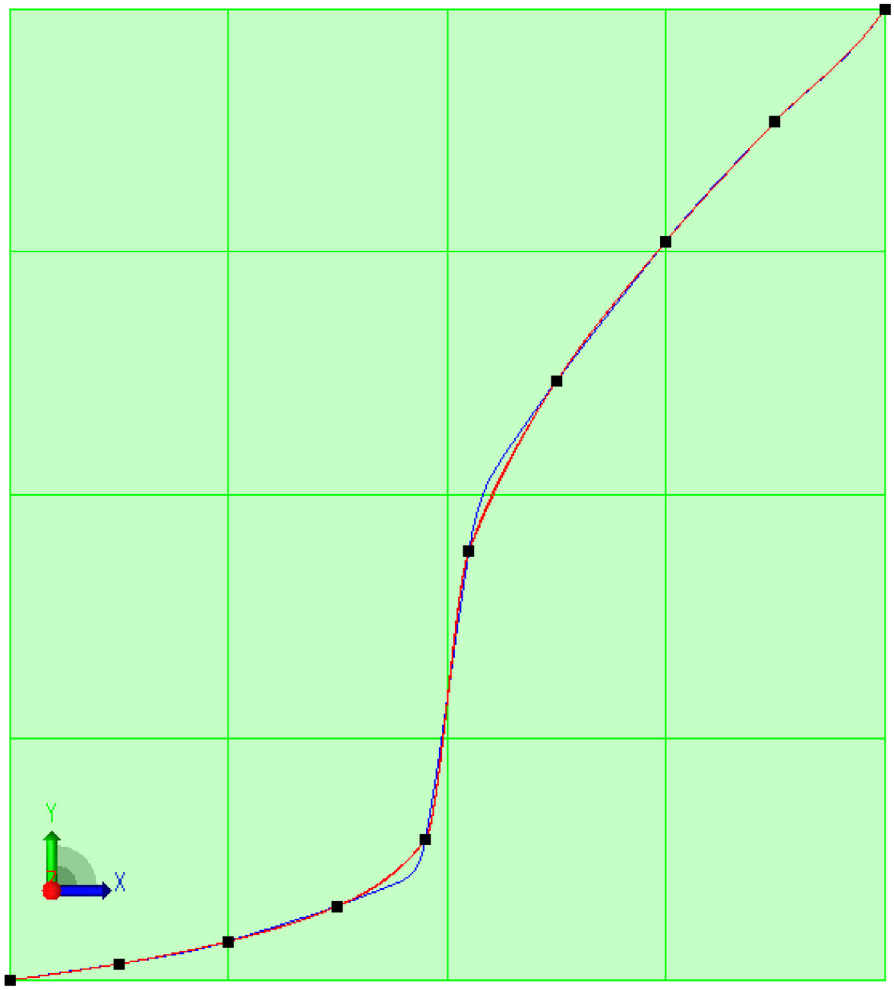


**Fig. 14.** Example 16: The $C^1$ shape preserving curve with its nodal derivatives estimated using the *Opt* method (blue) and the *Aa*, *Br* methods (red). (For interpretation of the references to color in this figure legend, the reader is referred to the web version of this article.)

| 2nd Derivative | $\mathcal{K}_{Opt}$ | $\mathcal{K}_{par}$ | $\mathcal{K}_{fd}$ | $\mathcal{K}_{FB}$ | $\mathcal{K}_{Br}$ | $\mathcal{K}_{Aw}$ | $\mathcal{K}_{Aa}$ | Min |
|---|---|---|---|---|---|---|---|---|
| $\max_i \lvert c''_{i-1}(x_i) - c''_i(x_i)\rvert$ | 227.30 | 3586.1 | 3586.1 | 2312.6 | 2735.9 | 2735.9 | 2735.9 | Opt |
| $\sum_i \lvert c''_{i-1}(x_i) - c''_i(x_i)\rvert$ | 619.70 | 4108.1 | 4108.1 | 2974.1 | 3331.6 | 3331.6 | 3331.6 | Opt |
| $\sum_i \int (c''_i(x))^2 dx$ | 2199.0 | 13098.3 | 13098.3 | 199.87 | 120.67 | 120.67 | 120.67 | Br,Aw,Aa |
| Curvature | $\mathcal{K}_{Opt}$ | $\mathcal{K}_{par}$ | $\mathcal{K}_{fd}$ | $\mathcal{K}_{FB}$ | $\mathcal{K}_{Br}$ | $\mathcal{K}_{Aw}$ | $\mathcal{K}_{Aa}$ | Min |
| $\max_i \lvert \kappa_{i-1}(x_i) - \kappa_i(x_i)\rvert$ | 227.30 | 318.06 | 318.06 | 337.68 | 243.39 | 243.39 | 243.39 | Opt |
| $\sum_i \lvert \kappa_{i-1}(x_i) - \kappa_i(x_i)\rvert$ | 231.37 | 336.02 | 336.02 | 434.48 | 410.55 | 410.55 | 410.55 | Opt |
| $\sum_i \int (\kappa_i(x))^2 dx$ | 2.79 | 0.92 | 0.92 | 6.32 | 25.81 | 25.81 | 25.81 | par,fd |

**Example 19.** Data from Sarfraz, et al. [24]: data, degree distributions and fairness measures for various derivative estimation methods. The results are shown in Fig. 17.

| Points $(x_i, f_i)$ | $\mathcal{K}_{Opt}$ | $\mathcal{K}_{par}$ | $\mathcal{K}_{fd}$ | $\mathcal{K}_{FB}$ | $\mathcal{K}_{Br}$ | $\mathcal{K}_{Aw}$ | $\mathcal{K}_{Aa}$ |
|---|---|---|---|---|---|---|---|
| (2,10) | 6 | 6 | 6 | 6 | 6 | 6 | 6 |
| (3,2) | 16 | 13 | 4 | 3 | 3 | 4 | 8 |
| (7,3) | 3 | 3 | 3 | 3 | 3 | 3 | 3 |
| (8,7) | 3 | 3 | 3 | 3 | 3 | 3 | 3 |
| (9,2) | 13 | 23 | 7 | 3 | 3 | 5 | 6 |
| (13,3) | 4 | 3 | 6 | 6 | 6 | 6 | 7 |
| (14,10) | | | | | | | |

End point derivatives: $v_0 = -9.65$ and $v_6 = 8.35$.

(*continued on next page*)

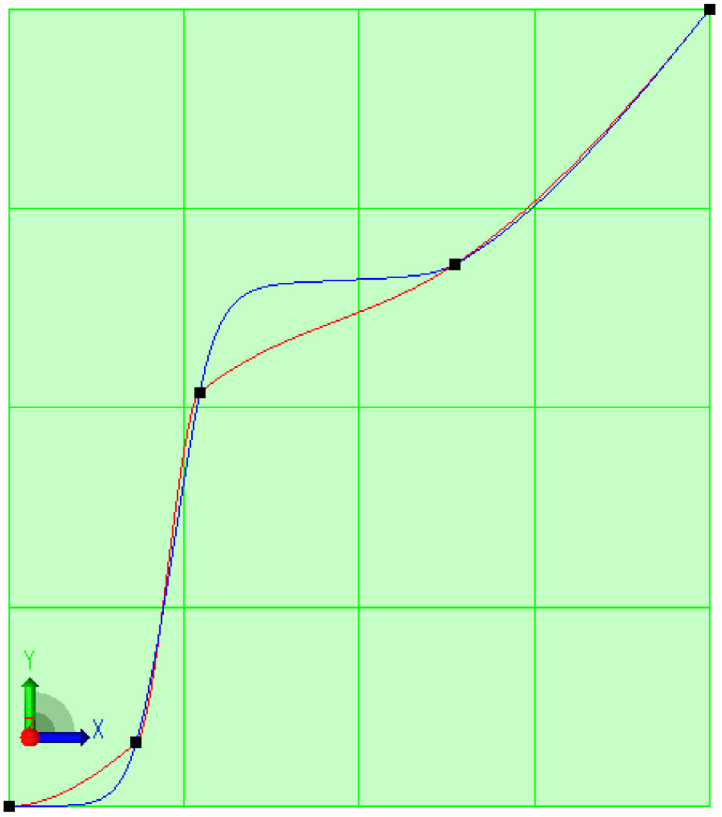


**Fig. 15.** Example 17: The $C^1$ shape preserving curve with its nodal derivatives estimated using the *Opt* method (blue) and the *Br* method (red). (For interpretation of the references to color in this figure legend, the reader is referred to the web version of this article.)

(*continued*)

| Points $(x_i, f_i)$ | $\mathcal{K}_{Opt}$ | $\mathcal{K}_{par}$ | $\mathcal{K}_{fd}$ | $\mathcal{K}_{FB}$ | $\mathcal{K}_{Br}$ | $\mathcal{K}_{Aw}$ | $\mathcal{K}_{Aa}$ | |
|---|---|---|---|---|---|---|---|---|
| | | | | | | | | Min |
| Max degree | 16 | 23 | 7 | 6 | 6 | 6 | 8 | FB,Br,Aw |
| Sum of degrees | 45 | 51 | 29 | 24 | 24 | 27 | 33 | FB,Br |

| 2nd Derivative | $\mathcal{K}_{Opt}$ | $\mathcal{K}_{par}$ | $\mathcal{K}_{fd}$ | $\mathcal{K}_{FB}$ | $\mathcal{K}_{Br}$ | $\mathcal{K}_{Aw}$ | $\mathcal{K}_{Aa}$ | Min |
|---|---|---|---|---|---|---|---|---|
| $\max_i \lvert c''_{i-1}(x_i) - c''_i(x_i)\rvert$ | 47.94 | 47.94 | 47.94 | 47.90 | 47.76 | 47.94 | 47.42 | Br,Aa |
| $\sum_i \lvert c''_{i-1}(x_i) - c''_i(x_i)\rvert$ | 105.97 | 94.02 | 134.85 | 143.61 | 146.25 | 139.32 | 154.09 | par |
| $\sum_i \int (c''_i(x))^2 dx$ | 46.79 | 48.00 | 46.34 | 46.40 | 46.70 | 46.10 | 46.94 | fd,FB,Aw |
| Curvature | $\mathcal{K}_{Opt}$ | $\mathcal{K}_{par}$ | $\mathcal{K}_{fd}$ | $\mathcal{K}_{FB}$ | $\mathcal{K}_{Br}$ | $\mathcal{K}_{Aw}$ | $\mathcal{K}_{Aa}$ | Min |
| $\max_i \lvert \kappa_{i-1}(x_i) - \kappa_i(x_i)\rvert$ | 47.94 | 47.94 | 47.94 | 47.90 | 47.76 | 47.94 | 47.42 | Br,Aa |
| $\sum_i \lvert \kappa_{i-1}(x_i) - \kappa_i(x_i)\rvert$ | 94.10 | 92.48 | 97.12 | 117.87 | 133.68 | 103.19 | 149.42 | par |
| $\sum_i \int (\kappa_i(x))^2 dx$ | 1.94 | 1.94 | 2.14 | 2.52 | 3.26 | 2.15 | 4.16 | Opt,par |

**Example 20.** Data from Hussain & Sarfraz [26]: data, degree distributions and fairness measures for various derivative estimation methods. The results are shown in Fig. 18.

| Points $(x_i, f_i)$ | $\mathcal{K}_{Opt}$ | $\mathcal{K}_{par}$ | $\mathcal{K}_{fd}$ | $\mathcal{K}_{FB}$ | $\mathcal{K}_{Br}$ | $\mathcal{K}_{Aw}$ | $\mathcal{K}_{Aa}$ |
|---|---|---|---|---|---|---|---|
| (0,0) | 3 | 3 | 3 | 3 | 3 | 3 | 3 |
| (6,15) | 1 | 1 | 1 | 1 | 1 | 1 | 1 |
| (10,15) | 10 | 20 | 4 | 3 | 4 | 14 | 3 |
| (29.5,25) | 6 | 6 | 11 | 10 | 11 | 5 | 11 |
| (30,30) | | | | | | | |

End point derivatives: $v_0 = 4$ and $v_4 = 11$.

Min

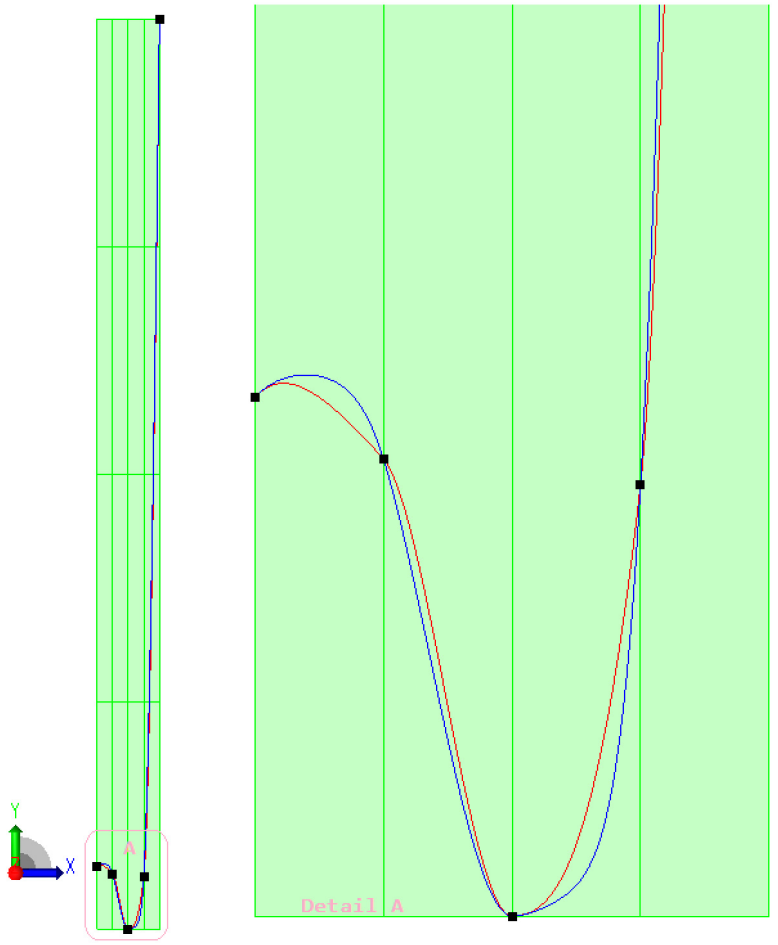


**Fig. 16.** Example 18: The $C^1$ shape preserving curve with its nodal derivatives estimated using the *Opt* method (blue) and the *FB* method (red). (For interpretation of the references to color in this figure legend, the reader is referred to the web version of this article.)

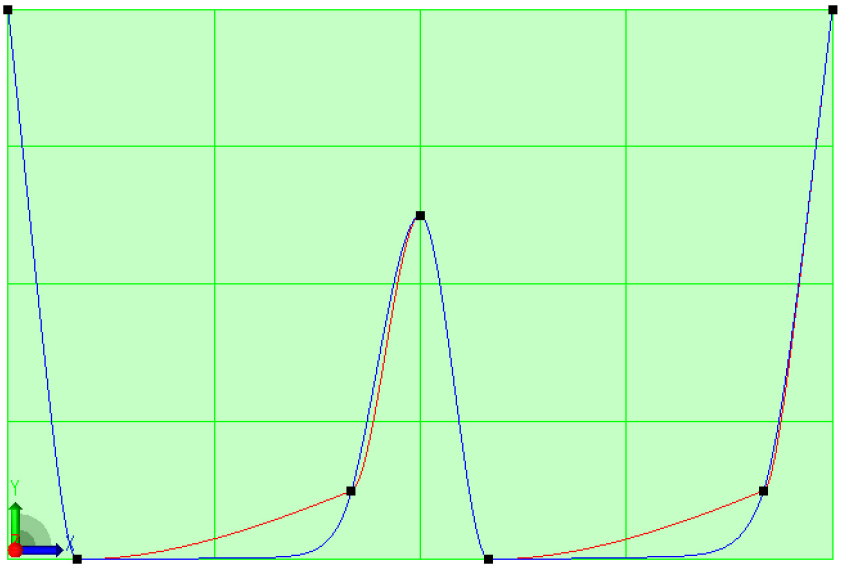


**Fig. 17.** Example 19: The $C^1$ shape preserving curve with its nodal derivatives estimated using the *Opt* method (blue) and the *Br* method (red). (For interpretation of the references to color in this figure legend, the reader is referred to the web version of this article.)

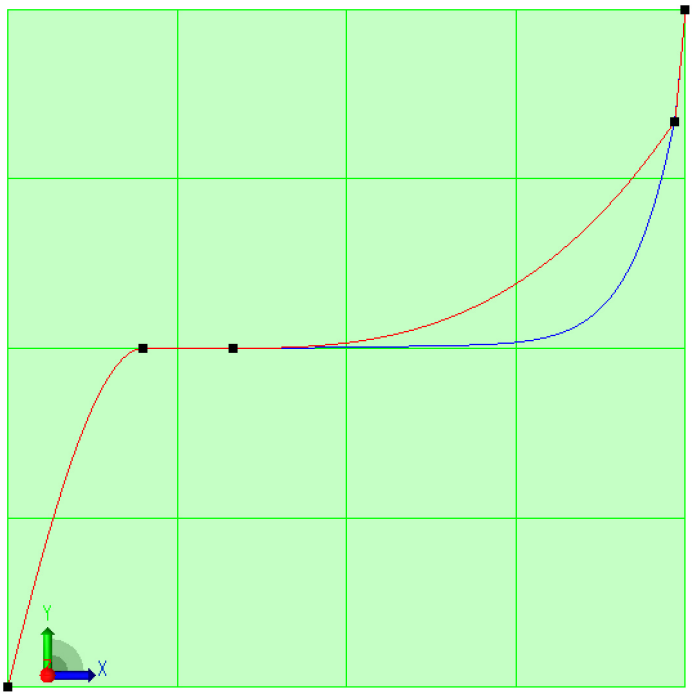


**Fig. 18.** Example 20: The $C^1$ shape preserving curve with its nodal derivatives estimated using the *Opt* method (blue) and the *Aa* method (red). (For interpretation of the references to color in this figure legend, the reader is referred to the web version of this article.)

(*continued*)

| Points $(x_i, f_i)$ | $\mathcal{K}_{Opt}$ | $\mathcal{K}_{par}$ | $\mathcal{K}_{fd}$ | $\mathcal{K}_{FB}$ | $\mathcal{K}_{Br}$ | $\mathcal{K}_{Aw}$ | $\mathcal{K}_{Aa}$ | |
|---|---|---|---|---|---|---|---|---|
| Max degree | 10 | 20 | 11 | 10 | 11 | 14 | 11 | Opt,FB |
| Sum of degrees | 20 | 30 | 19 | 17 | 19 | 23 | 18 | FB |

| 2nd Derivative | $\mathcal{K}_{Opt}$ | $\mathcal{K}_{par}$ | $\mathcal{K}_{fd}$ | $\mathcal{K}_{FB}$ | $\mathcal{K}_{Br}$ | $\mathcal{K}_{Aw}$ | $\mathcal{K}_{Aa}$ | Min |
|---|---|---|---|---|---|---|---|---|
| $\max_i \lvert c''_{i-1}(x_i) - c''_i(x_i)\rvert$ | 57.53 | 1.17 | 203.32 | 171.87 | 203.12 | 26.53 | 217.04 | par |
| $\sum_i \lvert c''_{i-1}(x_i) - c''_i(x_i)\rvert$ | 58.71 | 1.50 | 204.58 | 173.05 | 204.39 | 27.71 | 218.35 | par |
| $\sum_i \int (c''_i(x))^2 dx$ | 1.29 | 1.00 | 0.12 | 0.12 | 0.12 | 4.35 | 0.11 | Aa |
| Curvature | $\mathcal{K}_{Opt}$ | $\mathcal{K}_{par}$ | $\mathcal{K}_{fd}$ | $\mathcal{K}_{FB}$ | $\mathcal{K}_{Br}$ | $\mathcal{K}_{Aw}$ | $\mathcal{K}_{Aa}$ | Min |
| $\max_i \lvert \kappa_{i-1}(x_i) - \kappa_i(x_i)\rvert$ | 1.17 | 1.17 | 104.10 | 33.97 | 102.69 | 1.17 | 210.88 | Opt,par,Aw |
| $\sum_i \lvert \kappa_{i-1}(x_i) - \kappa_i(x_i)\rvert$ | 1.60 | 1.63 | 105.37 | 35.15 | 103.96 | 1.27 | 212.19 | Aw |
| $\sum_i \int (\kappa_i(x))^2 dx$ | 4.3e−04 | 3.1e−03 | 0.08 | 0.04 | 0.08 | 9.2e−05 | 0.19 | Aw |

**Example 21.** Data from Han et al. [34]: data, degree distributions and fairness measures for various derivative estimation methods. The results are shown in Fig. 19.

| Points $(x_i, f_i)$ | $\mathcal{K}_{Opt}$ | $\mathcal{K}_{par}$ | $\mathcal{K}_{fd}$ | $\mathcal{K}_{FB}$ | $\mathcal{K}_{Br}$ | $\mathcal{K}_{Aw}$ | $\mathcal{K}_{Aa}$ | |
|---|---|---|---|---|---|---|---|---|
| (1,14) | 3 | 3 | 3 | 3 | 3 | 3 | 3 | |
| (2,8) | 4 | 3 | 9 | 8 | 11 | 8 | 12 | |
| (3,3) | 5 | 10 | 3 | 3 | 3 | 5 | 5 | |
| (8,0.8) | 1 | 1 | 1 | 1 | 1 | 1 | 1 | |
| (10,0.8) | 3 | 3 | 3 | 3 | 3 | 3 | 3 | |
| (11,0.45) | 10 | 14 | 8 | 5 | 3 | 3 | 3 | |
| (12,0.4) | 3 | 3 | 3 | 3 | 5 | 3 | 7 | |
| (14,0.37) | | | | | | | | |
| End point derivatives: $v_0 = -6.5$ and $v_7 = 0.00833333$. | | | | | | | | |
| | | | | | | | | Min |
| Max degree | 10 | 14 | 9 | 8 | 11 | 8 | 12 | FB,Aw |
| Sum of degrees | 29 | 37 | 30 | 26 | 29 | 26 | 34 | FB,Aw |

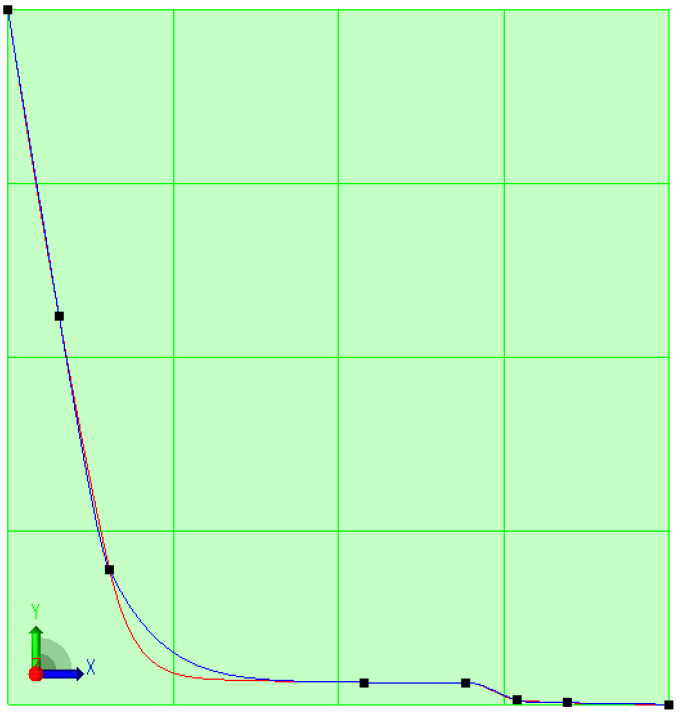


**Fig. 19.** Example 21: The $C^1$ shape preserving curve with its nodal derivatives estimated using the *Opt* method (blue) and the *par* method (red). (For interpretation of the references to color in this figure legend, the reader is referred to the web version of this article.)

| 2nd Derivative | $\mathcal{K}_{Opt}$ | $\mathcal{K}_{par}$ | $\mathcal{K}_{fd}$ | $\mathcal{K}_{FB}$ | $\mathcal{K}_{Br}$ | $\mathcal{K}_{Aw}$ | $\mathcal{K}_{Aa}$ | Min |
|---|---|---|---|---|---|---|---|---|
| $\max_i \lvert c''_{i-1}(x_i) - c''_i(x_i)\rvert$ | 9.97 | 5.56 | 33.74 | 30.57 | 47.46 | 23.96 | 55.89 | par |
| $\sum_i \lvert c''_{i-1}(x_i) - c''_i(x_i)\rvert$ | 14.87 | 8.63 | 36.38 | 33.93 | 52.26 | 28.80 | 60.81 | par |
| $\sum_i \int (c''_i(x))^2 dx$ | 1.75 | 0.09 | 13.56 | 11.35 | 25.14 | 7.64 | 33.89 | par |
| Curvature | $\mathcal{K}_{Opt}$ | $\mathcal{K}_{par}$ | $\mathcal{K}_{fd}$ | $\mathcal{K}_{FB}$ | $\mathcal{K}_{Br}$ | $\mathcal{K}_{Aw}$ | $\mathcal{K}_{Aa}$ | Min |
| $\max_i \lvert \kappa_{i-1}(x_i) - \kappa_i(x_i)\rvert$ | 1.93 | 1.70 | 8.85 | 9.00 | 26.77 | 2.63 | 46.69 | par |
| $\sum_i \lvert \kappa_{i-1}(x_i) - \kappa_i(x_i)\rvert$ | 4.21 | 2.58 | 10.72 | 12.25 | 30.63 | 6.30 | 50.81 | par |
| $\sum_i \int (\kappa_i(x))^2 dx$ | 0.07 | 0.05 | 0.04 | 0.04 | 0.04 | 0.04 | 0.04 | FB |

**Example 22.** Data from Abbas et al. [28]: data, degree distributions and fairness measures for various derivative estimation methods. The results are shown in Fig. 20.

| Points $(x_i, f_i)$ | $\mathcal{K}_{Opt}$ | $\mathcal{K}_{par}$ | $\mathcal{K}_{fd}$ | $\mathcal{K}_{FB}$ | $\mathcal{K}_{Br}$ | $\mathcal{K}_{Aw}$ | $\mathcal{K}_{Aa}$ | |
|---|---|---|---|---|---|---|---|---|
| (10,0.31) | 3 | 20 | 20 | 16 | 21 | 21 | 21 | |
| (12.5,0.4) | 61 | 54 | 90 | 41 | 19 | 11 | 23 | |
| (15,0.5) | 3 | 15 | 4 | 4 | 3 | 7 | 3 | |
| (19.2,1.86) | 3 | 14 | 3 | 3 | 4 | 3 | 6 | |
| (19.6,3.02) | 3 | 3 | 8 | 5 | 8 | 5 | 12 | |
| (19.8,4.44) | 3 | 3 | 3 | 3 | 3 | 3 | 3 | |
| (19.9,5.27) | 6 | 5 | 8 | 9 | 6 | 4 | 7 | |
| (20,6.06) | 3 | 3 | 3 | 3 | 3 | 3 | 3 | |
| (20.05,6.45) | 3 | 3 | 3 | 3 | 3 | 3 | 3 | |
| (20.11,7.02) | | | | | | | | |
| End point derivatives: $v_0 = 0$ and $v_9 = 10.4273$. | | | | | | | | |
| | | | | | | | | Min |
| Max degree | 61 | 54 | 90 | 41 | 21 | 21 | 23 | Br,Aw |
| Sum of degrees | 88 | 120 | 142 | 87 | 70 | 60 | 81 | Aw |

| 2nd Derivative | $\mathcal{K}_{Opt}$ | $\mathcal{K}_{par}$ | $\mathcal{K}_{fd}$ | $\mathcal{K}_{FB}$ | $\mathcal{K}_{Br}$ | $\mathcal{K}_{Aw}$ | $\mathcal{K}_{Aa}$ | Min |
|---|---|---|---|---|---|---|---|---|
| $\max_i \lvert c''_{i-1}(x_i) - c''_i(x_i)\rvert$ | 24.27 | 77.98 | 109.76 | 75.20 | 123.87 | 43.64 | 211.76 | Opt |
| $\sum_i \lvert c''_{i-1}(x_i) - c''_i(x_i)\rvert$ | 82.09 | 175.50 | 268.70 | 207.35 | 261.27 | 120.53 | 383.06 | Opt |
| $\sum_i \int (c''_i(x))^2 dx$ | 3.90 | 47.25 | 5.92 | 7.18 | 4.52 | 4.42 | 5.15 | Opt |
| Curvature | $\mathcal{K}_{Opt}$ | $\mathcal{K}_{par}$ | $\mathcal{K}_{fd}$ | $\mathcal{K}_{FB}$ | $\mathcal{K}_{Br}$ | $\mathcal{K}_{Aw}$ | $\mathcal{K}_{Aa}$ | Min |

(*continued on next page*)

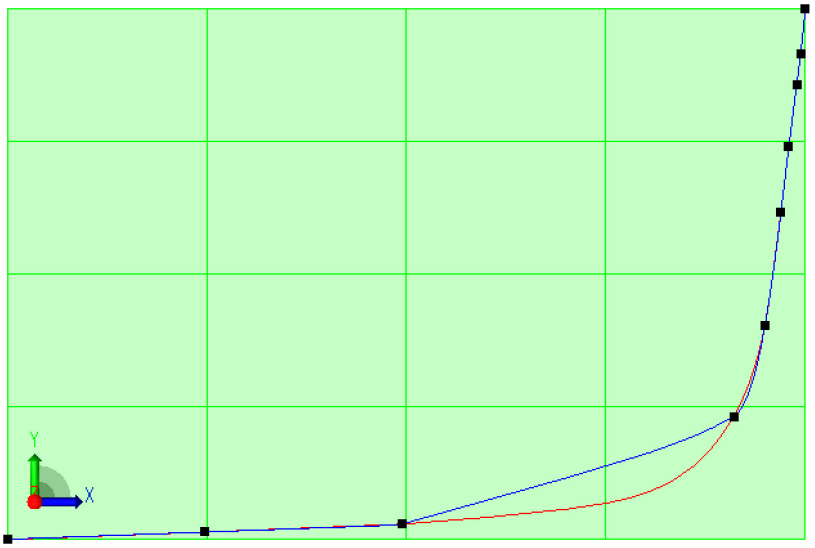


**Fig. 20.** Example 22: The $C^1$ shape preserving curve with its nodal derivatives estimated using the *Opt* method (blue) and the *Aw* method (red). (For interpretation of the references to color in this figure legend, the reader is referred to the web version of this article.)

(*continued*)

| 2nd Derivative | $\mathcal{K}_{Opt}$ | $\mathcal{K}_{par}$ | $\mathcal{K}_{fd}$ | $\mathcal{K}_{FB}$ | $\mathcal{K}_{Br}$ | $\mathcal{K}_{Aw}$ | $\mathcal{K}_{Aa}$ | Min |
|---|---|---|---|---|---|---|---|---|
| $\max_i \lvert\kappa_{i-1}(x_i) - \kappa_i(x_i)\rvert$ | 207.23 | 78.25 | 354.40 | 24.16 | 17.16 | 0.37 | 38.18 | Aw |
| $\sum_i \lvert\kappa_{i-1}(x_i) - \kappa_i(x_i)\rvert$ | 217.58 | 79.17 | 366.95 | 30.20 | 22.33 | 0.57 | 48.43 | Aw |
| $\sum_i \int (\kappa_i(x))^2 dx$ | 0.42 | 0.44 | 0.81 | 0.28 | 1.22 | 0.54 | 2.88 | FB |

**Example 23.** Data from Abbas et al. [28]: data, degree distributions and fairness measures for various derivative estimation methods. The results are shown in Fig. 21.

| Points $(x_i, f_i)$ | $\mathcal{K}_{Opt}$ | $\mathcal{K}_{par}$ | $\mathcal{K}_{fd}$ | $\mathcal{K}_{FB}$ | $\mathcal{K}_{Br}$ | $\mathcal{K}_{Aw}$ | $\mathcal{K}_{Aa}$ | |
|---|---|---|---|---|---|---|---|---|
| (1,0) | 1 | 1 | 1 | 1 | 1 | 1 | 1 | |
| (2,0) | 3 | 5 | 4 | 3 | 3 | 3 | 4 | |
| (12,4.2) | 3 | 3 | 3 | 3 | 3 | 3 | 3 | |
| (18,20.8) | 5 | 5 | 5 | 5 | 7 | 7 | 7 | |
| (24,34.3) | 3 | 102 | 102 | 102 | 42 | 42 | 42 | |
| (30,37.8) | 3 | 3 | 3 | 3 | 3 | 3 | 3 | |
| (36,41.2) | 4 | 3 | 3 | 3 | 3 | 3 | 3 | |
| (40,43.7) | | | | | | | | |
| End point derivatives: $v_0 = 0$ and $v_7 = 0.648333$. | | | | | | | | |
| | | | | | | | | Min |
| Max degree | 5 | 102 | 102 | 102 | 42 | 42 | 42 | Opt |
| Sum of degrees | 22 | 122 | 121 | 120 | 62 | 62 | 63 | Opt |

| 2nd Derivative | $\mathcal{K}_{Opt}$ | $\mathcal{K}_{par}$ | $\mathcal{K}_{fd}$ | $\mathcal{K}_{FB}$ | $\mathcal{K}_{Br}$ | $\mathcal{K}_{Aw}$ | $\mathcal{K}_{Aa}$ | Min |
|---|---|---|---|---|---|---|---|---|
| $\max_i \lvert c''_{i-1}(x_i) - c''_i(x_i)\rvert$ | 1.37 | 1.23 | 1.23 | 1.46 | 2.07 | 2.07 | 2.07 | par,fd |
| $\sum_i \lvert c''_{i-1}(x_i) - c''_i(x_i)\rvert$ | 3.05 | 2.29 | 3.19 | 3.90 | 5.03 | 4.71 | 5.19 | par |
| $\sum_i \int (c''_i(x))^2 dx$ | 0.17 | 0.21 | 0.18 | 0.20 | 0.32 | 0.31 | 0.32 | Opt |
| Curvature | $\mathcal{K}_{Opt}$ | $\mathcal{K}_{par}$ | $\mathcal{K}_{fd}$ | $\mathcal{K}_{FB}$ | $\mathcal{K}_{Br}$ | $\mathcal{K}_{Aw}$ | $\mathcal{K}_{Aa}$ | Min |
| $\max_i \lvert\kappa_{i-1}(x_i) - \kappa_i(x_i)\rvert$ | 0.88 | 182.79 | 182.79 | 183.11 | 25.29 | 25.29 | 25.29 | Opt |
| $\sum_i \lvert\kappa_{i-1}(x_i) - \kappa_i(x_i)\rvert$ | 1.38 | 182.91 | 183.10 | 183.65 | 26.27 | 25.93 | 26.48 | Opt |
| $\sum_i \int (\kappa_i(x))^2 dx$ | 9.9e−03 | 0.05 | 0.05 | 0.04 | 0.06 | 0.04 | 0.07 | Opt |

**Example 24.** Data from Sarfraz et al. [25]: data, degree distributions and fairness measures for various derivative estimation methods. The results are shown in Fig. 22.

| Points $(x_i, f_i)$ | $\mathcal{K}_{Opt}$ | $\mathcal{K}_{par}$ | $\mathcal{K}_{fd}$ | $\mathcal{K}_{FB}$ | $\mathcal{K}_{Br}$ | $\mathcal{K}_{Aw}$ | $\mathcal{K}_{Aa}$ |
|---|---|---|---|---|---|---|---|
| (2,12) | 6 | 6 | 6 | 6 | 6 | 6 | 6 |
| (3,4.5) | 11 | 9 | 3 | 3 | 3 | 4 | 11 |

(*continued on next page*)

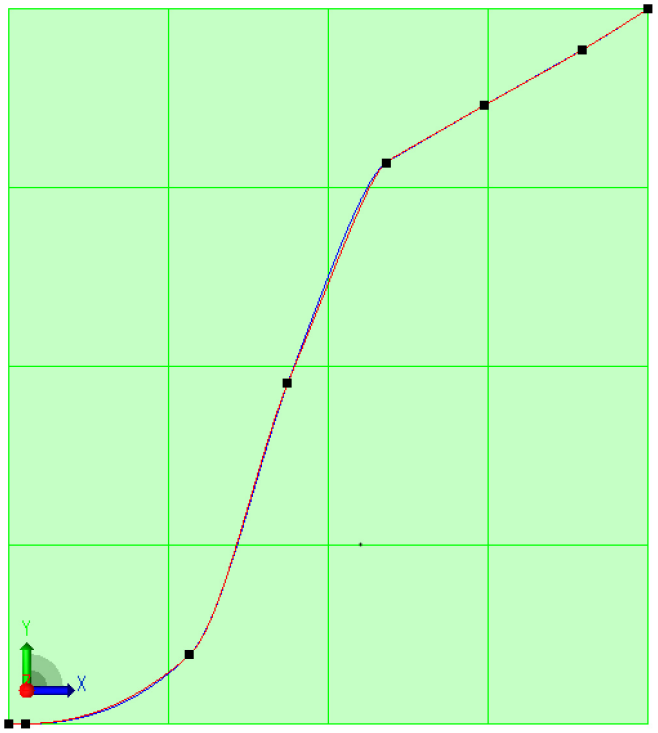


**Fig. 21.** Example 23: The $C^1$ shape preserving curve with its nodal derivatives estimated using the *Opt* method (blue) and the *Aw* method (red). (For interpretation of the references to color in this figure legend, the reader is referred to the web version of this article.)

(*continued*)

| Points $(x_i, f_i)$ | $\mathcal{K}_{Opt}$ | $\mathcal{K}_{par}$ | $\mathcal{K}_{fd}$ | $\mathcal{K}_{FB}$ | $\mathcal{K}_{Br}$ | $\mathcal{K}_{Aw}$ | $\mathcal{K}_{Aa}$ | |
|---|---|---|---|---|---|---|---|---|
| (7,6.5) | 3 | 3 | 3 | 3 | 3 | 3 | 3 | |
| (8,12) | 3 | 3 | 3 | 3 | 3 | 3 | 3 | |
| (9,7.5) | 8 | 14 | 5 | 3 | 3 | 5 | 8 | |
| (13,9.5) | 4 | 3 | 6 | 6 | 6 | 6 | 7 | |
| (14,18) | | | | | | | | |
| End point derivatives: $v_0 = -9.1$ and $v_6 = 10.1$. | | | | | | | | |
| | | | | | | | | Min |
| Max degree | 11 | 14 | 6 | 6 | 6 | 6 | 11 | fd,FB,Br,Aw |
| Sum of degrees | 35 | 38 | 26 | 24 | 24 | 27 | 38 | FB,Br |

| 2nd Derivative | $\mathcal{K}_{Opt}$ | $\mathcal{K}_{par}$ | $\mathcal{K}_{fd}$ | $\mathcal{K}_{FB}$ | $\mathcal{K}_{Br}$ | $\mathcal{K}_{Aw}$ | $\mathcal{K}_{Aa}$ | Min |
|---|---|---|---|---|---|---|---|---|
| $\max_i \lvert c''_{i-1}(x_i) - c''_i(x_i)\rvert$ | 44.88 | 44.88 | 44.88 | 44.76 | 46.06 | 44.81 | 56.37 | Opt,par,fd,FB,Aw |
| $\sum_i \lvert c''_{i-1}(x_i) - c''_i(x_i)\rvert$ | 90.79 | 100.05 | 137.03 | 144.69 | 151.48 | 134.95 | 162.31 | Opt |
| $\sum_i \int (c''_i(x))^2 dx$ | 51.04 | 66.45 | 45.93 | 46.06 | 46.77 | 45.46 | 47.35 | Aw |
| Curvature | $\mathcal{K}_{Opt}$ | $\mathcal{K}_{par}$ | $\mathcal{K}_{fd}$ | $\mathcal{K}_{FB}$ | $\mathcal{K}_{Br}$ | $\mathcal{K}_{Aw}$ | $\mathcal{K}_{Aa}$ | Min |
| $\max_i \lvert \kappa_{i-1}(x_i) - \kappa_i(x_i)\rvert$ | 44.88 | 44.88 | 44.88 | 44.76 | 44.52 | 44.81 | 43.47 | Aa |
| $\sum_i \lvert \kappa_{i-1}(x_i) - \kappa_i(x_i)\rvert$ | 77.04 | 74.97 | 82.09 | 90.63 | 111.97 | 79.84 | 141.32 | par |
| $\sum_i \int (\kappa_i(x))^2 dx$ | 2.03 | 2.03 | 2.10 | 2.16 | 2.52 | 2.07 | 3.39 | Opt,par |

**Example 25.** Data from Sarfraz et al. [25]: data, degree distributions and fairness measures for various derivative estimation methods. The results are shown in Fig. 23.

| Points $(x_i, f_i)$ | $\mathcal{K}_{Opt}$ | $\mathcal{K}_{par}$ | $\mathcal{K}_{fd}$ | $\mathcal{K}_{FB}$ | $\mathcal{K}_{Br}$ | $\mathcal{K}_{Aw}$ | $\mathcal{K}_{Aa}$ |
|---|---|---|---|---|---|---|---|
| (−4,5) | 3 | 3 | 3 | 3 | 3 | 3 | 3 |
| (−3.5,0) | 5 | 8 | 3 | 3 | 3 | 3 | 9 |
| (−2,−3.5) | 3 | 6 | 5 | 3 | 3 | 3 | 3 |
| (0,−4) | 3 | 3 | 3 | 3 | 3 | 3 | 3 |
| (2,3.5) | 3 | 3 | 3 | 3 | 3 | 3 | 3 |
| (3.5,0) | 5 | 5 | 5 | 5 | 5 | 5 | 5 |

(*continued on next page*)

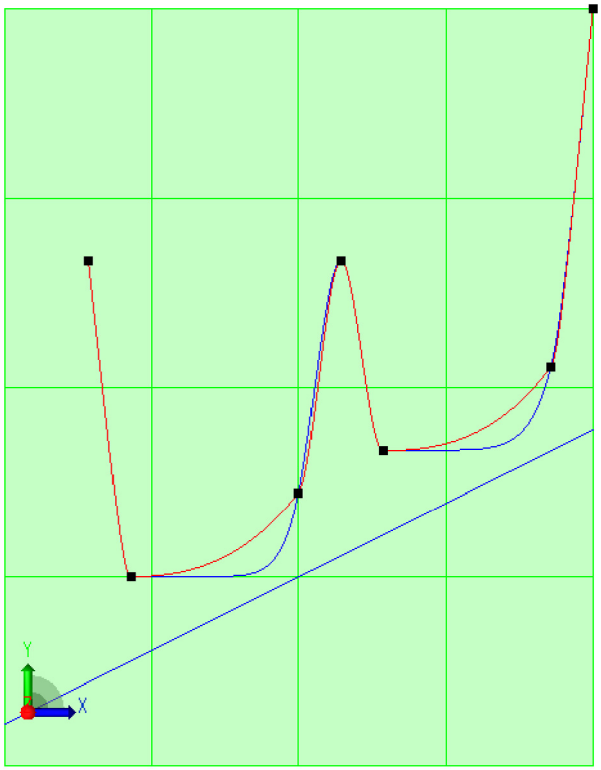


**Fig. 22.** Example 24: The $C^1$ shape preserving curve with its nodal derivatives estimated using the *Opt* method (blue) and the *FB* method (red). (For interpretation of the references to color in this figure legend, the reader is referred to the web version of this article.)

(*continued*)

| Points $(x_i, f_i)$ | $\mathcal{K}_{Opt}$ | $\mathcal{K}_{par}$ | $\mathcal{K}_{fd}$ | $\mathcal{K}_{FB}$ | $\mathcal{K}_{Br}$ | $\mathcal{K}_{Aw}$ | $\mathcal{K}_{Aa}$ | |
|---|---|---|---|---|---|---|---|---|
| (4,5) | | | | | | | | |
| End point derivatives: $v_0 = 0$ and $v_6 = 13.0833$. | | | | | | | | |
| | | | | | | | | Min |
| Max degree | 5 | 8 | 5 | 5 | 5 | 5 | 9 | Opt,fd,FB,Br,Aw |
| Sum of degrees | 22 | 28 | 22 | 20 | 20 | 20 | 26 | FB,Br,Aw |

| 2nd Derivative | $\mathcal{K}_{Opt}$ | $\mathcal{K}_{par}$ | $\mathcal{K}_{fd}$ | $\mathcal{K}_{FB}$ | $\mathcal{K}_{Br}$ | $\mathcal{K}_{Aw}$ | $\mathcal{K}_{Aa}$ | Min |
|---|---|---|---|---|---|---|---|---|
| $\max_i \lvert c''_{i-1}(x_i) - c''_i(x_i)\rvert$ | 89.11 | 89.11 | 89.11 | 89.11 | 92.18 | 89.11 | 98.94 | Opt,par,fd,FB,Aw |
| $\sum_i \lvert c''_{i-1}(x_i) - c''_i(x_i)\rvert$ | 117.21 | 130.14 | 186.28 | 180.58 | 197.63 | 172.51 | 212.39 | Opt |
| $\sum_i \int (c''_i(x))^2 dx$ | 15.21 | 24.53 | 52.33 | 47.85 | 60.12 | 42.01 | 70.28 | Opt |
| Curvature | $\mathcal{K}_{Opt}$ | $\mathcal{K}_{par}$ | $\mathcal{K}_{fd}$ | $\mathcal{K}_{FB}$ | $\mathcal{K}_{Br}$ | $\mathcal{K}_{Aw}$ | $\mathcal{K}_{Aa}$ | Min |
| $\max_i \lvert \kappa_{i-1}(x_i) - \kappa_i(x_i)\rvert$ | 89.11 | 89.11 | 89.11 | 89.11 | 89.11 | 89.11 | 89.11 | Opt,par,fd,FB,Br,Aw,Aa |
| $\sum_i \lvert \kappa_{i-1}(x_i) - \kappa_i(x_i)\rvert$ | 102.56 | 102.88 | 103.65 | 103.33 | 106.67 | 102.71 | 115.70 | Opt,par,FB,Aw |
| $\sum_i \int (\kappa_i(x))^2 dx$ | 44.58 | 53.16 | 72.65 | 69.80 | 77.22 | 65.99 | 81.95 | Opt |

**Example 26.** Data from Kvasov [21]: data, degree distributions and fairness measures for various derivative estimation methods. The results are shown in Fig. 24.

| Points $(x_i, f_i)$ | $\mathcal{K}_{Opt}$ | $\mathcal{K}_{par}$ | $\mathcal{K}_{fd}$ | $\mathcal{K}_{FB}$ | $\mathcal{K}_{Br}$ | $\mathcal{K}_{Aw}$ | $\mathcal{K}_{Aa}$ |
|---|---|---|---|---|---|---|---|
| (0,0) | 3 | 3 | 3 | 3 | 3 | 3 | 3 |
| (2,3) | 3 | 3 | 4 | 3 | 3 | 4 | 3 |
| (3,3.6) | 5 | 4 | 4 | 4 | 3 | 3 | 3 |
| (4,3.8) | 12 | 12 | 12 | 9 | 5 | 5 | 5 |
| (5,4.1) | 3 | 5 | 5 | 6 | 8 | 8 | 8 |
| (6,5.5) | 5 | 5 | 5 | 3 | 5 | 5 | 5 |
| (7,7.2) | 3 | 3 | 3 | 3 | 3 | 3 | 3 |
| (8,9) | 3 | 3 | 3 | 3 | 3 | 3 | 3 |

(*continued on next page*)

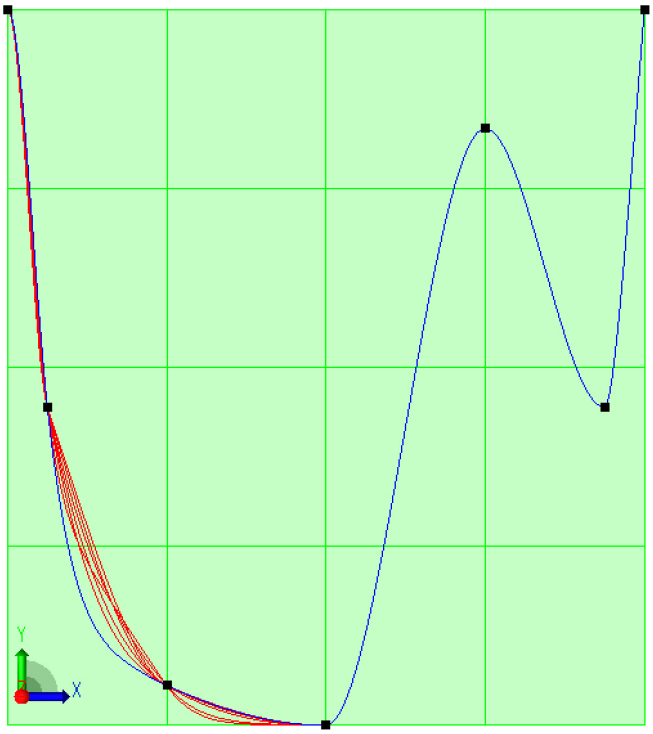


**Fig. 23.** Example 25: The $C^1$ shape preserving curve with its nodal derivatives estimated using the *Opt* method (blue) and all the other methods (red). (For interpretation of the references to color in this figure legend, the reader is referred to the web version of this article.)

(*continued*)

| Points $(x_i, f_i)$ | $\mathcal{K}_{Opt}$ | $\mathcal{K}_{par}$ | $\mathcal{K}_{fd}$ | $\mathcal{K}_{FB}$ | $\mathcal{K}_{Br}$ | $\mathcal{K}_{Aw}$ | $\mathcal{K}_{Aa}$ | |
|---|---|---|---|---|---|---|---|---|
| (9,4) | 3 | 3 | 3 | 3 | 3 | 3 | 3 | |
| (10,2) | | | | | | | | |
| End point derivatives: $v_0 = 2.1$ and $v_9 = -0.5$. | | | | | | | | |
| | | | | | | | | Min |
| Max degree | 12 | 12 | 12 | 9 | 8 | 8 | 8 | Br,Aw,Aa |
| Sum of degrees | 40 | 41 | 42 | 37 | 36 | 37 | 36 | Br,Aa |

| 2nd Derivative | $\mathcal{K}_{Opt}$ | $\mathcal{K}_{par}$ | $\mathcal{K}_{fd}$ | $\mathcal{K}_{FB}$ | $\mathcal{K}_{Br}$ | $\mathcal{K}_{Aw}$ | $\mathcal{K}_{Aa}$ | Min |
|---|---|---|---|---|---|---|---|---|
| $\max_i \lvert c''_{i-1}(x_i) - c''_i(x_i)\rvert$ | 13.20 | 15.70 | 15.70 | 16.06 | 18.14 | 18.14 | 18.14 | Opt |
| $\sum_i \lvert c''_{i-1}(x_i) - c''_i(x_i)\rvert$ | 35.80 | 38.47 | 40.87 | 37.68 | 46.36 | 47.56 | 46.76 | Opt |
| $\sum_i \int (c''_i(x))^2 dx$ | 3.87 | 4.55 | 4.54 | 4.47 | 5.35 | 5.37 | 5.34 | Opt |
| Curvature | $\mathcal{K}_{Opt}$ | $\mathcal{K}_{par}$ | $\mathcal{K}_{fd}$ | $\mathcal{K}_{FB}$ | $\mathcal{K}_{Br}$ | $\mathcal{K}_{Aw}$ | $\mathcal{K}_{Aa}$ | Min |
| $\max_i \lvert \kappa_{i-1}(x_i) - \kappa_i(x_i)\rvert$ | 12.80 | 15.70 | 15.70 | 16.06 | 16.98 | 16.98 | 16.98 | Opt |
| $\sum_i \lvert \kappa_{i-1}(x_i) - \kappa_i(x_i)\rvert$ | 18.69 | 19.42 | 20.13 | 19.07 | 23.13 | 23.94 | 23.23 | Opt |
| $\sum_i \int (\kappa_i(x))^2 dx$ | 0.23 | 0.18 | 0.18 | 0.20 | 0.25 | 0.25 | 0.25 | par |

**Example 27.** Data from Kvasov [21]: data, degree distributions and fairness measures for various derivative estimation methods. The results are shown in Fig. 25.

| Points $(x_i, f_i)$ | $\mathcal{K}_{Opt}$ | $\mathcal{K}_{par}$ | $\mathcal{K}_{fd}$ | $\mathcal{K}_{FB}$ | $\mathcal{K}_{Br}$ | $\mathcal{K}_{Aw}$ | $\mathcal{K}_{Aa}$ |
|---|---|---|---|---|---|---|---|
| (0,2) | 3 | 3 | 3 | 3 | 3 | 3 | 3 |
| (0.2,1.4) | 3 | 6 | 6 | 6 | 3 | 3 | 3 |
| (0.4,1.2) | 7 | 3 | 3 | 3 | 3 | 3 | 3 |
| (0.6,1.08348) | 3 | 3 | 3 | 3 | 3 | 3 | 3 |
| (0.8,1.0202) | 3 | 3 | 3 | 3 | 3 | 3 | 3 |
| (1,1) | 3 | 3 | 3 | 3 | 3 | 3 | 3 |
| (1.2,1.0202) | 3 | 3 | 3 | 3 | 3 | 3 | 3 |
| (1.4,1.08348) | 7 | 3 | 3 | 3 | 3 | 3 | 3 |

(*continued on next page*)

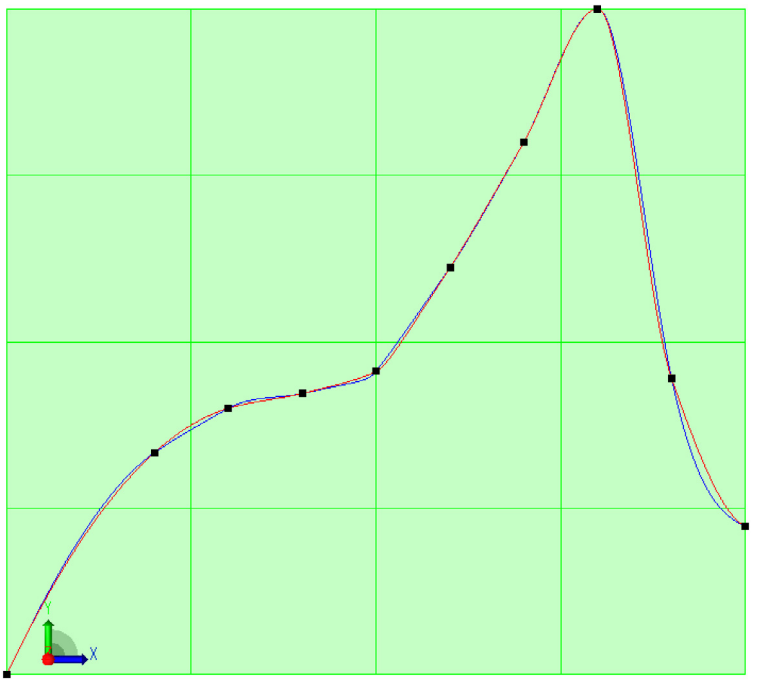


**Fig. 24.** Example 26: The $C^1$ shape preserving curve with its nodal derivatives estimated using the *Opt* method (blue) and the *Br* method (red). (For interpretation of the references to color in this figure legend, the reader is referred to the web version of this article.)

(*continued*)

| Points $(x_i, f_i)$ | $\mathcal{K}_{Opt}$ | $\mathcal{K}_{par}$ | $\mathcal{K}_{fd}$ | $\mathcal{K}_{FB}$ | $\mathcal{K}_{Br}$ | $\mathcal{K}_{Aw}$ | $\mathcal{K}_{Aa}$ | |
|---|---|---|---|---|---|---|---|---|
| (1.6,1.2) | 3 | 6 | 6 | 6 | 3 | 3 | 3 | |
| (1.8,1.4) | 3 | 3 | 3 | 3 | 3 | 3 | 3 | |
| (2,2) | | | | | | | | |
| End point derivatives: $v_0 = -4.5$ and $v_{10} = 4.5$. | | | | | | | | |
| | | | | | | | | Min |
| Max degree | 7 | 6 | 6 | 6 | 3 | 3 | 3 | Br,Aw,Aa |
| Sum of degrees | 38 | 36 | 36 | 36 | 30 | 30 | 30 | Br,Aw,Aa |

| 2nd Derivative | $\mathcal{K}_{Opt}$ | $\mathcal{K}_{par}$ | $\mathcal{K}_{fd}$ | $\mathcal{K}_{FB}$ | $\mathcal{K}_{Br}$ | $\mathcal{K}_{Aw}$ | $\mathcal{K}_{Aa}$ | Min |
|---|---|---|---|---|---|---|---|---|
| $\max_i \lvert c''_{i-1}(x_i) - c''_i(x_i)\rvert$ | 10.94 | 24.95 | 24.95 | 14.80 | 7.64 | 7.64 | 7.64 | Br,Aw,Aa |
| $\sum_i \lvert c''_{i-1}(x_i) - c''_i(x_i)\rvert$ | 32.15 | 57.70 | 57.70 | 37.43 | 25.36 | 25.36 | 25.36 | Br,Aw,Aa |
| $\sum_i \int (c''_i(x))^2 dx$ | 1.38 | 3.36 | 3.36 | 2.51 | 1.38 | 1.38 | 1.38 | Opt,Br,Aw,Aa |
| Curvature | $\mathcal{K}_{Opt}$ | $\mathcal{K}_{par}$ | $\mathcal{K}_{fd}$ | $\mathcal{K}_{FB}$ | $\mathcal{K}_{Br}$ | $\mathcal{K}_{Aw}$ | $\mathcal{K}_{Aa}$ | Min |
| $\max_i \lvert \kappa_{i-1}(x_i) - \kappa_i(x_i)\rvert$ | 2.25 | 2.23 | 2.23 | 1.69 | 2.22 | 2.22 | 2.22 | FB |
| $\sum_i \lvert \kappa_{i-1}(x_i) - \kappa_i(x_i)\rvert$ | 11.28 | 9.08 | 9.08 | 8.28 | 10.81 | 10.81 | 10.81 | FB |
| $\sum_i \int (\kappa_i(x))^2 dx$ | 0.05 | 0.04 | 0.04 | 0.04 | 0.04 | 0.04 | 0.04 | Br,Aw,Aa |

**Example 28.** Data from Kvasov [21]: data, degree distributions and fairness measures for various derivative estimation methods. The results are shown in Fig. 26.

| Points $(x_i, f_i)$ | $\mathcal{K}_{Opt}$ | $\mathcal{K}_{par}$ | $\mathcal{K}_{fd}$ | $\mathcal{K}_{FB}$ | $\mathcal{K}_{Br}$ | $\mathcal{K}_{Aw}$ | $\mathcal{K}_{Aa}$ | |
|---|---|---|---|---|---|---|---|---|
| (0,5) | 4 | 3 | 6 | 5 | 6 | 4 | 6 | |
| (1,7) | 3 | 4 | 3 | 3 | 4 | 3 | 43 | |
| (5,9) | 1 | 1 | 1 | 1 | 1 | 1 | 1 | |
| (8,9) | 4 | 4 | 4 | 4 | 4 | 4 | 4 | |
| (10,1) | | | | | | | | |
| End point derivatives: $v_0 = 2.3$ and $v_4 = -5.6$. | | | | | | | | |
| | | | | | | | | Min |
| Max degree | 4 | 4 | 6 | 5 | 6 | 4 | 43 | Opt,par,Aw |
| Sum of degrees | 12 | 12 | 14 | 13 | 15 | 12 | 54 | Opt,par,Aw |

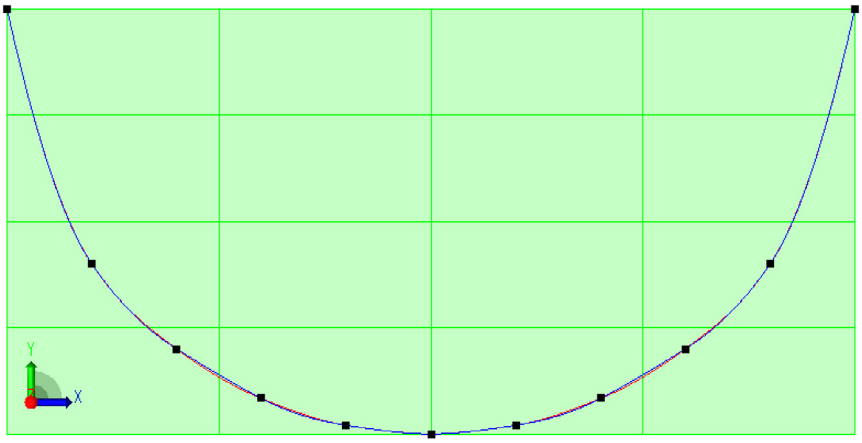


**Fig. 25.** Example 27: The $C^1$ shape preserving curve with its nodal derivatives estimated using the *Opt* method (blue) and the *Aa* method (red). (For interpretation of the references to color in this figure legend, the reader is referred to the web version of this article.)

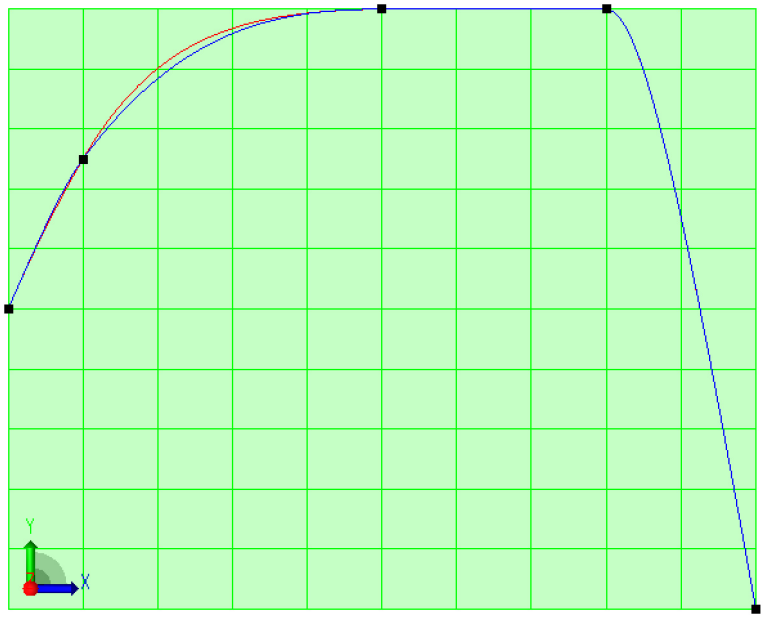


**Fig. 26.** Example 28: The $C^1$ shape preserving curve with its nodal derivatives estimated using the *Opt* method (blue) and the *Aw*, *par* methods (red). (For interpretation of the references to color in this figure legend, the reader is referred to the web version of this article.)

| 2nd Derivative | $\mathcal{K}_{Opt}$ | $\mathcal{K}_{par}$ | $\mathcal{K}_{fd}$ | $\mathcal{K}_{FB}$ | $\mathcal{K}_{Br}$ | $\mathcal{K}_{Aw}$ | $\mathcal{K}_{Aa}$ | Min |
|---|---|---|---|---|---|---|---|---|
| $\max_i \lvert c''_{i-1}(x_i) - c''_i(x_i)\rvert$ | 7.80 | 7.80 | 7.80 | 7.80 | 7.80 | 7.80 | 9.64 | Opt,par,fd,FB,Br,Aw |
| $\sum_i \lvert c''_{i-1}(x_i) - c''_i(x_i)\rvert$ | 9.75 | 8.47 | 15.22 | 12.73 | 15.89 | 10.35 | 18.17 | par |
| $\sum_i \int (c''_i(x))^2 dx$ | 0.09 | 0.01 | 0.64 | 0.32 | 0.74 | 0.12 | 1.12 | par |
| Curvature | $\mathcal{K}_{Opt}$ | $\mathcal{K}_{par}$ | $\mathcal{K}_{fd}$ | $\mathcal{K}_{FB}$ | $\mathcal{K}_{Br}$ | $\mathcal{K}_{Aw}$ | $\mathcal{K}_{Aa}$ | Min |
| $\max_i \lvert \kappa_{i-1}(x_i) - \kappa_i(x_i)\rvert$ | 7.80 | 7.80 | 7.80 | 7.80 | 7.80 | 7.80 | 150.41 | Opt,par,fd,FB,Br,Aw |
| $\sum_i \lvert \kappa_{i-1}(x_i) - \kappa_i(x_i)\rvert$ | 8.27 | 7.99 | 11.52 | 9.71 | 12.38 | 8.52 | 164.49 | par |
| $\sum_i \int (\kappa_i(x))^2 dx$ | 0.82 | 0.82 | 0.82 | 0.82 | 0.82 | 0.82 | 0.82 | Opt,par,fd,FB,Br,Aw,Aa |

**Example 29.** Data from Aràndiga [35]: data, degree distributions and fairness measures for various derivative estimation methods. The results are shown in Fig. 27.

| Points $(x_i, f_i)$ | $\mathcal{K}_{Opt}$ | $\mathcal{K}_{par}$ | $\mathcal{K}_{fd}$ | $\mathcal{K}_{FB}$ | $\mathcal{K}_{Br}$ | $\mathcal{K}_{Aw}$ | $\mathcal{K}_{Aa}$ | |
|---|---|---|---|---|---|---|---|---|
| (1,1) | 1 | 1 | 1 | 1 | 1 | 1 | 1 | |
| (2,1) | 1 | 1 | 1 | 1 | 1 | 1 | 1 | |
| (3,1) | 1 | 1 | 1 | 1 | 1 | 1 | 1 | |
| (4,1) | 1 | 1 | 1 | 1 | 1 | 1 | 1 | |
| (5,1) | 3 | 3 | 3 | 3 | 3 | 3 | 3 | |
| (6,1.05) | 1 | 1 | 1 | 1 | 1 | 1 | 1 | |
| (7,1.05) | 1 | 1 | 1 | 1 | 1 | 1 | 1 | |
| (8,1.05) | 1 | 1 | 1 | 1 | 1 | 1 | 1 | |
| (9,1.05) | 8 | 5 | 5 | 3 | 3 | 3 | 3 | |
| (10,1.5) | 3 | 3 | 3 | 3 | 3 | 3 | 3 | |
| (11,5) | 1 | 1 | 1 | 1 | 1 | 1 | 1 | |
| (12,5) | 1 | 1 | 1 | 1 | 1 | 1 | 1 | |
| (13,5) | 1 | 1 | 1 | 1 | 1 | 1 | 1 | |
| (14,5) | 3 | 3 | 3 | 3 | 4 | 4 | 4 | |
| (15,6) | 3 | 3 | 3 | 3 | 3 | 3 | 3 | |
| (16,8.5) | 1 | 1 | 1 | 1 | 1 | 1 | 1 | |
| (17,8.5) | | | | | | | | |
| End point derivatives: $v_0 = 0$ and $v_{16} = 0$. | | | | | | | | |
| | | | | | | | | Min |
| Max degree | 8 | 5 | 5 | 3 | 4 | 4 | 4 | FB |
| Sum of degrees | 31 | 28 | 28 | 26 | 27 | 27 | 27 | FB |

| 2nd Derivative | $\mathcal{K}_{Opt}$ | $\mathcal{K}_{par}$ | $\mathcal{K}_{fd}$ | $\mathcal{K}_{FB}$ | $\mathcal{K}_{Br}$ | $\mathcal{K}_{Aw}$ | $\mathcal{K}_{Aa}$ | Min |
|---|---|---|---|---|---|---|---|---|
| $\max_i \lvert c''_{i-1}(x_i) - c''_i(x_i)\rvert$ | 17.38 | 17.05 | 17.05 | 18.85 | 19.41 | 19.41 | 19.41 | par,fd |
| $\sum_i \lvert c''_{i-1}(x_i) - c''_i(x_i)\rvert$ | 44.10 | 44.58 | 44.58 | 57.11 | 63.29 | 63.29 | 63.29 | Opt |
| $\sum_i \int (c''_i(x))^2 dx$ | 11.07 | 6.17 | 6.17 | 6.36 | 6.73 | 6.73 | 6.73 | par,fd |
| Curvature | $\mathcal{K}_{Opt}$ | $\mathcal{K}_{par}$ | $\mathcal{K}_{fd}$ | $\mathcal{K}_{FB}$ | $\mathcal{K}_{Br}$ | $\mathcal{K}_{Aw}$ | $\mathcal{K}_{Aa}$ | Min |
| $\max_i \lvert \kappa_{i-1}(x_i) - \kappa_i(x_i)\rvert$ | 14.00 | 17.05 | 17.05 | 18.85 | 19.41 | 19.41 | 19.41 | Opt |
| $\sum_i \lvert \kappa_{i-1}(x_i) - \kappa_i(x_i)\rvert$ | 26.13 | 33.38 | 33.38 | 40.16 | 47.06 | 47.06 | 47.06 | Opt |
| $\sum_i \int (\kappa_i(x))^2 dx$ | 0.03 | 0.06 | 0.06 | 0.07 | 0.10 | 0.10 | 0.10 | Opt |

**Example 30.** Data from Yankova [31]: data, degree distributions and fairness measures for various derivative estimation methods. The results are shown in Fig. 28.

| Points $(x_i, f_i)$ | $\mathcal{K}_{Opt}$ | $\mathcal{K}_{par}$ | $\mathcal{K}_{fd}$ | $\mathcal{K}_{FB}$ | $\mathcal{K}_{Br}$ | $\mathcal{K}_{Aw}$ | $\mathcal{K}_{Aa}$ | |
|---|---|---|---|---|---|---|---|---|
| (−1,1) | 3 | 4 | 3 | 3 | 3 | 3 | 5 | |
| (0.8,1.4) | 3 | 4 | 3 | 3 | 3 | 3 | 3 | |
| (1.7,2.2) | 3 | 3 | 3 | 3 | 3 | 3 | 3 | |
| (3,5) | 3 | 3 | 3 | 3 | 3 | 3 | 3 | |
| (4.1,1) | 4 | 7 | 5 | 5 | 7 | 8 | 6 | |
| (4.9,−1) | 3 | 3 | 4 | 3 | 4 | 3 | 8 | |
| (6,1) | 3 | 3 | 3 | 3 | 3 | 3 | 3 | |
| (6.4,3) | 3 | 3 | 5 | 3 | 5 | 3 | 19 | |
| (8,6) | | | | | | | | |
| End point derivatives: $v_0 = 0$ and $v_8 = 0$. | | | | | | | | |
| | | | | | | | | Min |
| Max degree | 4 | 7 | 5 | 5 | 7 | 8 | 19 | Opt |
| Sum of degrees | 25 | 30 | 29 | 26 | 31 | 29 | 50 | Opt |

| 2nd Derivative | $\mathcal{K}_{Opt}$ | $\mathcal{K}_{par}$ | $\mathcal{K}_{fd}$ | $\mathcal{K}_{FB}$ | $\mathcal{K}_{Br}$ | $\mathcal{K}_{Aw}$ | $\mathcal{K}_{Aa}$ | Min |
|---|---|---|---|---|---|---|---|---|
| $\max_i \lvert c''_{i-1}(x_i) - c''_i(x_i)\rvert$ | 10.21 | 19.41 | 36.15 | 26.06 | 37.38 | 21.25 | 50.98 | Opt |
| $\sum_i \lvert c''_{i-1}(x_i) - c''_i(x_i)\rvert$ | 25.01 | 51.59 | 97.72 | 82.12 | 111.37 | 81.83 | 122.08 | Opt |
| $\sum_i \int (c''_i(x))^2 dx$ | 3.84 | 7.80 | 11.96 | 8.40 | 14.64 | 10.57 | 16.90 | Opt |
| Curvature | $\mathcal{K}_{Opt}$ | $\mathcal{K}_{par}$ | $\mathcal{K}_{fd}$ | $\mathcal{K}_{FB}$ | $\mathcal{K}_{Br}$ | $\mathcal{K}_{Aw}$ | $\mathcal{K}_{Aa}$ | Min |
| $\max_i \lvert \kappa_{i-1}(x_i) - \kappa_i(x_i)\rvert$ | 10.21 | 19.41 | 9.29 | 11.39 | 15.23 | 21.25 | 6.43 | Aa |
| $\sum_i \lvert \kappa_{i-1}(x_i) - \kappa_i(x_i)\rvert$ | 17.35 | 27.53 | 19.96 | 20.46 | 28.37 | 31.29 | 22.25 | Opt |
| $\sum_i \int (\kappa_i(x))^2 dx$ | 1.48 | 1.64 | 1.86 | 1.73 | 1.95 | 1.77 | 2.09 | Opt |

## 13. Conclusions

This research was initialized by the very practical need/problem of fitting a shape preserving polynomial spline to the given point data of Examples 1 and 2. Our initial investigation revealed inability of the current spline technology to create acceptable shape preserving interpolants to these data. This research has shown also the classical notion of monotonicity preservation (see Criterion 2 in Section 2) to be problematic, leading to introduction of the alternative *weak monotonicity*

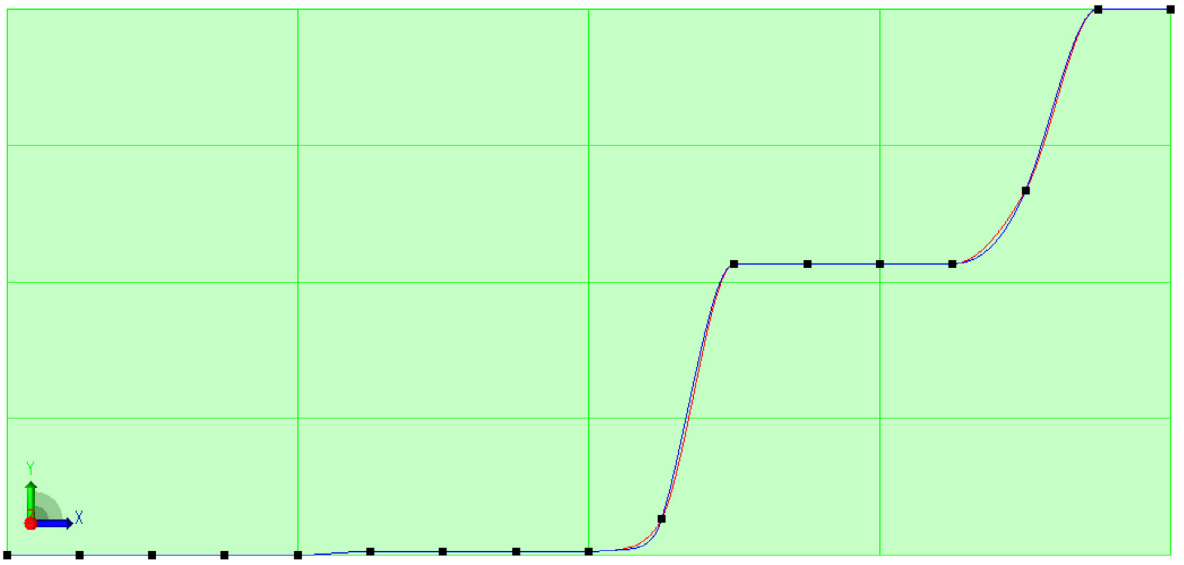


**Fig. 27.** Example 29: The $C^1$ shape preserving curve with its nodal derivatives estimated using the *Opt* method (blue) and the *FB* method (red). (For interpretation of the references to color in this figure legend, the reader is referred to the web version of this article.)

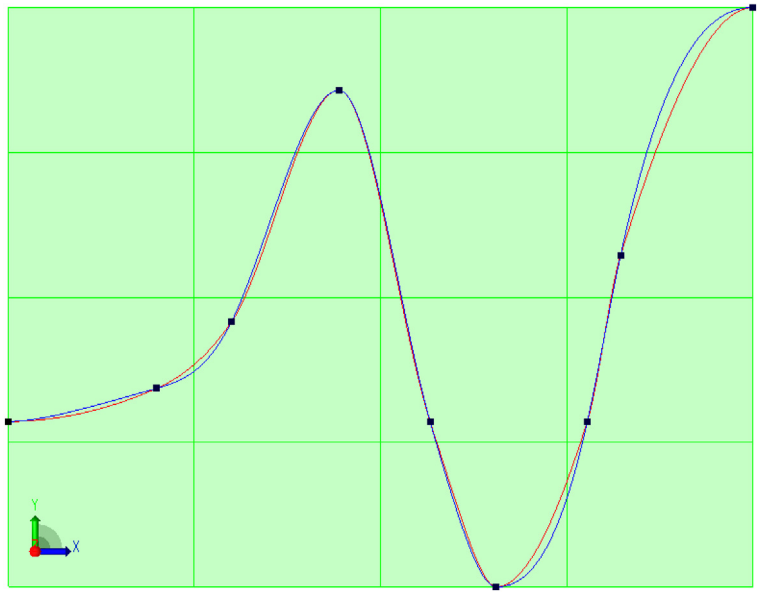


**Fig. 28.** Example 30: The $C^1$ shape preserving curve with its nodal derivatives estimated using the *Opt* method (blue) and the *FB* method (red). (For interpretation of the references to color in this figure legend, the reader is referred to the web version of this article.)

Criterion 4 (Section 3). The Sign, Monotonicity and Convexity preservation problem (detailed in Sections 2 and 3) is solved, in Sections 5–9, using a $C^1$ Hermite variable degree spline, with polynomial segments having the same structure as in [42]. Based on these results, we showed the ability of that spline to achieve shape preserving interpolation with a linear complexity algorithm, given in Section 10. We also studied the convergence of the algorithm for many methods for estimating the nodal derivatives. We developed a new global method for derivative estimation, which was compared against other methods from the literature. The comparison was done in the context of the algorithm of Chapter 10, using a wide range of examples from the pertinent literature. Tables 1–3 show that:

**Table 1**
Results from all the examples regarding degree distributions.

| | Max Degree | Sum of Degrees |
|---|---|---|
| Example 1 | Opt,fd,Br | Opt |
| Example 2 | Opt,FB | Opt,par,fd,FB,Br,Aa |
| Example 3 | FB | Br |
| Example 4 | Opt,par,fd,FB,Br,Aw,Aa | Opt |
| Example 5 | Opt,Br,Aa | Opt,Br,Aa |
| Example 6 | par | par |
| Example 7 | FB | FB |
| Example 8 | Opt | Opt |
| Example 9 | Br,Aw,Aa | Br,Aw,Aa |
| Example 10 | Aa | Aa |
| Example 11 | Opt | Opt |
| Example 12 | FB | FB |
| Example 13 | Opt,FB | Opt,FB |
| Example 14 | Opt,Br,Aw,Aa | Br,Aw,Aa |
| Example 15 | Aw | Aw |
| Example 16 | Br,Aa | Aa |
| Example 17 | Br | Br |
| Example 18 | FB | FB |
| Example 19 | FB,Br,Aw | FB,Br |
| Example 20 | Opt,FB | FB |
| Example 21 | FB,Aw | FB,Aw |
| Example 22 | Br,Aw | Aw |
| Example 23 | Opt | Opt |
| Example 24 | fd,FB,Br,Aw | FB,Br |
| Example 25 | Opt,fd,FB,Br,Aw | FB,Br,Aw |
| Example 26 | Br,Aw,Aa | Br,Aa |
| Example 27 | Br,Aw,Aa | Br,Aw,Aa |
| Example 28 | Opt,par,Aw | Opt,par,Aw |
| Example 29 | FB | FB |
| Example 30 | Opt | Opt |

Number of times each method appears to perform best

| | Max Degree | Sum of Degrees |
|---|---|---|
| Aa | 8 | 8 |
| Aw | 12 | 8 |
| Br | 13 | 11 |
| FB | 13 | 11 |
| Opt | 13 | 10 |
| fd | 4 | 1 |
| par | 3 | 3 |

- Table 1 does not allow us compare the results of the derivative estimation methods, having the minimum degree distribution as a criterion. We see that the methods giving the lowest degree distributions are either local non-linear of quadratic convergence rate (*Br*, *Aw*, *Aa*) or local non-linear of linear convergence rate (*FB*) and global of linear convergence rate (*Opt*). The local linear methods (*fd* and *par*) seem to give the poorest results, although their convergence rate is of quadratic order.
- The *Opt* method tends to minimize the gaps of the second derivative at the interpolation nodes more frequently than the other methods. It also minimizes in most of the cases the integral of the second order derivative of the interpolant.
- The *Opt* method tends to minimize the gaps of the curvature graphs as the nodes of interpolation, as well as the integral of the square curvature, more frequently than the other methods.
- Apart from the above, we have also counted the number of monotonic segments of the curvature. The minimum has been achieved almost uniformly by all methods.

We presented the results representing the spline as a composite Bézier curve, which in turn makes the algorithm being directly adaptable by an ordinary CAD system. Our current research focuses on techniques to reduce the polynomial degree of the shape preserving interpolant.

## Acknowledgments

This work was supported by DNV GL - Digital Solutions (former name: DNV GL - Software). The first of the authors would like to express his thankfulness to Sven-Kåre Evenseth, who, as the Head of Section Fixed Structure Analysis Products, DNV GL - Software, continuously supported research activities of the members of the section. The authors would like also to thank the anonymous reviewers for their valuable comments.

**Table 2**
Results from all the examples on 2nd derivative.

| | $\max \lvert c''_{i-1}(x_i) - c''_i(x_i)\rvert$ | $\sum \lvert c''_{i-1}(x_i) - c''_i(x_i)\rvert$ | $\sum_i \int (c''_i(x))^2 dx$ |
|---|---|---|---|
| Example 1 | Opt | Opt | par |
| Example 2 | Opt | Opt | Opt |
| Example 3 | par | par | par |
| Example 4 | Opt,fd,FB,Br,Aw,Aa | Opt | Opt |
| Example 5 | par | par,Aw | Aa |
| Example 6 | par | Aw | Opt |
| Example 10 | par | par | par |
| Example 11 | Opt | Opt | Opt |
| Example 12 | Opt | Opt | par,fd |
| Example 13 | Opt | FB | fd |
| Example 14 | Br,Aw,Aa | Br,Aw,Aa | Br,Aw,Aa |
| Example 15 | par | par | par |
| Example 16 | par | par | par |
| Example 17 | par | par | Opt |
| Example 18 | Opt | Opt | Br,Aw,Aa |
| Example 19 | Br,Aa | par | fd,FB,Aw |
| Example 20 | par | par | Aa |
| Example 21 | par | par | par |
| Example 22 | Opt | Opt | Opt |
| Example 23 | par,fd | par | Opt |
| Example 24 | Opt,par,fd,FB,Aw | Opt | Aw |
| Example 25 | Opt,par,fd,FB,Aw | Opt | Opt |
| Example 26 | Opt | Opt | Opt |
| Example 27 | Br,Aw,Aa | Br,Aw,Aa | Opt,Br,Aw,Aa |
| Example 28 | Opt,par,fd,FB,Br,Aw | par | par |
| Example 29 | par,fd | Opt | par,fd |
| Example 30 | Opt | Opt | Opt |

Number of times each method appears to perform best

| | $\max \lvert c''_{i-1}(x_i) - c''_i(x_i)\rvert$ | $\sum \lvert c''_{i-1}(x_i) - c''_i(x_i)\rvert$ | $\sum_i \int (c''_i(x))^2 dx$ |
|---|---|---|---|
| Aa | 4 | 2 | 5 |
| Aw | 6 | 4 | 5 |
| Br | 5 | 2 | 3 |
| FB | 4 | 1 | 1 |
| Opt | 13 | 12 | 11 |
| fd | 6 | 0 | 4 |
| par | 14 | 11 | 9 |

**Table 3**
Results from all the examples on curvature.

| | $\max \lvert \kappa_{i-1}(x_i) - \kappa_i(x_i)\rvert$ | $\sum \lvert \kappa_{i-1}(x_i) - \kappa_i(x_i)\rvert$ | $\sum_i \int (\kappa_i(x))^2 dx$ |
|---|---|---|---|
| Example 1 | Opt | Opt | Aa |
| Example 2 | Opt | Opt | Opt,Br,Aw |
| Example 3 | Aw | par | Opt |
| Example 4 | Opt,par,fd,FB,Br,Aw,Aa | Opt,fd | Aa |
| Example 5 | fd | fd | fd |
| Example 6 | par | par | FB |
| Example 10 | Opt | Opt | Opt |
| Example 11 | Opt | Opt | Opt |
| Example 12 | Opt | Opt | FB |
| Example 13 | par | par | par |
| Example 14 | Br,Aw,Aa | Br,Aw,Aa | Br,Aw,Aa |
| Example 15 | fd | par | fd |
| Example 16 | Opt | Opt | Opt |
| Example 17 | Opt | Opt | par |
| Example 18 | Opt | Opt | par,fd |
| Example 19 | Br,Aa | par | Opt,par |
| Example 20 | Opt,par,Aw | Aw | Aw |
| Example 21 | par | par | FB |
| Example 22 | Aw | Aw | FB |
| Example 23 | Opt | Opt | Opt |
| Example 24 | Aa | par | Opt,par |
| Example 25 | Opt,par,fd,FB,Br,Aw,Aa | Opt,par,FB,Aw | Opt |
| Example 26 | Opt | Opt | par |

(*continued on next page*)

**Table 3** (*continued*)

| | $\max \lvert\kappa_{i-1}(x_i) - \kappa_i(x_i)\rvert$ | $\sum \lvert\kappa_{i-1}(x_i) - \kappa_i(x_i)\rvert$ | $\sum_i \int(\kappa_i(x))^2 dx$ |
|---|---|---|---|
| Example 27 | FB | FB | Br,Aw,Aa |
| Example 28 | Opt,par,fd,FB,Br,Aw | par | Opt,par,fd,FB,Br,Aw,Aa |
| Example 29 | Opt | Opt | Opt |
| Example 30 | Aa | Opt | Opt |

Number of times each method appears to perform best

| | $\max \lvert\kappa_{i-1}(x_i) - \kappa_i(x_i)\rvert$ | $\sum \lvert\kappa_{i-1}(x_i) - \kappa_i(x_i)\rvert$ | $\sum_i \int(\kappa_i(x))^2 dx$ |
|---|---|---|---|
| Aa | 6 | 1 | 5 |
| Aw | 7 | 4 | 5 |
| Br | 5 | 1 | 4 |
| FB | 4 | 2 | 5 |
| Opt | 15 | 14 | 12 |
| fd | 5 | 2 | 4 |
| par | 7 | 9 | 7 |

## References


[1] P.D. Caduto, Foundation Design Principles and Practices, Prentice Hall Inc, 2001.
[2] G. Madabhushi, J. Knappett, S. Haigh, Design of Pile Foundations in Liquefiable Soils, Imperial College Press, 2010.
[3] J.M. Hyman, Accurate monotonicity preserving interpolation, SIAM J. Sci. Stat. Comput. 4 (1983) 645–654.
[4] A.M. Lekkas, T.I. Fossen, Integral los path following for curved paths based on a monotone cubic hermite spline parametrization, IEEE Trans. Control Syst. Techn. 22 (2014) 2287–2301.
[5] R. Kozera, L. Noakes, P. Szmielew, Quartic orders and sharpness in trajectory estimation for smooth cumulative chord cubics, in: L.J. Chmielewski, et al. (Eds.), ICCVG 2014, in: LNCS, vol. 8671, Springer International Publishing, 2014, p. 916.
[6] D.F Mc Allister, E. Passow, J.A. Roulier, Algorithms for computing shape preserving spline interpolations to data, Math. Comp. 31 (1977) 717–725.
[7] S. Pruess, Shape preserving $C^2$ cubic spline interpolation, IMA J. Numer. Anal. 13 (1993) 493–507.
[8] L.M. Kocic, G.V. Milovanovic, Shape preserving approximations by polynomials and splines, Comput. Math. Appl. 33 (1997) 59–97.
[9] D. Schweikert, An interpolation curve using splines in tension, J. Math. Phys. 45 (1966) 312–317.
[10] H. Späth, Exponential spline interpolation, Computing 4 (1969) 225–233.
[11] L.L. Schumaker, On shape preserving quadratic spline interpolation, SIAM J. Numer. Anal. 20 (1983) 854–864.
[12] F.N. Fritsch, R.E. Carlson, Monotone piecewise cubic interpolation, SIAM J. Numer. Anal. 17 (1980) 238–246.
[13] P. Costantini, On monotone and convex spline interpolation, Math. Comp. 46 (1986) 203–214.
[14] P. Costantini, An algorithm for computing shape-preserving interpolating splines of arbitrary degree, J. Comput Appl. Math. 22 (1988) 89–136.
[15] Numerical Algorithms Group Ltd, Oxford, UK, NAG Library Manual, Mark 26. https://www.nag.co.uk/numeric/fl/nagdoc_fl26/nagdoc_fl26.pdf.
[16] F.N. Fritsch, J. Butland, A method for constructing local monotone piecewise cubic interpolants, SIAM J. Sci. Stat. Comput. 5 (1984) 300–304.
[17] R. Delbourgo, J. Gregory, Shape preserving piecewise rational interpolation, SIAM J. Sci. Stat. Comput. 6 (1985) 967–976.
[18] P. Costantini, Curve and surface construction using variable degree polynomial splines, CAGD 17 (2000) 419–446.
[19] P. Costantini, C. Manni, Geometric construction of generalized cubic splines, in: it Rendiconti di Matematica, Serie VII, vol. 26, Roma, 2006, pp. 327–338.
[20] P. Costantini, P. Kaklis, C. Manni, Polynomial cubic splines with tension properties, CAGD 27 (2010) 592–610.
[21] B.I. Kvasov, Monotone and convex interpolation by weighted quadratic splines, Adv. Comput. Math. 40 (2014) 91–116.
[22] M. Sarfraz, A rational cubic spline for the visualization of monotonic data: an alternate approach, Comput. Graph. 27 (2003) 107–121.
[23] M. Sarfraz, S. Butt, M.Z. Hussain, Visualization of shaped data by a rational cubic spline interpolation, Comput. Graph. 25 (2001) 833–845.
[24] M. Safraz, M.Z. Hussain, F.S. Chaudary, Shape preserving cubic spline for data visualization, Comput. Graph. CAD/CAM 01 (2005) 185–193.
[25] M. Sarfraz, M.Z. Hussain, M. Hussain, Shape-preserving curve interpolation, Int. J. Comput. Math. 89 (2012) 35–53.
[26] M.Z. Hussain, M. Sarfraz, Positivity-preserving interpolation of positive data by rational cubics, J. Comput. 218 (2008) 446–458.
[27] M. Abbas, A.A. Majid, M.N.H. Awang, J.M. Ali, Monotonicity preserving interpolation using rational spline, in: Proc. of the Intern. MultiConference of Eng. and Comp. Scientists, Vol I. Hong Kong, 2011.
[28] M. Abbas, A.A. Majid, J.M. Ali, Monotonicity-preserving c2 rational cubic spline for monotone data, Appl. Math. Comput. 219 (2012) 2885–2895.
[29] Meng Tian, Monotonicity-preserving piecewise rational cubic interpolation, Int. J. Math. Anal. 5 (2011) 99–104.
[30] Yan Wang, Jieqing Tan, Zhiming Li, Tian Bai, Weighted rational quartic spline interpolation, J. Inf. Comp. Sci. 10 (2013) 2651–2658.
[31] T. Yankova, Piecewise rational interpolation by witch of Agnesi, Comp. Appl. Math. 36 (2017) 1205–1216.
[32] K.O. Riedel, Locally optimal knots and tension parameters for exponential splines, J. Comput. 196 (2006) 94–114.
[33] M. Kamada, R. Enkhbat, Spline interpolation in piecewise constant tension, in: Laurent Fesquet, Bruno Torrésani (Eds.), SAMPTA09, Marseille, France, 2004, pp. 373–376.
[34] Xi-An Han, Yi Chen Ma, Xi Li Huang, The cubic trigonometric Bézier curve with two shape parameters, Appl. Math. Lett. 22 (2009) 226–231.
[35] F. Aràndiga, R. Donata, M. Santagueda, The PCHIP subdivision scheme, Appl. Math. Comput. 8 (2015) 1–13.
[36] F. Kuijt, R. Van Damme, Shape preserving interpolatory subdivision schemes for nonuniform data, J. Approx. Theory 114 (2002) 1–32.
[37] T. Lyche, J.-L. Merrien, $C^1$ interpolatory subdivision with shape constraints for curves, SIAM J. Numer. Anal. 44 (2006) 1095–1121.
[38] P. Novara, L. Romani, On the interpolating 5-point ternary subdivision scheme: a revised proof of convexity-preservation and an application-oriented extension, Math. Comp. Simulation 147 (C) (2018) 194–209.
[39] F. Pitolli, Ternary shape-preserving subdivision schemes, Math. Comp. Simulation 106 (2014) 185–194.
[40] P. Viswanathan, A.K.B. Chand, R.P. Agarwal, Preserving convexity through rational cubic spline fractal interpolation function, J. Comput. 263 (2014) 262–276.
[41] P. Viswanathan, A.K.B. Chand, Shape preserving rational cubic spline fractal interpolation, Numer. Anal. (2016). arXiv:1503.02458v2 (math.NA).
[42] P.D. Kaklis, D.G. Pandelis, Convexity-preserving polynomial splines of non-uniform degree, IMA J. Numer. Anal. 10 (1990) 223–234.
[43] A. Messac, A. Sivanandan, A new family of convex splines for data interpolation, CAGD 15 (1997) 39–59.
[44] P.D. Kaklis, N.S. Sapidis, Convexity-preserving interpolatory parametric splines of non-uniform polynomial degree, CAGD 12 (1995) 1–26.
[45] P.D. Kaklis, M.I. Karavelas, Shape preserving interpolation in $R^3$, IMA J. Numer. Anal. 17 (1997) 373–419.

[46] N.C. Gabrielides, P.D. Kaklis, $C^4$ Interpolatory shape preserving polynomial splines of variable degree, in: G. Brunnet, H. Bieri, G. Farin (Eds.), Geometric Modelling, Dugstuhl 1999 (Computing Supplement 14), 2001, pp. 119–154.
[47] N.C. Gabrielides, $C^1$ Hermite shape preserving polynomial splines in $R^3$, 3D Res. 3 (2012) 1–12.
[48] DNV GL - Digital Solutions, Conceptual modelling of offshore and maritime structures - GeniE, 2018. https://www.dnvgl.com/services/conceptual-modelling-of-offshore-and-maritime-structures-genie-89128.
[49] R.L. Dougherty, A. Edelman, J.M. Hyman, Nonnegativity-, monotonicity-, or convexity-preserving cubic and quintic Hermite interpolation, Math. Comp. 52 (1989) 471–494.
[50] N.S. Sapidis, P.D. Kaklis, A hybrid method for shape–preserving interpolation with curvature-continuous quintic splines, Comput. Suppl. 10 (1995) 285–301.
[51] F. Aràndiga, On the order of nonuniform monotone cubic Hermite interpolants, SIAM J. Numer. Anal. 51 (2013) 2613–2633.
[52] K.W. Brodlie, Methods for drawing curves, in: R.A. Earnshaw (Ed.), Fundamental Algorithms for Computer Graphics, in: NATO ASI Series, vol. 17, Springer, Berlin, Heidelberg, 1985.
[53] P. Rentrop, An algorithm for the computation of the exponential spline, Numer. Math. 35 (1980) 81–93.
[54] D.F. McAllister, J.A. Roulier, Interpolation by convex quadratic splines, Math. Comp. 32 (1978) 1154–1162.
[55] H. Akima, A new method for interpolation and smooth curve fitting based on local procedures, J. ACM 17 (1970) 589–602.
[56] S. Butt, K.W. Brodlie, Preserving positivity using piecewise cubic interpolation, Comput. Graph. 17 (1993) 55–64.
[57] C. Conti, R. Morandi, Piecewise $C^1$-shape-preserving Hermite interpolation, Computing 56 (1996) 323–341.
[58] H. Späth, One Dimensional Spline Interpolation Algorithms, AK Peters, Natick, 1997.
[59] C. Manni, On shape preserving $C^2$ Hermite interpolation, BIT 41 (2001) 127–148.
[60] C.F. Gerald, P.O. Wheatley, Applied Numerical Analysis, seventh ed., Pearson, Upper Saddle River, 2003.